The Tough get Tougher?

Investigation of Vertically Oriented Carbon Nanotubes Materials at Interlaminar Region of Polyphenylene Sulfide Thermoplastic Composites

By: Mark Fiorentino

in partial fulfillment of the requirements for the degree of

Master of Science

Aerospace Engineering - Structural Integrity and Composites – Manufacturing Track

at the Delft University of Technology,

to be defended publicly on October 24th 2018 at 14:00.

Supervisor:	Asst. Prof. dr. I. F. Villegas	TU Delft
Thesis committee:	Asst. Prof. ir. J. Sinke	TU Delft
	Prof. dr. S. van der Zwaag	Tu Delft
	dr. H. Luinge	TenCate

Table of Contents

List of Figures

List of Abbreviations

CAI	Compression after impact
CFRP	Carbon fiber reinforced polymer
CF/TP	Carbon fiber thermoplastic
CF/TS	Carbon fiber thermoset
CNT	Carbon nanotube
CF	Carbon fiber
CT	Computed tomography
CVD	Chemical vapor deposition
CLC	Combined loading compression

DOE	Design of experiments
DCB	Double cantilever beam
EDS	Energy Dispersive Spectroscopy
ENF	End-notch flexure
Tg	Gas-transition temperature
ILSS	Interlaminar shear strength
MPT	Mandrel Peel Test
TM	Melting temperature
MMA	Methylmethacrylate
MWCNT	Multi-wall Carbon Nano-tube
OOA	Out of Autoclave
Pa·s	Pascal second
pJ	Picojoules
PC	Polycarbonate
PEI	Polyetherimide
PEEK	Polyetheretherketone
PI	Polyimide
PMMA	Polymethylmethacrylate
PPS	Polyphenylene sulfide
RC	Resin Content
SBS	Short beam shear
SEM	Scanning Electron Microscope
SS	Stainless Steel
SWCNT	Single-wall Carbon Nano-tube
TP	Thermoplastic
TS	Thermoset
UD	Unidirectional fiber
VACNT	Vertically aligned carbon nanotube

Abstract

Vertically aligned carbon nanotube (VACNT) materials, also referred to as aligned-carbon nanotubes or *Nanostitch*, have been shown to add significantly to out-of-plane mechanical properties when applied to the interlaminar region of traditional thermoset (TS) composite materials. These enhancements included increased interlaminar shear strength (ILSS), fracture toughness, fatigue life, and damage tolerance. These noted increases in mechanical properties occur due to the placement of VACNT materials between the fiber layers of composite materials (perpendicular to the fiber layers) such that the numerous free ends of the VACNTs interdigitate with the fibers of the composite. This *bridging* across the traditionally weak matrix layer of the composite materials with the extremely strong VACNTs has the effect of increasing the out-of-plane properties of composite materials. These increases can prove to be beneficial by allowing for stronger, lighter, and more damage tolerant composite structures. Recent advancements in the large-scale industrial production of VACNTs has opened new avenues for their use in a variety of composite materials.

This project investigates the combination of high-performance Polyphenylene sulfide (PPS) thermoplastic (TP) uni-directional (UD) and fabric woven carbon fiber materials with these newly available VACNTs. The inspiration for this investigation is to establish if the toughness of PPS can be enhanced to a level of that PEEK or other similar high-performance TP composite-based materials. Additionally, the method for embedding of VACNTs into TP based composite materials may provide an avenue for future uses such as welding or heating applications.

In this examination ~20µm and ~50µm VACNTs are respectively embedded and consolidated at the interlaminar region of UD and fabric PPS composite materials through the application of heat and pressures ranging from applied temperatures of 100^0C to 320^0C and 0.5 to 10 bar respectively. It was found that by varying percentage of VACNTs could be transferred from their presented substrate and embedded to both UD and fabric materials depending on the temperature and pressures used to embed them. The vertical orientation of the VACNTs following the embedding process was observed to be more intact with respective applied pressures and temperatures of 1bar and 200^0C. For higher pressures and temperatures, buckling and matting of the VACNTs was witnessed. During the consolidation of multiple plies with VACNTs at the interlaminar layer, it was further observed that buckling and matting of VACNTs occurred to varying degrees. For ~50µm VACNTs tested with fabric materials, the VACNTs were found to drift and conglomerate in the resin-rich pockets created by the undulations of the fabric materials, while for ~20µm VACNTs tested with UD did not show similar behaviors.

Mechanical testing in the form of short-beam-shear (SBS), combined-loading-compression (CLC), and mandrel-peel-test (MPT) was used to characterize the impact that VACNTS at the interlaminar region of PPS TP materials on the respective shear, compression, and fracture toughness properties of the resulting materials. A significant decrease of 10.6% in short-beam strength was observed for UD PPS specimens with VACNTs compared to without. Similar decreases in compressive strengths of 8.5%

for UD PPS specimens were found. These decreases are thought be caused by matting and buckling of VACNTs which did not bridge the entirety of the interlaminar regions, causing stress concentrations rather than strengthening mechanisms. The results from the use of an MPT showed somewhat ambiguous results in that specimens with VACNTs showed a lower overall fracture toughness by 18.6%, but is believed to be due to the propagation of the crack front diverting off from the interlaminar region with VACNTs.

It is recommended that work be continued to with TP UD materials but not with fabric materials as the location and morphology of VACNTs with fabric materials cannot be maintained whereas they can to an extent with TP UD materials. Furthermore, an investigation into the embedding of VACNTs with TP films with the use of temperature and pressure should be performed. This appears to be a viable option for placement of VACNTs at the interlaminar region of TP/CF composites and may open the door to other uses such as TP welding, heating, and in-situ repair.

1 Introduction

Carbon nanotubes (CNT) have been touted by researchers and the press as the next best wonder material since their discovery in the early 1990s [1]. Their proposed high-tech uses include advanced electronics, space elevators, and an array of aerospace applications due to their unique electrical, thermal, and mechanical properties. In regards to structural applications, the high tensile strength and stiffness of CNTs, respectively 50-200 GPa and up to 1TPa, could be highly beneficial their uses for the transportation, aeronautical, and space applications [2]–[4]. In these applications, highly loaded structures can be made lighter leading to the ability to increase payload capacity or reduce fuel costs. Specifically, the use of CNTs in conjunction with fiber-based composite materials in the form of additives to matrix or fiber materials has been an area where much research has been done over the past several decades [5]. However, such cutting-edge applications with the use of CNTs and composite materials have been slow to show themselves in reality due to the complexity of working with CNTs and producing them in large scales.

Research into the production and use of VACNTs has shown recent promise as a readily applicable use of CNTs from a structural perspective within composite materials. It has been shown that VACNTs of a length in the range of ~10-100μm can be placed at the weak interlaminar matrix layer and greatly increase the interlaminar strength of the composite materials. This increase is achieved by placing the VACNTs perpendicular to the fibers of a laminate layer whereby the VACNTS bridge across the matrix region as shown in Figure 1. Significant increases in interlaminar shear, fatigue, and damage tolerance properties of thermoset (TS) composites supplemented by VACNTs has been shown.

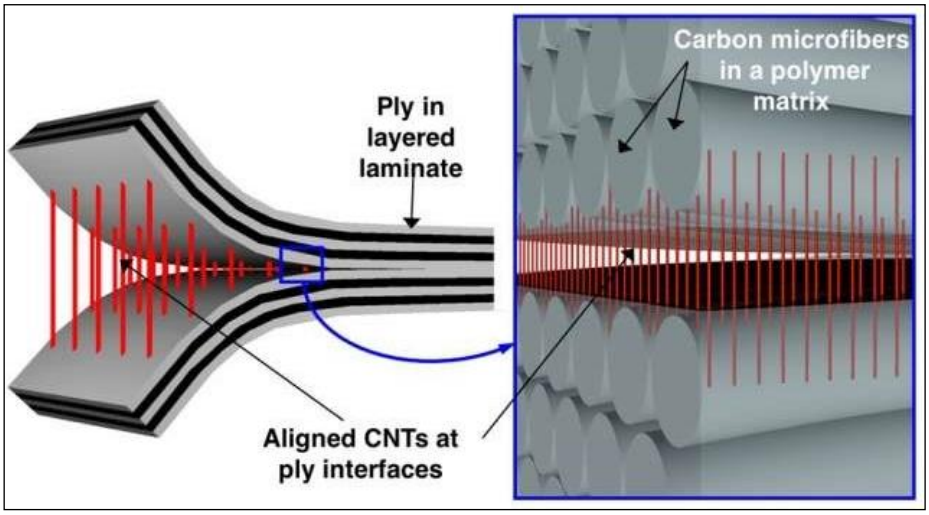

Figure 1 -VACNTs or aligned CNTs in composite laminate [6]

Recent advances with large-scale production of VACNTs has been made through the use of a continuously moving substrate growth process. In this process, large quantities of VACNTs can now be produced in short periods of time compared to the traditional time-intensive and small-scale

laboratory-based processes. This industrialization has led to novel uses of VACNTs that before were nearly impossible due to the low volume of VACNTs available for research which this project is based on.

Building on the newly created availability of VACNTs for research opportunities, the author has set the motivations for this thesis project firmly on the desire to understand if VACNTs can be used to similarly enhance the mechanical properties of thermoplastic (TP) composites as those observed with TS based composites. It is hypothesized that the already *tough* nature of TP composites, which is derived from the ductile nature of the TP resins used as a matrix, can be further enhanced with the use of VACNTs at the interlaminar layer. In the review of literature, it was observed that no in-depth research into this topic has been performed to date. Furthermore, in working closely with respective industrial partners who produce the VACNTs and TP composites, it was found that these partners desired to have a better understanding if this hypothesis proves true or not. This desire to better understand if VACNTs at the interlaminar layer can enhance the mechanical properties of TP composites form the motivation for this thesis project.

Based on the noted motivations, the detailed objective of this work is to investigate the use of VACNTs with PPS TP UD and fabric composite materials. The use of PPS as a matrix material to be used for this research was chosen for several different reasons. First, the processing temperature of PPS (320^0C) is considerably lower than that of other high-performance TP matrix materials such as PEEK, (380^0C) and therefore easier and less expensive to process with the available equipment. Secondly, the lower toughness properties of PPS TP composites compared to the other as TP materials, such as PEEK and PEI, set at a goal to see if it is possible to increase the toughness of PPS to that of or greater than these higher performance TP counterparts [7].

Overall this work sets to establish an understanding of both embedding and consolidation of VACNTs to PPS TP composite UD and fabric materials via the application of temperature and pressure. The embedding process is similar to that used for embedding VACNTs into TS pre-preg composite materials which use the *tacky* nature of TS pre-preg materials at room temperatures, along with applied pressures, as an adhesion method for transferring VACNTs from the substrate to the composite materials. However, since PPS is solid at room temperature, it is reasoned that no transfer of VACNTs to the TP composite material can take at room temperature and therefore must be performed at an elevated temperature along with applied pressures. An examination of the orientation of the VACNTs at the interlaminar region of the composite materials will be performed to understand how the embedding and consolidation processes affect the orientation of VACNTs. Lastly, mechanical testing will be performed to observe if any hypothesized increases or other changes in mechanical properties are achieved. This body of work sets to expand the use of VACNTs into composite materials and form a basis for future work in the form of embedding VACNTs into TP materials for structural enhancement and other uses such as welding or heating applications.

The work contained in the reporting of this project is presented in the following format: A review of pertinent background information and review of prior work by other researchers in section 2; statement of the research objectives in section 3; the methodology, results, and conclusions of the respective embedding and consolidation processes in section 4; the methodology, results, and conclusions for the various mechanical tests in section 5; overall conclusions and recommendations for future work in section 6.

2 Background and Prior Work

2.1 Carbon Fiber Reinforced Polymer Composites

The use of carbon fiber reinforced polymer (CFRP) composite structures came into large-scale use in the 1960s and 1970s first in use with aerospace applications [8]. In these applications, CFRPs have excelled with their low density, high strength and stiffness, and longer fatigue life compared to high strength metals which are typically used [9]–[11].

CFRPs are desirable for high-performance applications since they can be uniquely tailored, via the layup of the fibers in the composite, to achieve high mechanical properties in the respective in-plane fiber directions (see orientation in Figure 2). On the other hand, CFRPs are limited in their out-of-plane mechanical properties due to the low tensile strength of the polymer matrix which binds the various layers of the composite laminate. Out-of-plane loading can lead to failures in the form of matrix cracking, fiber breakage, and delamination between the fiber layers, which in turn can drastically reduce the overall strength and service life of a CFRP structure. Researchers have continually been working on efficient methods to increase this out-of-plane strength of composites. They have found some success with the use of Z-pinning, fiber stitching, and modifications to the fiber and matrix materials architecture with the addition of nano-sized materials [9], [12]–[14].

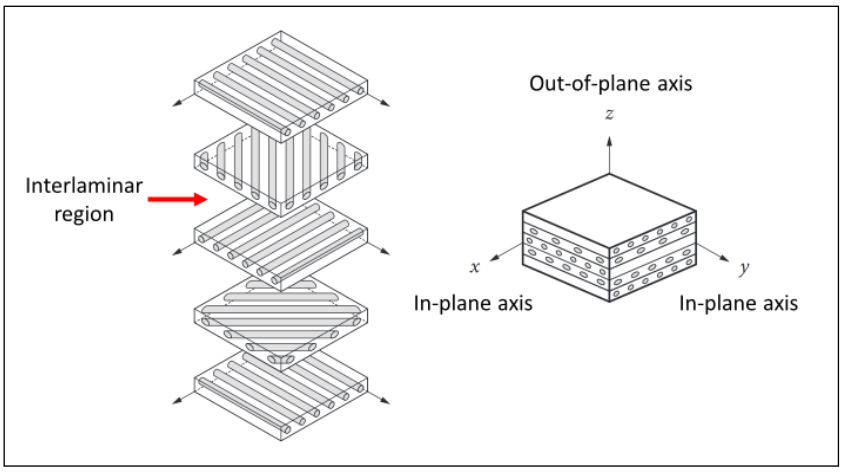

Figure 2 - Composite laminate orientation [11]

The two primary types of CFRPs are currently used in industry today are TS and TP composites. TS composite materials have formed the basis of the composites industry since its introduction, while TP composite materials came into widespread use later on and held a smaller, but growing, share of the industrial marketplace [12]. TS composite materials utilize matrix materials consisting of mixtures of unlinked polymer chains that through a curing process irreversibly crosslink to form a solid molecular structure. TP composite materials on the other hand employ matrix materials that consist of separate molecular chains which are held in place via intermolecular forces and can be re-formed with heat that is above the Tg of the polymer. TS materials, whether in their unmixed constituent components or as

pre-mixed pre-preg composite materials, have a limited shelf life whereas TP materials have the unique property of indefinite shelf life, allowing for long-term storage without any deterioration in properties. Regarding mechanical and physical properties CF/TP composites when compared to TS epoxy-based composites also been found to exhibit higher mode I and II fracture toughness values [15], residual mechanical properties after impact [16]–[18], and higher service temperatures values compared to TS materials [19].

2.2 Carbon Nanotube (CNT)

CNTs were first discovered in 1991 by S. Iijima [1]. Since that time there has been a nearly exponential year-over-year growth in the published research papers and patents focused on the topic of CNT manufacturing and applications [20]. Within those publications and patents, researchers have shown that with the addition of CNTs to the polymer matrix of a composite material mechanical and other properties of the composite can be drastically altered. Particularly, the severity of the as-mentioned failure mechanisms in the interlaminar region of a composite structure can be significantly reduced. These specific applications of CNTs take advantage of the high tensile strength and large surface area of CNTs to increase the mechanical strength of the matrix via simple mechanical bonding and adhesion between the CNTs and the matrix material of the composite [3]. As mentioned, research has shown that CNTs can reach a theoretical stiffness modulus of nearly 1TPa, roughly 2-4 times greater than that of most commercial carbon fibers; the workhorse material of the high-performance composite industry [23]. The underlying reason for the high stiffness is derived from the strong covalent carbon-carbon bonds that make up the CNT structure. Being arranged in single-wall or multi-wall configurations (SWCNT and MWCNT), CNTs are essentially layers of flat, two-dimensional graphene sheets that are wound up in a tubular fashion in either single or concentric tubes of carbon atoms as shown in Figure 3. CNTs can range in diameter from 0.5-10nm (single wall) to 1-100+nm (multi-wall) and have lengths from 10-1,000+μm, creating extremely high surface areas of over 1300m^2/gram [24].

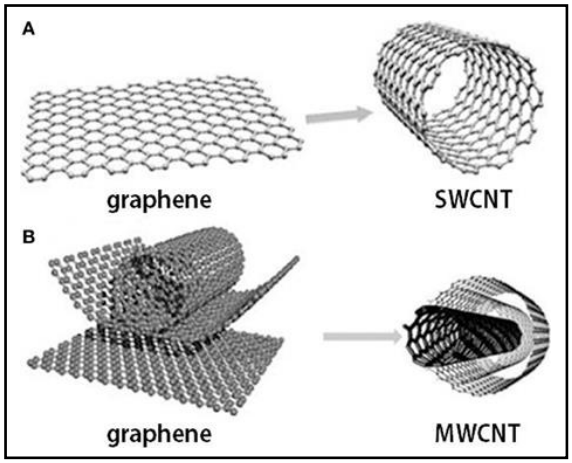

Figure 3 - Depiction of SWCNT and MWCNT construction [25]

2.3 Reinforcement of Composites with Carbon Nanotubes

As mentioned previously, researchers have investigated numerous methods to increase the out-of-plane properties of composite materials. One method has been the use of enhancing composites with the addition of CNTs and can be performed with three approaches which include the following.

1) Dispersion of CNTs with the polymer matrix
2) In-situ growth of CNTS on fibers, also known as *fuzzy fibers*
3) VACNTs located at the interlaminar region of composite plies.

The first method, addition of random CNTs into the polymer matrix region of a composite has been shown in some cases to increase Mode I and II fracture toughness and damage tolerance of a composite material by strengthening the matrix regions of the composite [26]–[28]. However, this style of nano-reinforcement often leads to issues with the CNTs not properly dispersing equally and conglomerating in dense areas within the matrix [22], [29]–[32]. This clumping of the CNTs leads to void pockets and areas of non-homogeneity in the matrix material. Recent advancements have however been shown to allow for more equal and homogeneous dispersion of CNTs into the polymer matrix of a wide variety of composite materials, leading to possible wide-scale use in the future.

The second method, known as *fuzzy fibers*, consists of a unique process by where individual SWCNTs and/or MWCNTs are grown on the surface of individual carbon fibers or carbon fiber woven materials [21], [33]–[39]. This process allows for the CNTs to be grown on the perimeter of a carbon fiber either randomly or radially out from the surface of the carbon fiber creating an interlocking mechanism between the other *fuzzy fibers* and the matrix of the composite as shown in Figure 4. Some researchers have shown that this type of CNT reinforcement can increase Mode I fracture toughness as well as other mechanical and electrical properties of the end-use composite material. One interesting feature of the *fuzzy fiber* architecture is that the capillary action of the CNTs attached to the surface of the carbon fibers helps to greatly wick matrix material into the composite rather than blocking the passage of the matrix material as can be seen with dispersed CNTs. One unfortunate pit-fall to the use of *fuzzy fiber* is that it has been shown to degrade and weaken the carbon fiber base materials by robbing carbon molecules away from the fiber to grow the CNTs, though work is progressing on addressing this known issue.

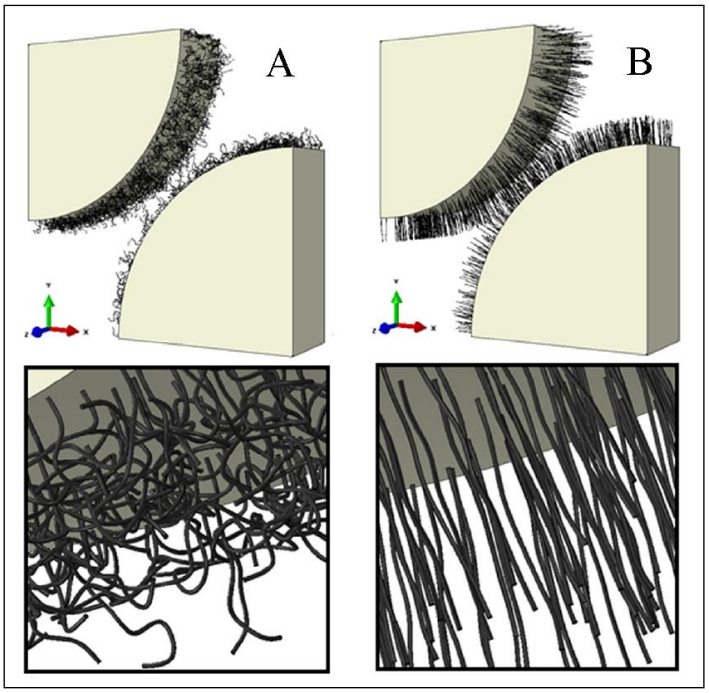

Figure 4 - Random and oriented fuzzy fibers [21]

The last method, the use of VACNTs oriented perpendicular to the composite fibers at the interfacial layer (shown in Figure 2), has been shown to increase the ILSS of composite materials. It performs this task by bridging the weak polymer interlaminar region with many CNTs, having extremely high specific tensile strengths, which happen to be lined up next to one another. The vertical orientation of these CNTs permits them to be accurately and consistently oriented across the matrix layer and come into contact with both the top and bottom side of each fiber layer within a composite. These VACNTs can be grown on a substrate (as shown in Figure 5) and transferred or embedded as a bulk material to the surface of a composite material ply.

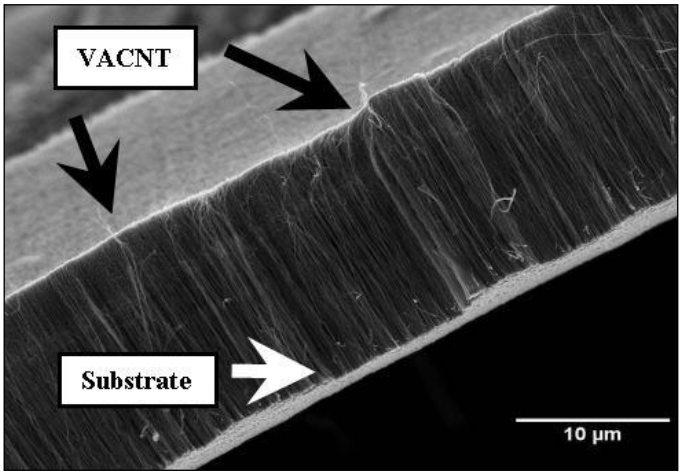

Figure 5 – SEM picture of VACNT material grown on substrate backing plate [40]

These composite plies can then be consolidated into full composite laminate materials where the VACNTs are shown to bridge the interlaminar, matrix dominated, region of the composite materials (as shown in Figure 6). This location of the VACNTs at the interlaminar region of a composite material removes the concern of proper dispersion of the CNTs throughout the polymer matrix material as previously described in the first method. It will be this form of CNT reinforcement which will be utilized and investigated in this thesis project.

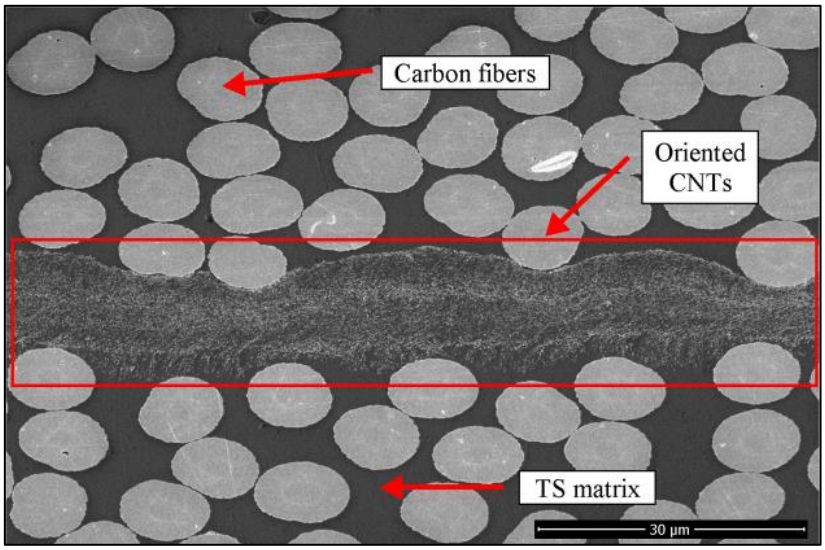

Figure 6 - VACNTs embedded at the interlaminar region of consolidated TS composite [1]

2.3.1 VACNTs – Background Information

To provide the reader with a high-level understanding VACNTs, a brief description of their history and production techniques is given here.

Since the discovery of VACNTs in 1997 various other researchers from around the globe have shown that a variety of methods to construct VACNTs [41], [42]. The primary method used is one of chemical vapor deposition (CVD), with other approaches including electrophoresis, graphite sputtering, and chemical grafting of bulk CNTs onto a substrate. The process of CVD will be focused on here since is the basis for the technology used to fabricate the VACNTs used in this thesis project. As a quick overview, the process to create VACNTs via a CVD process starts with the use of a substrate that is catalyzed by a material that will be used to nucleate the growth of individual CNTs on the substrate. These substrate materials are often high-temperature materials such as nickel, titanium, aluminum, or cobalt, though stainless steel (SS) substrates are often used for industrial purposes. [41], [43]–[45]. The catalyzed substrate is placed in an inert environment that is heated to high temperatures (ranging from roughly 500^0C to 1200^0C), and carbon-rich gasses are pumped into the environment. In a pyrolysis step, the carbon atoms from the carbon-rich gases transfer from the gas to the substrate where the carbon

1) Image courtesy N12 Technologies

atoms re-arrange themselves into either SWCNTs or MWCNTs. The parallel orientation of the CNTs to one another is governed via Van der Waals forces acting between CNTs themselves [46]. The resulting product is a bed of VACNTs which grow parallel to each other at a uniform rate mimicking that of blades of grass in a field [41][47]. This high-level overview of the process has many steps and parameters (temperature, time, substrate, catalyst, the chemical makeup of gas, and gas flow) that impact the final VACNT product. These affect the chief characteristics of the final VACNT material, which include density, length, diameter, and type of CNTs (SWCNTs and/or MWCNTs).

As mentioned the production of VACNTs has been traditionally performed on small-scale laboratory settings where the production of a roughly 50mm square areas of VACNTS could take several hours. This production period for a small yield size made large-scale use and research of VACNTs prohibitive. Recently work pioneered in the at MIT's Department of Aeronautics and Astronautics, has been licensed and industrialized by a company, N12 Technologies, of Cambridge, MA, USA. This VACNT material, commercial known as *Nanostitch* can be grown on a continuous production basis allowing for the high volumes of VACNTs which are now able to be used in new areas of research and industrial applications. It is this specific VACNT material which will be utilized for this thesis project.

The use of a SS as a substrate for the VACNTs, as will be done in this thesis project, is an important factor in several ways. First, the hypothesized transfer of VACNTS to the PPS composite materials will depend on the bond strength of the VACNTs to the substrate and if that bond can be easily broken while retaining the structure and orientation of the VACNTs. While it is not known the exact of strength of the bond between the VACNTs and the substrate used in this thesis project, it is has been shown in by I. Lahiri et al. that the energy to remove a single CNT from a metallic substrate ranges from 1-10 pJ, which correlates to an extremely low bond strength [48]. In practice it has been found that with the VACNTs, which will be used in this thesis project, have a strong enough bond to the substrate to be handled for processing without falling off, making handling of the raw substrate material possible. However, the VACNT-to-substrate bond is weak enough to permit VACNTs to be easily transferred from the substrate while maintaining their orientation. Secondly, the ability of the substrate to be easily handled during the testing for embedding of the VACNTs into PPS materials and later removed is key. The SS materials used as a substrate for the VACNTs used in this project was shown in practice to be an easy material to manipulate by hand and cut into sections simply with regular scissors or industrial shears for further processing.

2.4 Prior work / State-of-the-art

In this section, a brief review of the prior work and state-of-the-art research will be presented. As mentioned previously, this project has the goal to combine two largely unrelated topics, structural TP composites, and VACNTs at the interlaminar layer of those TP composites. The goal of this combination is to see if there are any changes in the mechanical properties of the combined composite materials. The goal of this research project is to understand and observe how and if these two materials

can be combined and what, if any, changes are observed in the mechanical properties of the combined composite material. As such, these two main topics and appropriate specific background research on those topics is discussed herein.

2.4.1 Thermoset VACNT focused research

To date, the vast majority of research on the use of VACNTs and composite materials for structural applications has focused on applications with TS composite materials. It is worth noting the highlights of this work as it forms the basis for the hypothesis of this work with TP composite materials.

Researchers from the Nano-Engineered Composite Structures (NECST) Lab, a group operating within the Department of Aeronautics and Astronautics at MIT in Cambridge, Massachusetts, USA, form one of the key centers for research into VACNTs and composite materials. This laboratory, over the past several years, has produced a volume of work related to the research and development of VACNTs which are relevant to this thesis project [6], [49]–[58]. The highlights that are relevant to this work include:

1) Garcia et al. found Mode I and Mode II fracture toughness of 1.5x – 2.5x and 3x respectively with UD thermoset pre-pregs and ~20µm VACNTs [6]. Noted that this length of VACNTs does not increase the thickness of the finished laminate. This length of VACNTs forms the basis for the work done with UD thermoplastic materials in this project.

2) R. Guzman de Villoria et al. found that improvements of 10%, 30%, and 40% respectively for open-hole compression ultimate strength, critical bearing strength, and L-shape laminate deflection using 20µm VACNTs [51], [53]. Bunching of VACNTs at interlaminar layer has been seen, but still yield increased mechanical properties as noted over pristine specimens.

3) J. Blanco et al. showed that analytical models for the geometric parameters of the VACNTs (individual CNT diameter, length, and density of VACNTs) could be directly related to Mode I fracture toughness of a TS composite material [52].

4) D. Lewis, in a recent MSc thesis project and published work, used SBS static and fatigue testing to find increases in ILSS of 8.5% regardless of VACNT length along with 3x increase in lifespan at 60% failure [57], [58]. Of interest is that a mistaken test cycle yielded an OOA application of VACNTs in pre-preg TS composites yielded extremely low voids. This accidental finding suggests that VACNTs act as air-channel pathways and have increased surface areas which allow air to escape easily [59].

5) X. Ni et al. found increases in-plane tensile strengths of 7.5% in TS UD composite specimens with the addition of 20µm VACNTs by use of double-edge notch tensile tests [56].

6) E. Kalfon-Cohen et al. used SBS testing on TS UD and fabric materials combined with 20, 50, 75, 100, and 300µm length VACNTs [54]. Found that for fabrics, VACNTs less than 50µm can

lead to voids in the finished composite. Did not see any noticeable increase in ILSS overall, but did notice a reduction in interfacial de-bonding of the composite plies in post tested specimens. This they reasoned had to do with the toughening of the VACNTs at the interlaminar region.

7) C. Furtado, in a recent, yet to be published, PhD 1st year seminar report investigated ~20µm length VACNTs with standard thickness (147gsm) and thin-ply (70gsm) thermoset UD materials [60]. Using double cantilevered beam (DCB) testing with thin-ply laminates and VACNTs, she found a ~5% increase in Mode I fracture toughness. She further found a decrease in Mode I fracture toughness of 6.3% using standard thickness fabric weave composite. For this interesting finding during post-testing analysis, it was shown that the fracture lines did not propagate through the VACNT regions, but rather around them. This gives credence to two possibilities. First being to the use of longer than 20µm VACNTs in fabric materials and secondly that tests other than DCB and end notch flexure testing (ENF) for fracture toughness characterization may be needed.

Outside of the group of researchers connected with MIT's NECSTLab as mentioned here, few other researchers were found to be working on VACNT materials at the interlaminar layer of TS or TP composites. Of note was that of B. G. Falzon et al. who found a respective increase of 61% and 161% in Mode I and II fracture toughness via DCB tests of low and high-temperature cure thermoset UD pre-preg composites when using 80-100µm VACNTs at the interlaminar region [61]. Conclusions of this study found that the 80-100µm VACNTs used may have been longer than necessary as they caused a noted increase in the laminate thickness due to the VACNTs.

Lastly, the in-house researchers from N12 Technologies have, for the past few years, published several white papers and articles both independently and in collaboration with other researchers [59], [62]–[65]. This body of work, all dealing with TS composites rather than TP materials, has been an extremely helpful starting point for many of the theories and methodologies of how test VACNTs and TP materials set out in this research project. Of note, several key takeaway findings, which are relevant to this thesis project, are listed here.

1) Increase in compression after impact (CAI) strength of 11-16% with various industry CF material brands [62], [65]. Proving the application of VACNTs to increase mechanical properties and usefulness across a spectrum of composite material manufacturers.

2) Increase in SBS static and fatigue testing by 33-34% and 200% respectively [59], [63]. Tested in similar nature to D. Lewis mentioned previously, providing proof of improvement of mechanical properties and a further data point to compare against for VACNTs with TP composites.

3) Increase in strength for ply-drop locations with the use of localized VACNTs instead of global use [64]. Offering possible future use for localized reinforcement with VACNTs.

4) Open Hole Compressing (OHC) strength increase of 7% over baseline [59]. Further providing evidence of usefulness of VACNTs at localized reinforcement.

5) Use of VACNTs in OOA applications where VACNTs permit <1% void content [59]. Wicking of VACNTs and micro air pathways permit removal of air during OOA compaction. Similar mechanisms could enhance wicking of PPS matrix in TP composite materials. This matches the accidental findings of D. Lewis as mentioned previously [60].

It is worth noting here that the author additionally visited the main production facility for N12 Technologies in January and July 2018 to review the various parameters, testing results, and other minor tips to working with the VACNT materials which proved to be invaluable.

2.4.2 Thermoplastic VACNT focused research

It was discovered that there is substantially less published research on the topic of adding CNTs or VACNTs to TP composite materials than that of TS composite-based materials. Of the relevant published findings, the majority of them have been focused on using VACNTs as electrically or thermally conductive components in TP materials rather than for mechanical properties of a TP composite. From these works, several interesting areas of research include the following

1) Researchers have shown that the embedding of VACNTs into polymethylmethacrylate (PMMA) and polycarbonate (PC) films can be performed easily at temperatures close (both above and below) the respective Tg of the polymers [66], [67]. This is an interesting finding in that it presents a possible method for embedding of VACNTs into a TP composite material close to its Tg.

2) E. Sunden et al. found good transferability of VACNTs to PC polymer films using microwave energy to heat an electrically conductive silicon substrate and VACNT materials, creating a highly localized heating of the VACNTs. This was then pressed into the nonconductive PC polymer surface. This may present a good alternative method for supplying energy to aid in the embedding process [68].

2.4.3 Testing related research

It is worth noting the work done by researchers focused on non-standardized testing methods which could be used to quantify the fracture toughness of the resultant materials for this thesis project. Researchers in the Netherlands at the University of Twente, the Thermoplastic Research Center (TPRC), and TU Deft [69]–[71] have helped to push the development and use of a Mandrel Peel Test (MPT) which can be used to evaluate mixed Mode I and II fracture toughness. Building off of work pioneered by Kawahita, Moore, Williams, et al. [72]–[74] they have worked to validate a MPT which can be used successfully with on thermoplastic composite materials. They have shown that the MPT can provide

comparable results to DCB testing to provide a mixed Mode I and II fracture toughness calculation in less time.

The MPT method, in regards to this thesis project, is hypothesized to be beneficial by providing a method to quantify fracture toughness of TP materials with VACNTs based on the findings of others. During correspondence with technical contacts at N12 Technologies, as well as evidenced in the work by C. Furtado [60], it was shown that the direct measurement of Mode I fracture toughness of a composite material with VACNTs at the interlaminar region via the traditional DCB test is often problematic. The results of this type of testing often yield nebulous results because the recording of the fracture tip location, which is necessary for the calculations of the test, is often irregular since the crack tip is often observed to veer off from the crack front at the intended interlaminar fracture surface. The MPT method is intended to avoid this issue by peeling off a specific laminate layer at the top of a thick laminate base, specifically for UD materials a $\pm 5^0$ scrim interface layer is used help drive the crack cross the interlaminar region. For clarity, the differences in the layout of the two types of tests are shown in Figure 7.

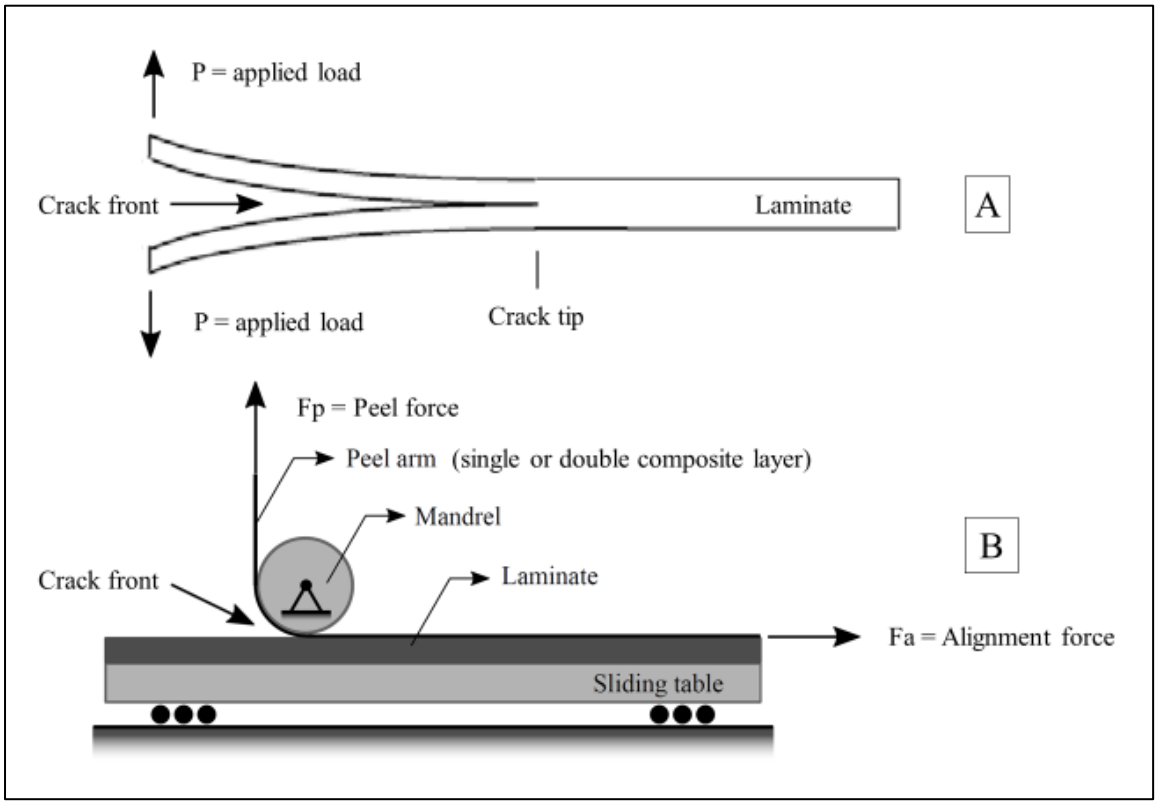

Figure 7 - DCB (A) and MPT (B) method layout

3 Research Objectives and Overview

It has been shown that the integration of VACNTs at the interlaminar region of TS based composites can be readily accomplished and can be related to significant increases in the out-of-plane mechanical properties of the resulting composite. Recent advancements in the production of VACNTs has allowed for wider scale use and research of VACNTs for other composite applications. These two impetuses along with the previously noted motivations to understand if VACNTs can enhance the out-of-plane mechanical properties of TP composites form the basis for the objectives for this study. Within this study, PPS based UD and fabric composites will be combined with VACNTs at the interlaminar layer and be tested to see if this is indeed the case. This study sets forth to examine this hypothesis through the use of several experimental tests and analysis techniques and are broken down into two principal areas of research.

1) Understanding of how pressure and temperature impact the embedding and consolidation of TP composites with VACNTs at the interlaminar region. This understanding will be quantitatively assessed by reviewing the percentages of VACNTs transferred from their substrate to the respective TP composite materials. Additionally, qualitative analysis of the VACNTs embedded to the surface and at the interlaminar regions of the TP composite materials will be made via optical microscopy (OM) and scanning electron microscopy (SEM) techniques with the goal of understanding how the orientation of the VACNTs is affected by the processing parameters
2) Mechanical testing of composite specimens with VACNTs at the interlaminar region to understand the influence of VACNTS ion TP composite materials. Specifically, the mechanical properties which influence out-of-plane strength, ILSS, compression strength, and fracture toughness will be investigated. This will be done through the use of SBS, CLC, and MPT methods.

As an overview of the research objectives for this thesis project, the details for what will and will not be included in the scope of the project are shown in Figure 8 for clarity.

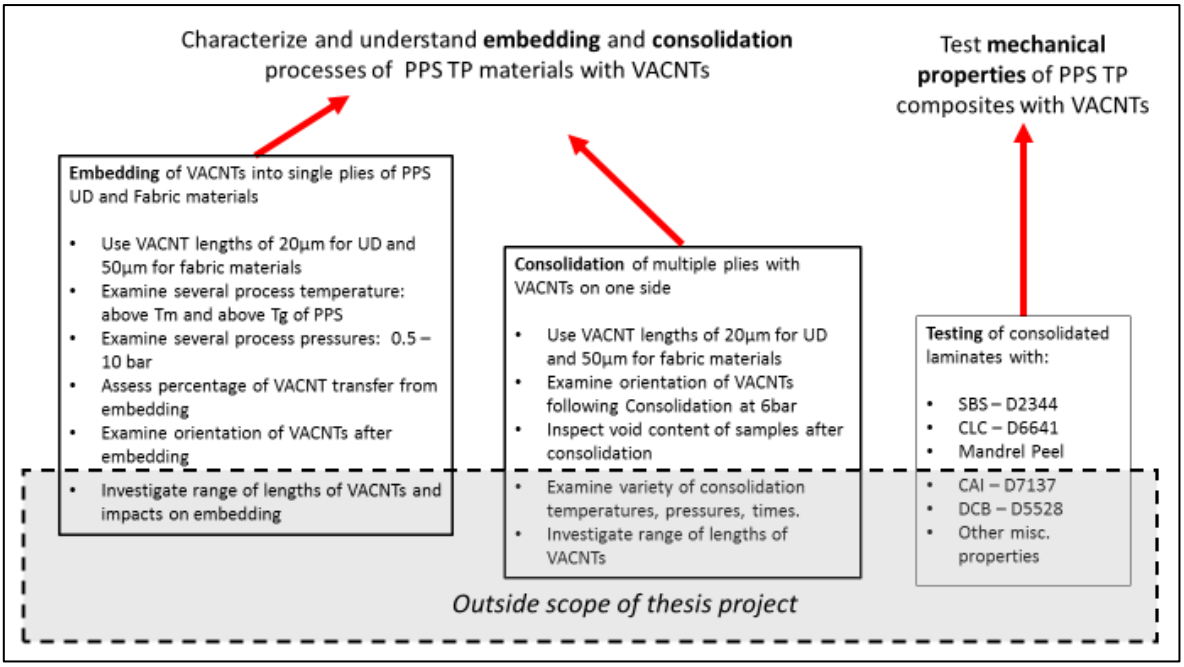

Figure 8 - Research Objective - Scope of work

3.1 Embedding and Consolidation

To evaluate the embedding and consolidation processes of VACNT combined with PPS TP composite materials, sections of SS substrate containing VACNTs measuring 30mm x 30mm will first be compressed into both UD and fabric PPS composite materials respectively with the use of heat and pressure. Embedding specimens will have VACNTs pressed into one side of a composite material while consolidated specimens will consist of one embedded specimen and a non-embedded composite ply consolidated together such that the VACNTs are at the interlaminar region as shown in Figure 9.

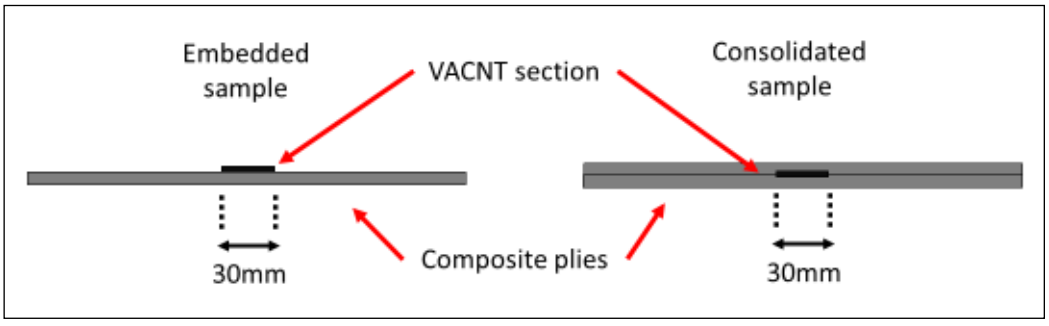

Figure 9 - Side view of Embedded and Consolidated specimens

The lengths of VACNTs used for the testing will be ~20µm long for UD materials and ~50µm for fabric materials. These lengths were chosen to be investigated primarily for the ability of the VACNTs to be incorporated into the composite material without an increase in laminate thickness. The respective lengths of the VACNTs correspond to the average interlaminar resin thickness of the UD and fabric materials. This is supported by the findings of several researchers working with VACNTs and

TS composite materials [6], [51], [53], [56], [60], [61]. Additionally, these two respective lengths of VACNTS were able to be produced in sufficient quantities to be used for this research project.

For the embedding processes, temperatures of 100^0C, 150^0C, 200^0C, and 320^0C will be used to examine how VACNT materials can be embedded into one side of the PPS TP material. These temperatures were chosen based on the previous research showing that VACNTs could be successfully embedded into PMMA, and PC TP resins at temperatures below the Tm and close to the Tg of the respective polymers [66], [67]. For reference, the Tm and Tg for PPS are noted as being 285^0C and 85^0C respectively [7]. Melt viscosity versus temperature data of PPS resin from 280^0C to 320^0C was found to show a nearly linear decrease in viscosity with increasing temperature in the range of 100-200 Pa·s [75]. In the absence of data below 280^0C the viscosity was characteristics were extrapolated to be higher than 200 Pa·s at temperatures lower than 280^0C. From this, it was reasoned that the PPS resin of the composite materials would exhibit gradual levels of decreasing viscosity with an increased temperature above its Tg, various degrees of VACNTs could be embedded at these specific temperatures. This estimated viscosity is much higher than the 0.025 to 1 Pa·s viscosity of the resins used in previously noted literature [6], [49]–[65] which is hypothesized to present significant differences in how the VACNTs can be embedded into TP composite materials. The higher 320^0C temperature was chosen primarily due to its use as the target point recommended by the material manufacturer for consolidation processes. The PPS resin was reasoned to be fully melted at 320^0C and should be able to adhere to the VACNTs. For each of these tested temperatures, pressures will be tested including 0.5, 1, 3, 5 and 10 bar of pressure. These pressures were chosen based on both on the limits of the consolidation pressures suggested by the TP composite manufacturer, in this case, 6-10 bar, but also with the thought that lower applied pressures would be less likely to distort or buckle the VACNTs while still allowing them to become embedded in the resin. To quantify the amount of VACNTs which are transferred from their SS substrate to the composite materials *ImageJ* processing software will be used to examine pictures of the remaining VACNTs on the SS substrate after embedding. The embedded composite specimens will additionally be examined using an SEM to characterize the general orientation of the VACNTs following the embedding process

3.2 Mechanical Testing

Several types of mechanical tests will be used to examine and quantify the influence of VACNTs at the interlaminar layer of consolidated PPS composite specimens. The planned set of tests that will be used in this thesis include SBS, CLC, and MPT. These were chosen since they would provide data on the ILSS, compressive strengths, and fracture toughness of the materials respectively. PPS and PEEK control specimens without VACNTs at the interlaminar layers will be used and tested as control specimens. These were chosen since they would provide a control consisting of the same PPS material as that tested with VACNTs, and it would allow comparison against a composite material, PEEK, with a known higher tensile strength and toughness value [76]. Following the experimental testing, using

OM and SEM tools, examinations will be made of the fracture surfaces. This will be used to gain a better understanding of the influence that VACNTs at the interlaminar region plays has on the resulting failure of the tested specimens. Additionally, it will permit an examination of the orientation and condition of the VACNTs with the goal to better understand if their addition influenced the results of the tests.

4 Embedding and Consolidation

The details of the materials used, process steps, analysis, and findings for both the embedding and consolidation stages of this thesis project are described in the following section. The input parameters of temperature and pressure needed for the embedding of VACNTs to a single-layer of composites are different than that needed for the consolidation of multiple layers of TP composites with VACNTs embedded on one side. As such, this section treats these sections separately.

4.1 Materials

This research projects structured around extensive experimental testing with two currently available commercially produced materials, VACNTs and CF/TP composites. The VACNTs used in this project were provided by N12 Technologies of Cambridge, MA. The VACNT materials, which during processing can be grown accurately to the desired length, are grown directly on either 30mm or 380mm wide SS strips. The length of the VACNT materials to be used in this project are ~20µm (for UD materials) and ~50µm (for fabric materials). Batch samples of the VACNTs used in this thesis project were measured by looking at side profiles of the samples using a JEOL JSM-7500 field emission SEM as shown in Figure 10. All measured samples were found to be within ±5µm and ±10µm of the respective 20µm and 50µm target heights.

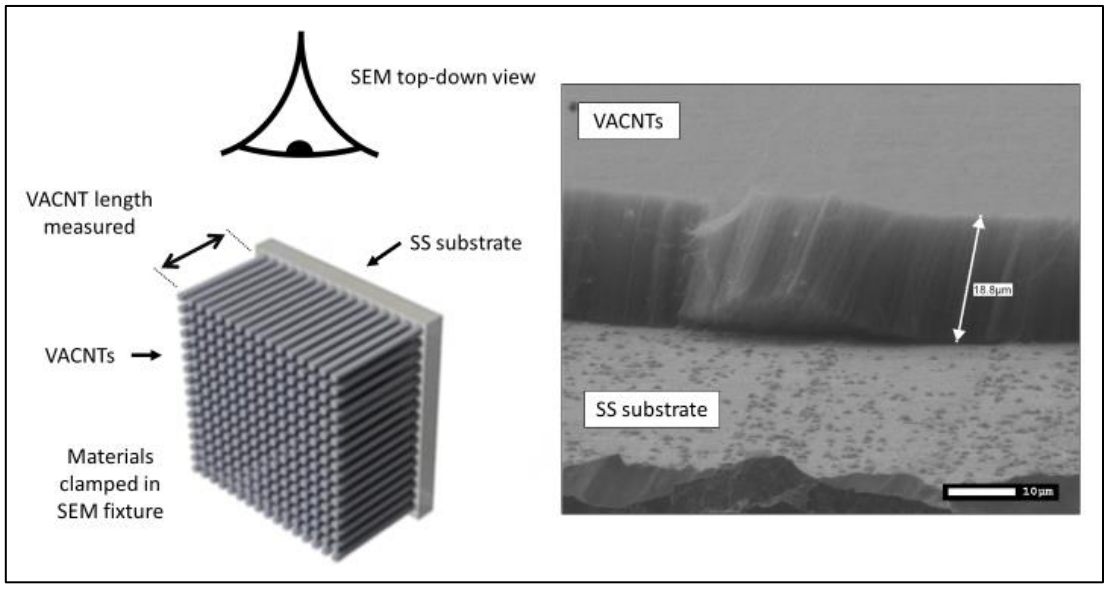

Figure 10 - SEM measurement of VACNT length[2]

The areal density of the VACNTs used is a proprietary figure of the manufacturer, but is estimated to be on the order of roughly 1.0 x 10^{13} - 1.0 x 10^{12} CNTs/cm^2 [41], [77]. For this project, the areal density of the VACNTs used can further be considered to have a density of roughly 20-30% of the maximum areal density able to be produced as indicated the supplier. A physical measurement of the

2) Partial image from [84]

areal density was not made due to the complexity of such measurements within the scope of this project. For clarity, strips of 30mm wide VACNT material are shown in Figure 11, and a section of 380mm wide VACNT material is shown in Figure 12.

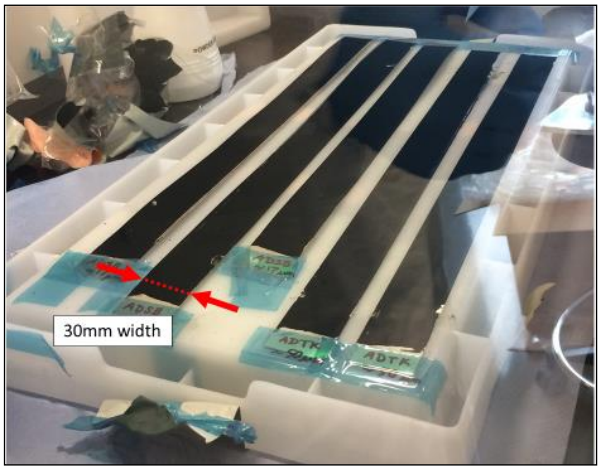

Figure 11 - 5X strips of 30mm wide VACNT material on SS substrate

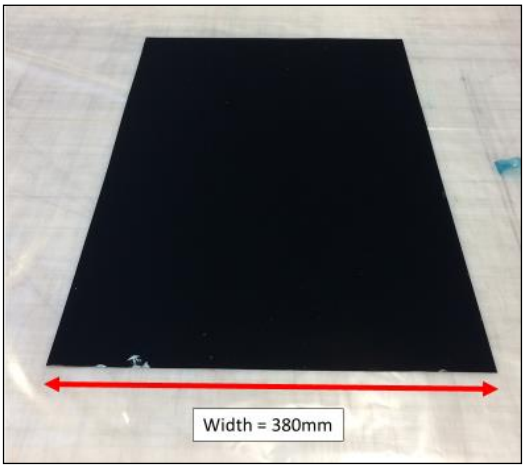

Figure 12 - Section of 380mm wide VACNT material on SS substrate

The composite materials used in this project are TenCate brand PPS and PEEK CF/TP pre-preg composites. The PPS based materials are Cetex® TC1100 AS4D 12K UD material (221 g/m^2 / 34% RC) and T300 3K 5HS satin weave fabric material (280 g/m^2 / 43% RC). Specifically, the PPS polymer is Fortron 214C1 PPS. The PEEK-based materials are Cetex® TC1200 AS4 12K UD material (146 g/m^2 / 34% RC) and T300 3K 5HS satin weave fabric material (280 g/m^2 / 42% RC)

4.2 Safety concerns

There are risks associated with working with any nano-scale materials such as the VACNTs used in this project. The primary concern is that the materials which are in the order of several nm in diameter and 10-100µm in length, may become airborne and be ingested or inhaled. As such, all operations where the VACNTs are exposed to the open-air during impregnation and consolidation are performed in enclosed areas such a fume hood or glove box. Additionally, precautions such as the use of N100/P100 particulate masks, eye protection, and latex gloves are used when handling VACNT materials that have not been embedded in some form of the polymer substrate. For testing where material fracture occurs, standard composite safety precautions was used for fractured material. It is assumed, based on industry convention, that any CNT materials embedded in a polymer before testing, will remain constrained in the polymer during fracture and does not pose any health risks.

4.3 Embedding

The process of embedding of VACNTs into PPS CF/TP material within this project centers around the use of VACNTs which are grown on a thin SS substrate and pressing them, under heat and pressure, against the composite materials. Through this process the VACNTs, which are loosely held

to the substrate are transferred to and meant to be held in place by the TP resin matrix on one side of a single CF/TP composite ply used for the embedding. It is hypothesized that VACNTS will be able to be embedded into PPS CF/TP materials to some extent, but it is unknown as to if the orientation of the VACNTs can be maintained and if there will be a high level of transfer from the substrate to CF/TP materials. As noted previously in section 3.1, for the embedding process a range of pressures from 0.5 to 10bar will be examined at temperatures of 100^0C, 150^0C, 200^0C, and 320^0C. This is done to obtain an understanding of how pressure and temperature impact the embedding and transfer of VACNTs to TP composite materials. Three embedding specimens were planned for each combination of pressure and temperature. An overview of the embedding process which was performed is shown in Figure 13 for clarity.

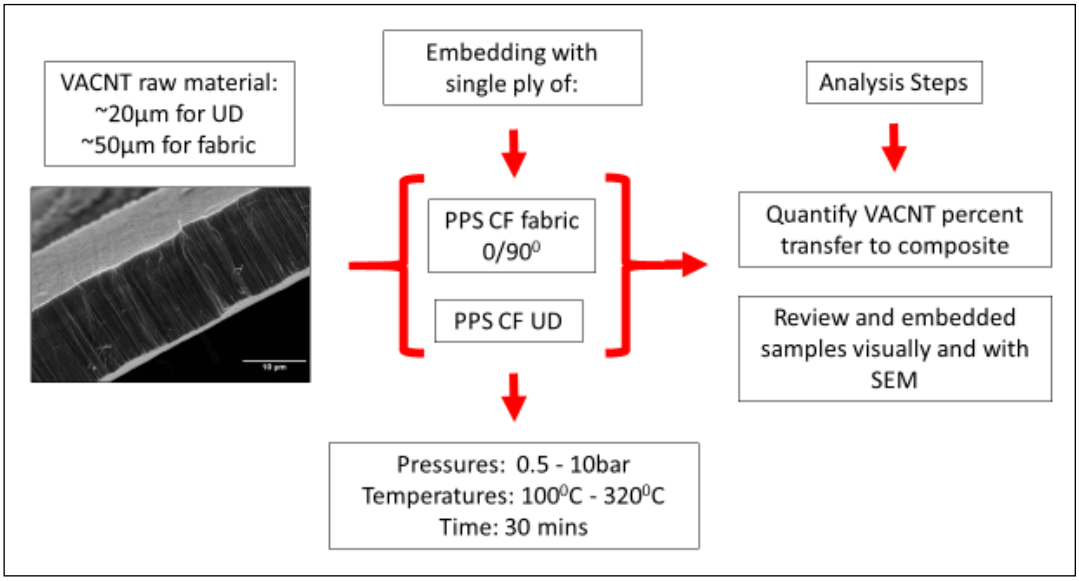

Figure 13 – Flow diagram - Embedding of VACNTs into PPS composite materials

4.3.1 Specimen Preparations

The preparation method of the test specimens used for the embedding process consists of preparing both the composite materials and the VACNT material, as it is attached to its substrate, and combining them to be pressed together with heat and pressure.

Several preliminary embedding tests were performed on PPS UD and fabric materials using the Votoch 60/60 high-temperature oven located within the DASML in the lead up to the final description for specimen preparation detailed below. This process consisted of using the oven for heat input and the use of a variety of weights placed atop the specimens to press the VACNT materials into the TP materials. This method was originally chosen since it would allow for the use of small specimen sizes of composite material (50mm x 50mm) and provide for easy testing of various low-pressure applications. A variety of tests consisting of a range of pressures and specimen preparation techniques were performed. These included the use of vacuum bags to surround the specimen and apply pressure, high-

temperature silicon rubber caul plates, and larger 100mm x 100mm composite specimens. It was determined from these tests that the small 50mm x 50mm composite specimen sizes did not provide adequate area for proper embedding. Furthermore, the final condition of the PPS polymer was found to turn brown during processing, which was believed to be due to edge effects of degradation of the PPS with oxygen occurring in the small specimens. Testing of larger 100mm x 100mm sized specimens was next trialed. Moving to the larger specimen size meant that larger weights would have to be used which became unwieldy inside the oven. This, in turn, pushed to the abandonment of the use of the oven for heating the specimens and to the adoption of the heated platen press for the embedding testing with larger 250mm x 250mm specimens. The 250mm x 250mm size was chosen such that it permits an adequate surface area to distribute pressure for the heated platen press that is used for the embedding and consolidation of specimens. The press that is used is a Joos brand press, model LAP 100, heated platen press with a 1000kN maximum capacity. The lower limit of applied force was measured by the use of a calibration loadcell to be roughly 5kN. This would equate to over 50 bars of pressure for a specimen of 30mm x 30mm as it used for testing of the VACNT per test and was deemed unacceptable for the testing. By utilizing a larger specimen size of 250mm x 250mm for the pressing, distributed pressures of as low as 0.8 bar can be achieved. The larger specimen size also was thought to allow for any edge effects, such as oxidation or resin flow-out from the CF/TP composite material, to not impact the area in the center where the VACNT embedding takes place.

The VACNT material, as supplied on the SS substrate, was cut and prepared into 30mm x 30mm (+/- 1mm) square sections. For working with 30mm wide VACNT materials, sharp industrial scissors were used to cut the long strips into 30mm long sections to allow for clean cuts of the SS substrate. For the wider 380mm wide VACNT materials, an industrial plate shear was used to cleanly cut the SS substrate into 30mm wide by 380mm long sections, which are then similarly cut into 30mm long sections with the aforementioned scissors.

For the placement of the VACNT sections onto the composite specimens to the backside (non VACNT side) of the substrate, two ~5mm x 5mm sections of polyimide (PI) adhesive tape are attached to the corners of the specimen as shown in Figure 14. These will be used to hold the substrate material to the composite section while the assembly was transferred into the press. The 30mm x 30mm VACNT substrate was placed by hand in the center of the 250mm x 250mm composite specimen, and the sides of the PI tape were lightly pressed down to keep the VACNT substrate specimen in place. Care was taken not to press down on the substrate at this time and possibly disturb the VACNTs on the front side of the substrate.

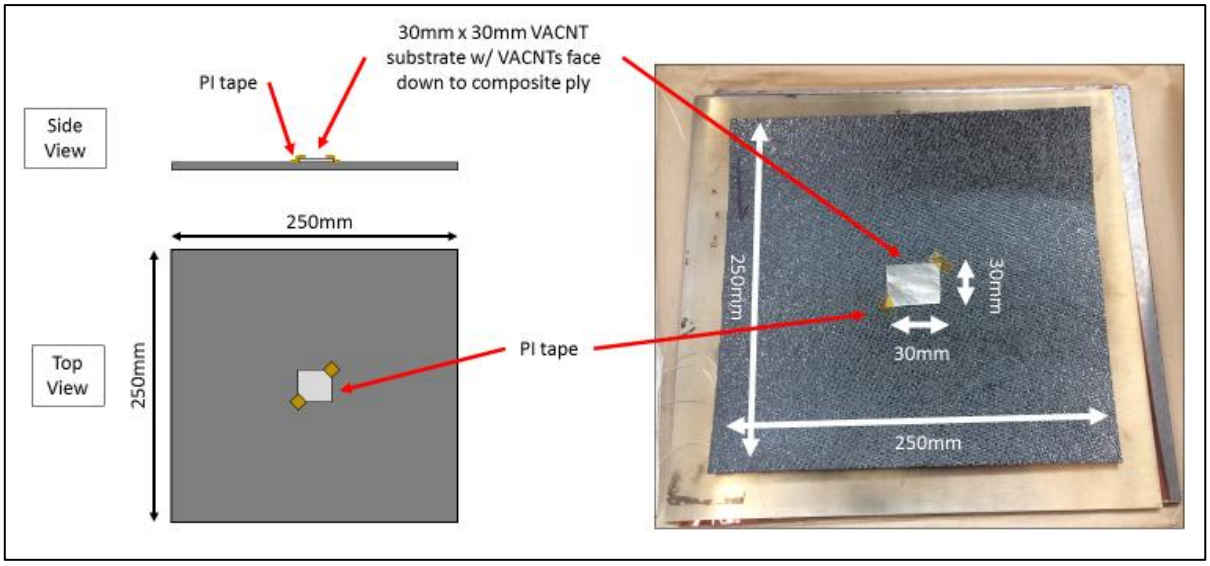

Figure 14 - Embedding specimen layout side and top view

4.3.2 Processing Procedure

As mentioned in the previous section, single layer TP specimens measuring 250mm x 250mm with VACNT materials attached to the center of the specimen are embedded with the application of heat and pressure. Two different methods of applying pressure are used depending on the level of pressure needed for the particular embedding process. For tested pressures ranging at 0.5bar, the lower platen of the platen press is used as a heated surface upon which a vacuum bag surrounds the composite specimen to compaction pressure to the specimen. For tested pressures ranging from 1bar and up to 10bar the platen press is used to clamp and apply compaction pressure and heat to both sides of the composite specimen.

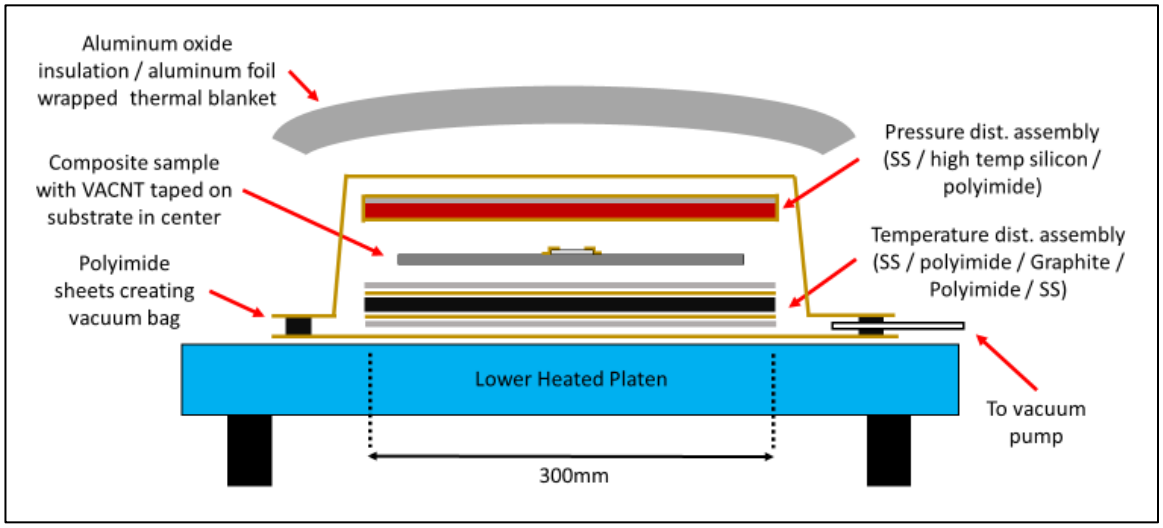

Figure 15 - Vacuum assisted press layout for embedding process 0.5 to <1bar

In Figure 15 the layout of the vacuum-assisted method for pressure application for 0.5bar is shown. The temperature distribution assembly is used on the bottom as shown to aid in the equal distribution of the temperature inputs from the platens of the press to the specimen. The pressure distribution assembly is used to aid in the uniform pressure distribution across the entire 250mm x 250mm composite specimen and any irregularities which are present by the slight height difference of the VACNT substrate compared to the surrounding composite material. A fiberglass thermal blanket made of 50mmm thick aluminum oxide insulation and wrapped in 0.07mm thick aluminum foil was constructed to roughly a 300mm x 300m total area and placed on top of the assembly to limit the loss of heat from the top of the vacuum bag assembly.

In Figure 16 the press layout of the method for pressure application from >1 to 10bar is shown. The organization of the material used for the pressing includes the same temperature distribution assemblies, a pressure distribution assembly, and PI film sheets to protect the surfaces of the press platens as in the vacuum-assisted method described previously. For the arrangement of the materials into the press, the composite specimen with the pre-applied VACNT substrate material is gently slid into to the center of the 300mm x 300mm lower temperature distribution assembly as shown in Figure 17. Care is taken as not to touch, shift, or shear the VACNT substrate taped to the top of the composite material which would possibly disturb the vertical orientation of the VACNTs. The pressure distribution assembly is gently placed by hand on top of the composite specimen, again as not to disturb the VACNT specimen, followed by the uppermost temperature distribution assembly.

For detailed information about the materials and steps used for the embedding processes reference Appendix A.

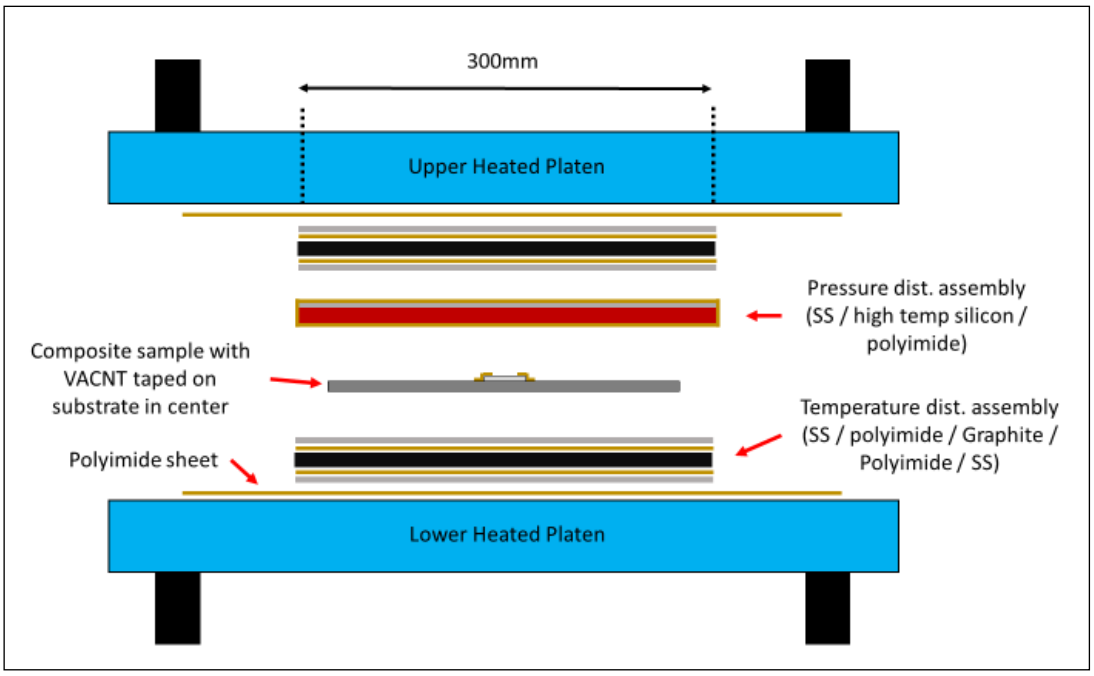

Figure 16 - Press layout for embedding process >1 – 10bar

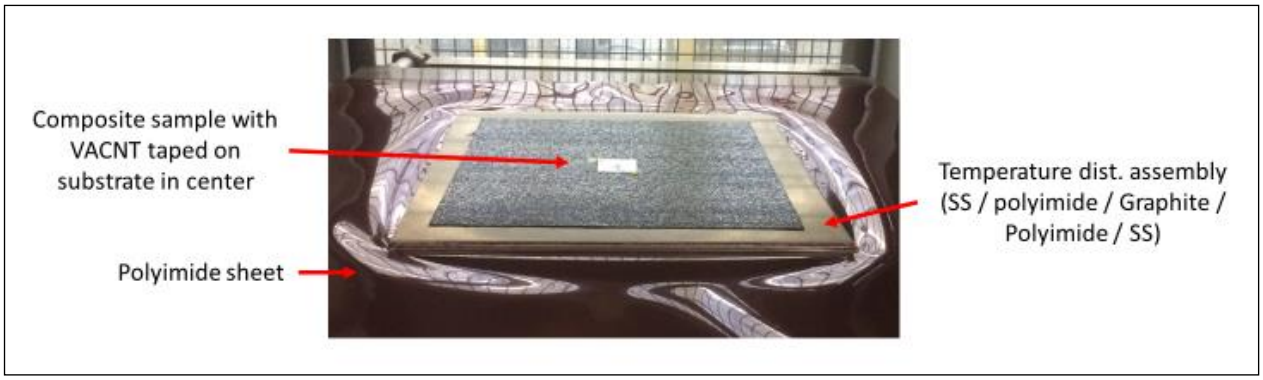

Figure 17 - Composite specimen placed on lower temperature distribution assembly

An example of the requested temperature and pressure profile of the embedding cycle is shown in Figure 18. The temperatures for embedding and reasoning for their use were previously mentioned in section 3.1. The temperature and pressure cycle were configured such that the maximum pressure that was indicated for the test, ranging from 0.5 to 10bar was applied only once the temperature set point as recorded from the internal thermocouples in the platen plates of the press has been reached. The application of pressure to the specimen was applied first by just light contact pressure. This style of simple temperature profile was chosen due to the limit the embedding process to a single pressure and reduce the number of variables for the experimentation.

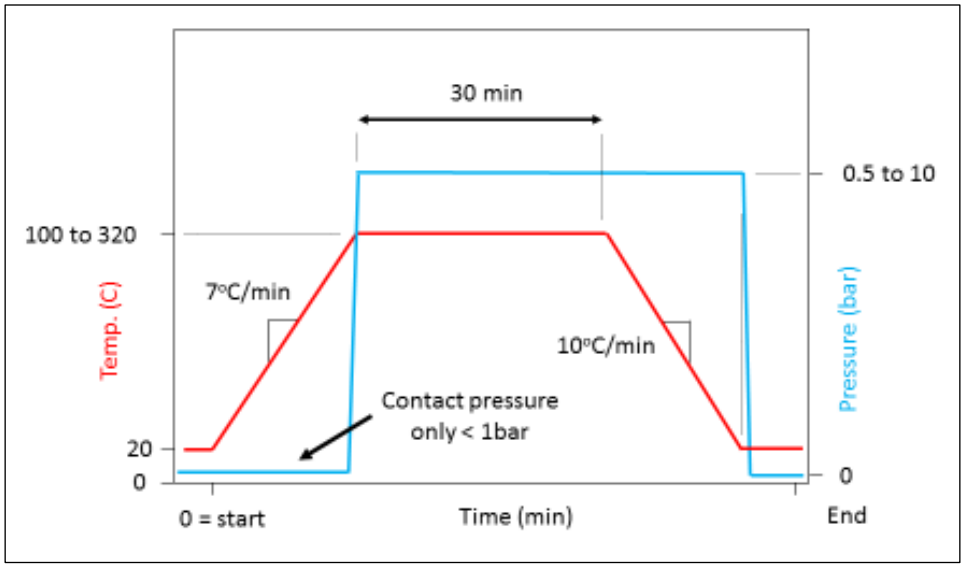

Figure 18 - Example temperature/pressure/time profile for the embedding process

After each specimen has been completed its embedding cycle is it removed from the press and transferred to a workbench. The embedded 250mm x 250mm specimens are cut down to roughly 100mm x 100mm centered about the area of the embedded VACNTs. This is done since the exterior composite materials are not needed for further analysis or testing and it makes the specimens easier to handle and examine. Lastly, the VACNT substrate is removed from the composite specimen using a

razor blade by peeling back one corner of the VACNT substrate carefully and removing the substrate by hand, taking care to handle the substrate by the edge as to not disturb any remaining VACNTs.

4.3.3 Analysis

The examination of the specimens following the embedding process consists of several steps including

1) Photographing overall composite specimens after the embedding process and indicating the condition of VACNT transfer region.
2) Photographing of the VACNT substrate surface which was in contact with the composite during the embedding process.
3) Quantification of the percentage of VACNT remaining on the substrate with *ImageJ* processing software.
4) Sectioning of the VACNT transfer region and qualitative examination by SEM to review the morphology of the VACNTs
5) Photographs of both sides of the composite (single-ply) specimen with embedded VACNTs are taken to record the overall resulting state of each specimen. Any remarkable or extraordinary features are noted such as visible voids, dry spots, or other anomalies.

Proper visual documentation via digital photography of the VACNT substrate surface was of critical for the analysis step. In this step, the percentage of remaining VACNTs on the surface was used as a tool to quantify the entire transfer of VACNTs during the embedding process.

Utilizing a Coolpix brand P600 digital camera, close up macro digital images of the resultant SS substrate surface, which initially contained VACNTS, were taken. Using *ImageJ* processing software, a calculation of percent area of remaining VACNTs on the SS substrate material can be made. The software allows for the digital conversion of the remaining VACNTs into a black and white contrasting image, and from that, a percentage of VACNTs remaining was made. For further information on the steps of this imaging process reference Appendix B. Shown in Figure 19 are VACNT examples from both a fabric and UD composite specimens, their corresponding black and white converted image, and percentages of VACNTs transferred.

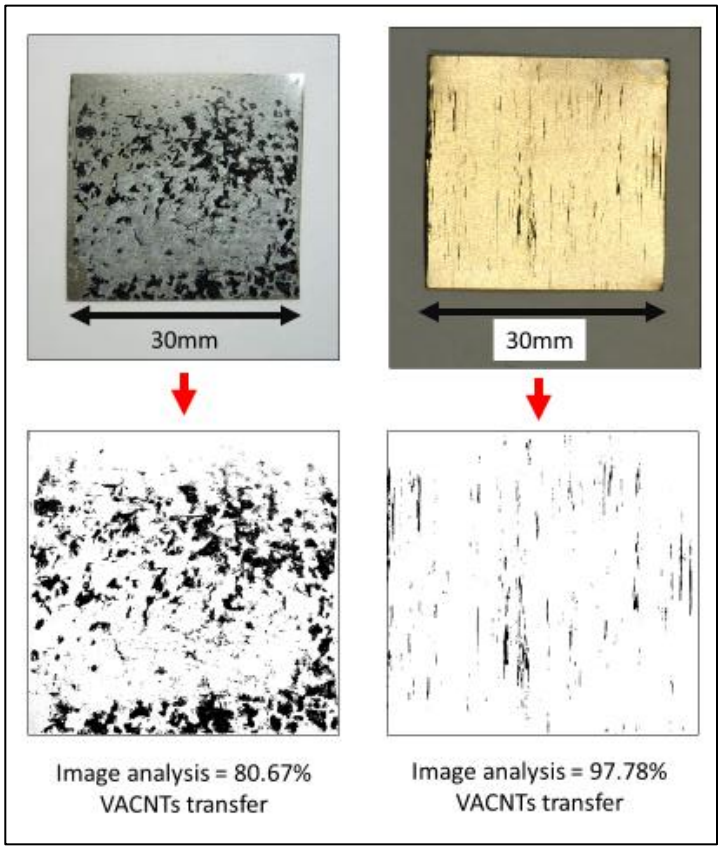

Figure 19 - VACNT substrate percent transfer analysis – 320^{0}C and 10bar (Fabric) / 5bar (UD)

Each composite specimen was then sectioned by hand with standard fabric scissors into six sections across the 30mm x 30mm of the VACNT embedding as shown in Figure 20 to be examined with SEM used for the previous observations. Through this investigation, a sampling of the qualitative condition, orientation, and length of embedding of VACNTs into the TP composite materials was made. Note that all surfaces of the six sections were not examined in this step. However the cut faces provide several cross-sectional surfaces to examine the location, condition, and orientation of any embedded VACNTs in the composite specimens.

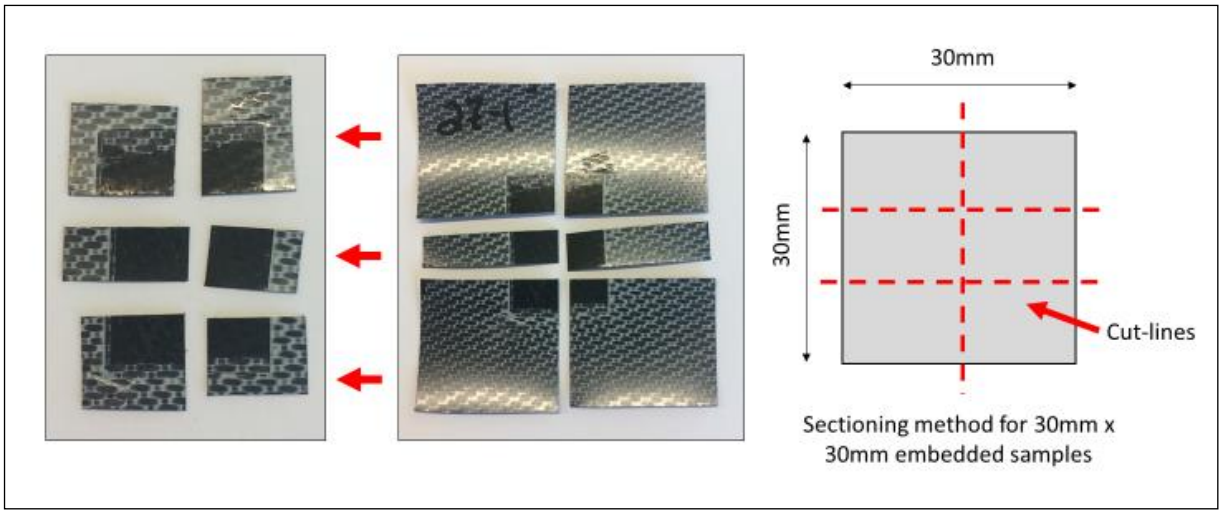

Figure 20 - Sectioning of VACNT area of embedded specimens

4.3.4 Results / Discussion

The results of the embedding processes with VACNTs and PPS UD and fabric materials are discussed herein succession. Note, that the embedding tests at 0.5bar of pressure for 150 and 200^{0}C for either the UD or Fabric specimens were not tested and hence not shown in the following figures. This was chosen after first embedding specimens at 100^{0}C and 320^{0}C and observing that the resultant transfer percentages at 0.5bar were deemed too low to be viable to continue testing with.

Shown in Figure 21 is the average percentages of the VACNTs transferred to the UD CF/TP specimens, from this it can be seen that with less pressure and temperature there are fewer VACNTs transferred to the UD composite materials. An example of this resulting transfer percentage versus a range of embedding pressure for UD materials is shown in Figure 22. An interesting byproduct of the embedding was that the VACNTs remaining on the substrate follow the pattern of the UD composite material which could indicate that the UD materials are not completely flat to start. Similar transfer patterns were observed for the other UD specimens tested at the other temperatures.

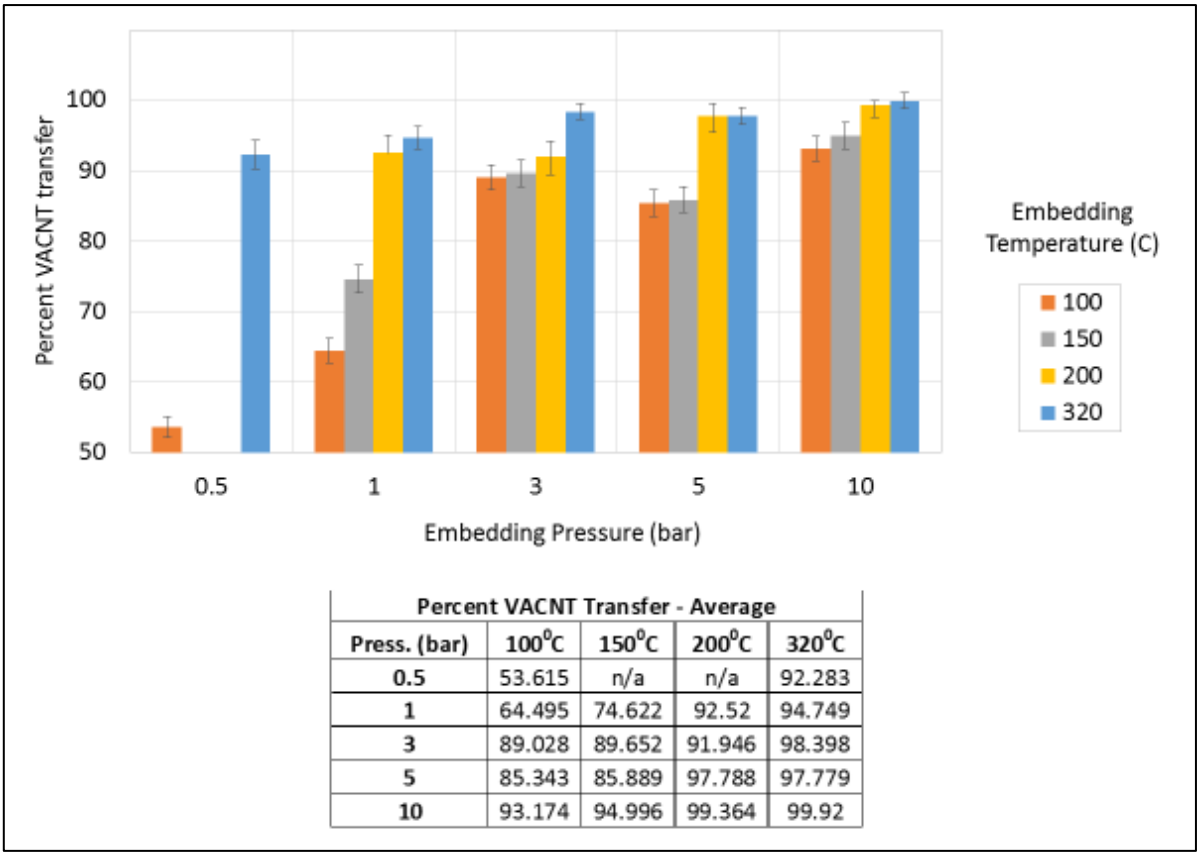

Percent VACNT Transfer - Average				
Press. (bar)	100°C	150°C	200°C	320°C
0.5	53.615	n/a	n/a	92.283
1	64.495	74.622	92.52	94.749
3	89.028	89.652	91.946	98.398
5	85.343	85.889	97.788	97.779
10	93.174	94.996	99.364	99.92

Figure 21 - Average percent VACNT transfer – UD

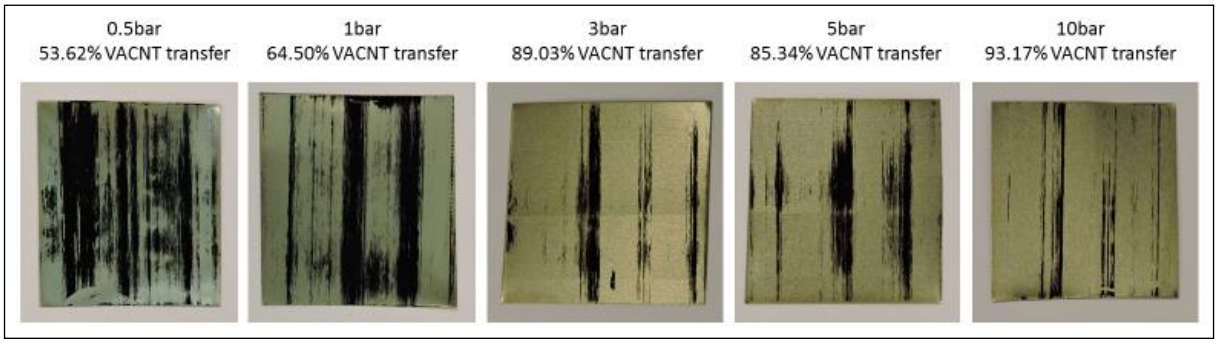

Figure 22 - VACNT substrate for varying pressures after embedding at 100°C with UD

To understand better why this correlation of pressure and temperature to the percentage of VACNTs transferred was occurring, qualitative observations were taken with an SEM to look at the surfaces of the VACNTs and the interfaces of the VACNTs to the composite materials. For low applied pressures of 0.5 and 1bar there appeared to be very little physical embedding of the VACNTs into the polymer surfaces for both fabric and UD materials. This was supported by the increase in the percentage of VACNTs left on the substrate as compared to higher pressures. A picture of this minimal degree of embedding of the VACNTs into the polymer can be seen in Figure 23. This qualitative review of the materials shows that the low embedding temperature most likely only allowed the PPS to become slightly viscous or tacky enough to allow some adhesion of the VACNTs. While there was a low amount

of embedding of the PPS into the VACNTs seen, the orientation of the VACNTs was largely seen to be intact with little to no buckling of the VACNTS and was similar to that found on the virgin material as seen in previously in the right-hand section of Figure 10.

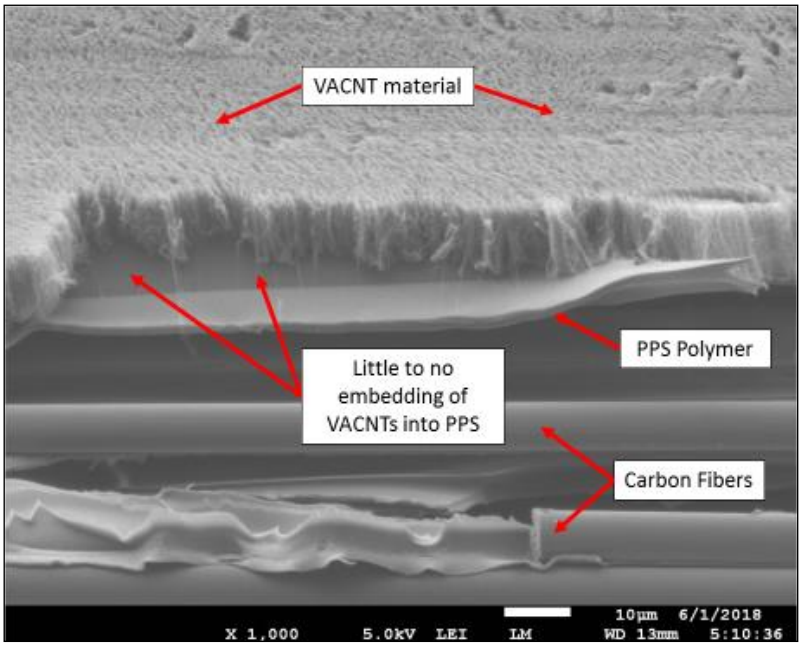

Figure 23 - VACNT interface region on UD - 100^{0}C at 0.5bar

Review of the embedded specimens via SEM techniques at higher pressures up to 10 bar, shows locations of a higher degree of embedding of the VACNTs into the PPS polymer, but with more matting and buckling of the VACNTs overall, as shown in Figure 24. This observed matting and buckling of the VACNTs follows with the logic that with increasing pressure, the VACNTs will be more likely to buckle under the applied load.

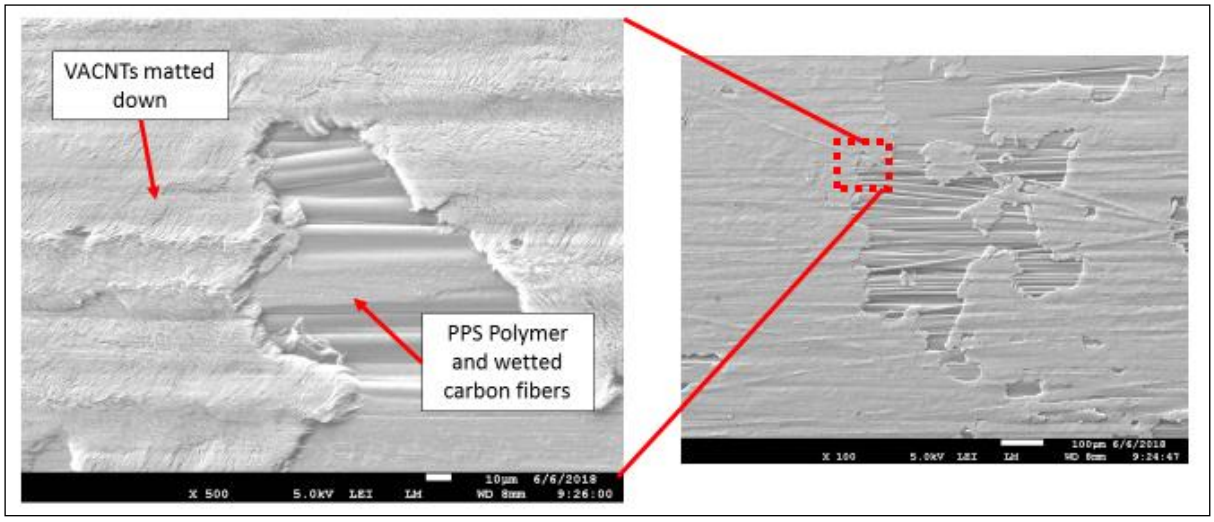

Figure 24 - VACNT interface region on UD - 100^{0}C at 10bar – 100x and 500x magnification

Examinations of embeddings at higher temperatures showed similar trends in embedding and buckling of VACNTs as with those shown for 100^0C embeddings. One distinct change in the conditions and percentage of transfer of VACNTs was seen in specimens embedded at 320^0C at pressures of 0.5 to 1bar. With these parameters, the VACNTs were shown to be mostly fully embedded into the UD material with good wetting with the PPS polymer. In some instances, it was seen that at film of PPS would form on the top side of what was largely unbuckled or matted VACNTs as seen in Figure 25.

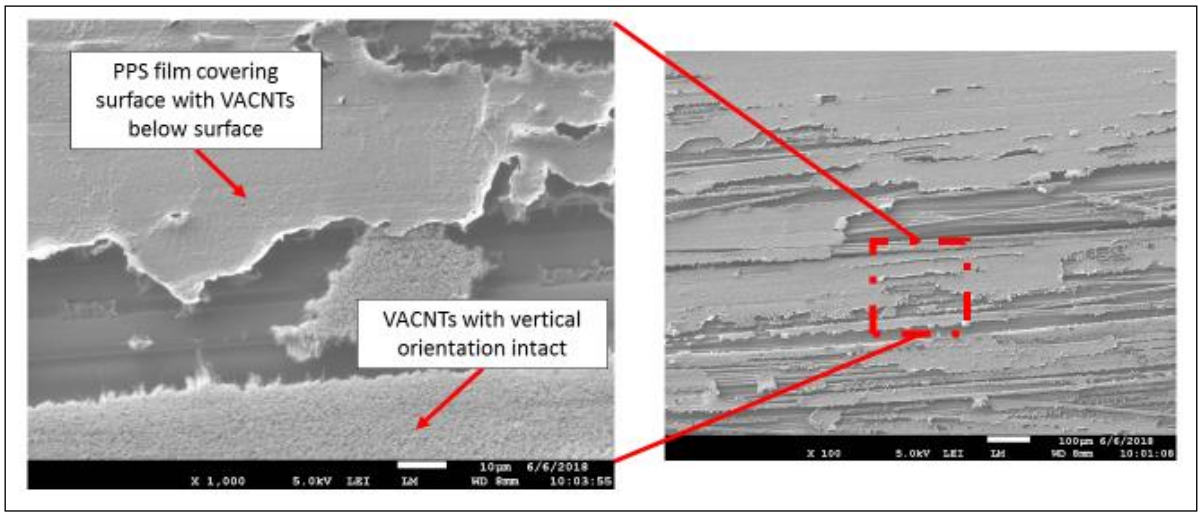

Figure 25 - VACNT interface region on UD - 320^0C at 1bar

The composition of this film was determined to be PPS polymer through the electron dispersive spectroscopy (EDS) functionality of the JEOL SEM used for the previous observations. Five areas of specimens that contained the film were analyzed, and it was observed that in the areas where the film is present presented heavy concentrations of sulfur were present, whereas in areas of the VACNTs showed heavy concentration of carbon. An example of this is analysis is shown in Figure 26 where the sulfur-rich regions in blue are thought to be the sulfide component PPS polymer and the carbon-rich regions in red are thought to be the carbon from the VACNTs. A subsequent check of the as-removed substrate from specimens processed at the same process parameters, which both did and did not show the film, was performed and no large-scale sulfur concentrations were detected. This leads to the conclusion that PPS has melted and formed a skin on the surface of the VACNTs under the embedding parameters of 320^0C and pressures of 0.5 to 1bar. This film may present as a protective or constraining layer that may be beneficial for later consolidation with multiple layers be keeping the orientation of the VACNTs intact rather than if they are uncovered on the embedded surface.

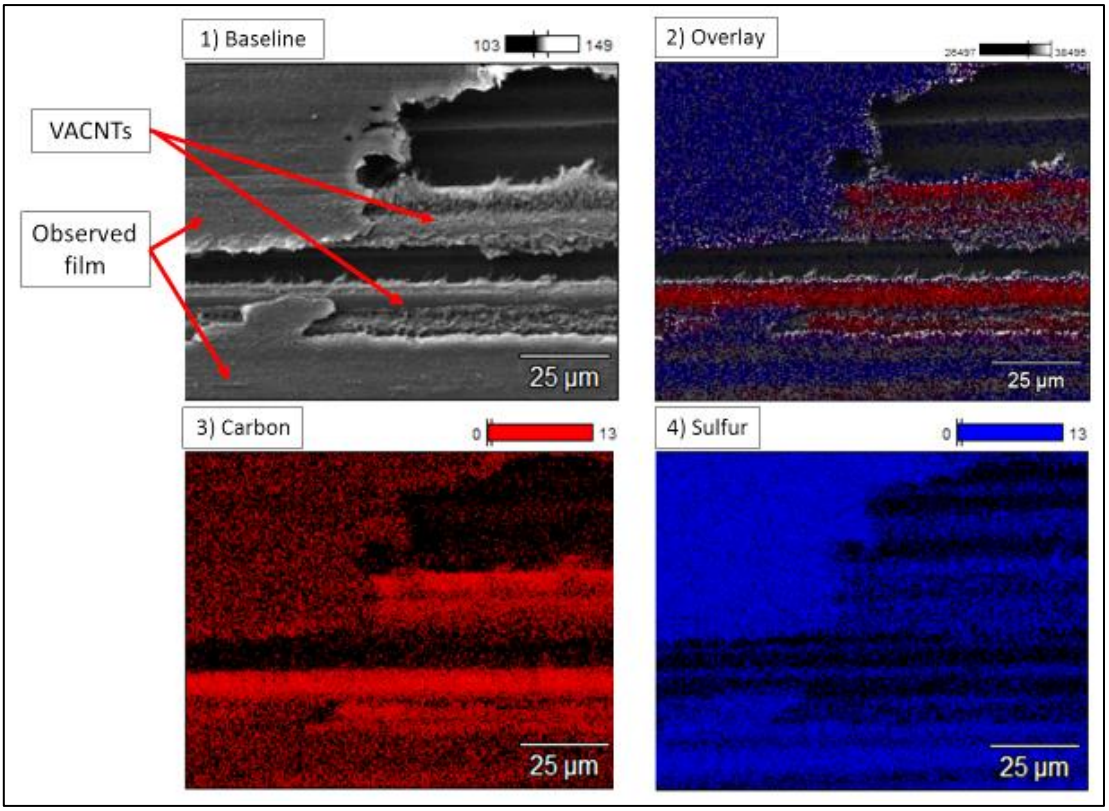

Figure 26 - EDS analysis of film

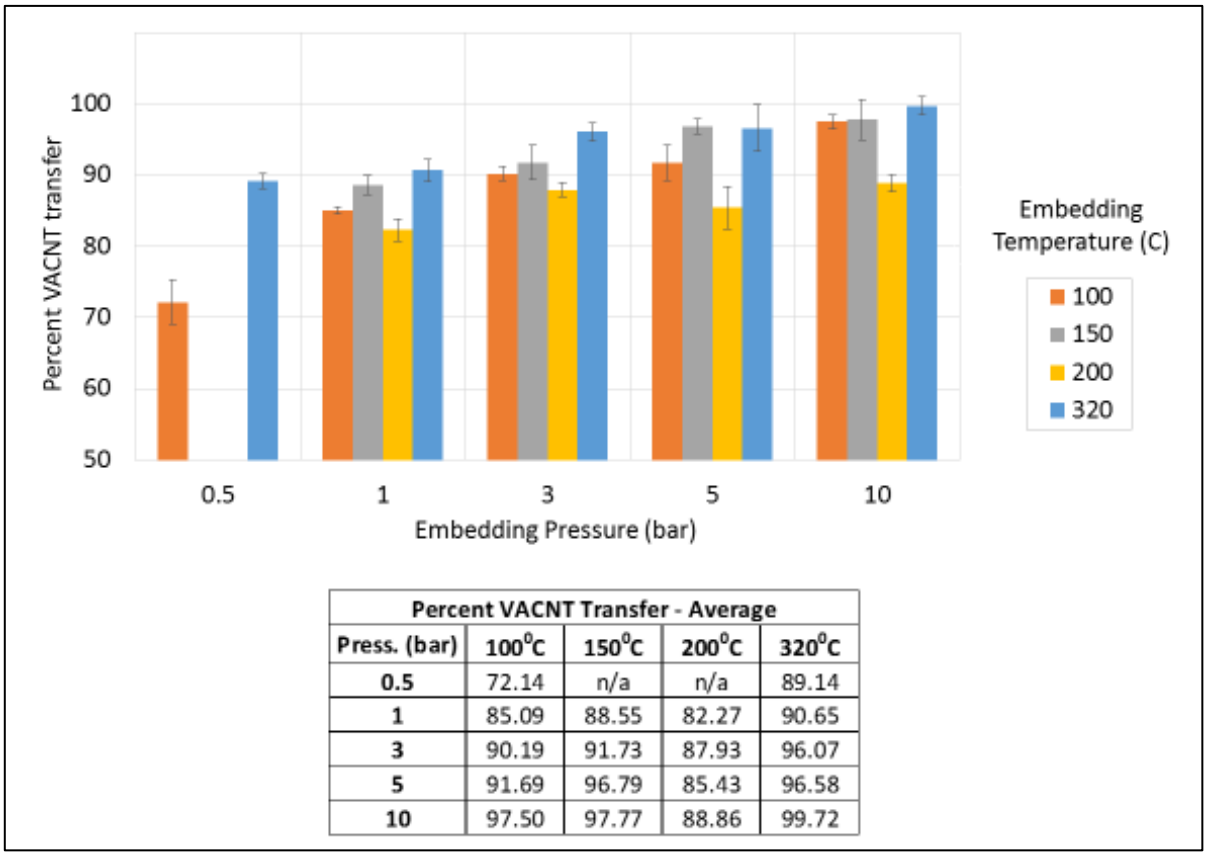

Percent VACNT Transfer - Average				
Press. (bar)	100°C	150°C	200°C	320°C
0.5	72.14	n/a	n/a	89.14
1	85.09	88.55	82.27	90.65
3	90.19	91.73	87.93	96.07
5	91.69	96.79	85.43	96.58
10	97.50	97.77	88.86	99.72

Figure 27 - Average percent VACNT transfer – Fabric

From Figure 27 a relationship between lower applied pressures and temperatures to lower percentages of VACNTs transferred to the fabric composite materials can be seen, similar to the UD materials discussed previously. An example of this relationship between transfer percentages versus a range of embedding pressure for fabric materials is shown in Figure 28**,** with similar observed for fabric specimens tested at other the other temperatures. The average transfer percentages for transfers at 200^0C as shown in Figure 27 are lower than that of the 150^0C and 320^0C, and the reason for this is not completely understood at this time. One interesting feature of the transfer patterns of the VACNTs with fabric is that a speckling of VACNTs was present which correlate to the high and low undulations of the fibers inherent in the fabric composite materials. This is similar to the linear patterns seen with UD materials as shown previously in Figure 22.

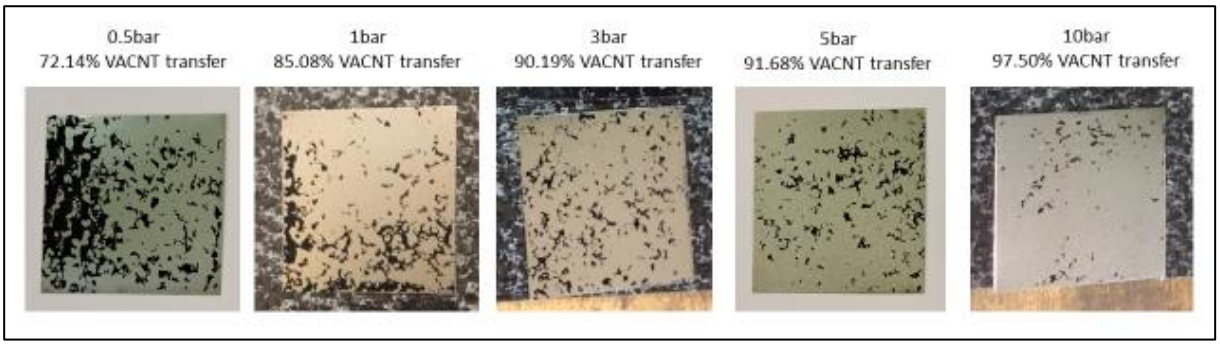

Figure 28 - VACNT substrate for varying pressures after embedding at 100^0C with fabric CF/TP

As with the UD materials qualitative observations were performed on surfaces of the embedded VACNTs with same JEOL SEM mentioned previously. It was found again, as with the UD materials, that with embedding temperatures below the 285^0C Tm of PPS there was little to no wetting of the PPS polymer into the VACNTs was seen. At the same time, the VACNTs were observed to retain much of their orientation without any noticeable buckling as shown in Figure 29. Similar buckling as seen with UD materials were seen in pressure above 1bar with increasing amounts of matting of VACNTs seen with increasing embedding pressure.

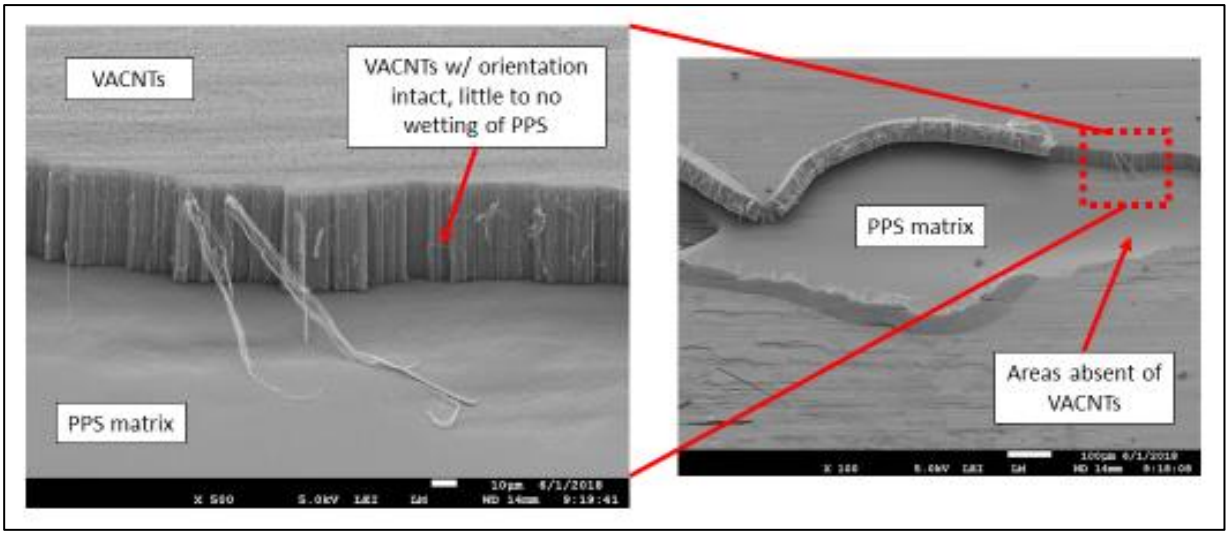

Figure 29 - VACNT interface region on Fabric – 100^0C at 1bar

One intriguing observation which was seen with both UD and fabric embedded materials was that at embeddings performed at 320^0C and 5 and 10bar, some white material was seen to adhere to the substrate during the embedding process. An example of this is shown in Figure 30. The presence of the PPS on the substrate was confirmed with the EDS functionality of the JEOL SEM used for the previous observations. The incidence of PPS on the substrate was plausible since the PPS at the 320^0C is above its Tm of 285^0C, but may indicate that more than enough time, pressure, and temperature (or a combination of the three) was used for the embedding process. As such, the use of high pressures of 5 and 10 bar at 320^0C will not be used in conjunction with further processing of embedding of specimens for mechanical testing later on in this project.

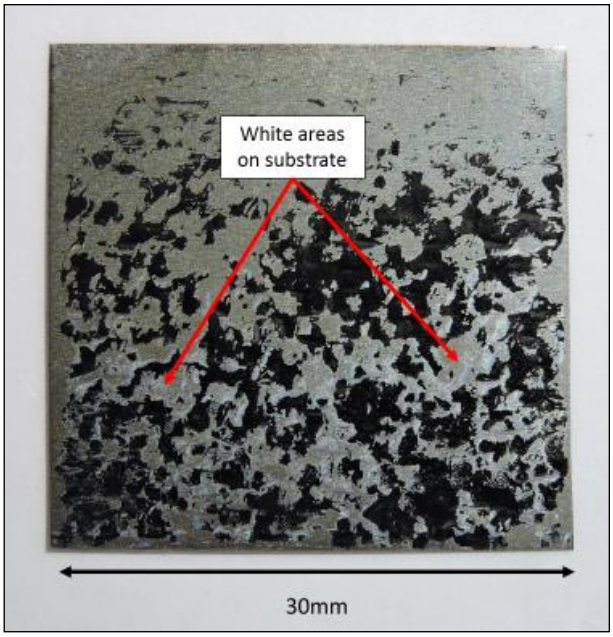

Figure 30 – VACNT substrate after embedding – 320^0C at 5bar

An observation related to the material handling more than embedding was found for both UD and fabric materials embedded at 320^0C. Specimens embedded at this temperature had a chance to melt and fully recrystallize upon cooling. The outcome of this was that for fabric specimens that consisted of a single 0/90 fabric ply the composite ply took a severely curved shape due to the un-symmetrical layup of the fabric ply. This proved to make the specimens difficult to process and also presented a challenge to try to work for the consolidation of multiple layers. From this finding, it was decided to not use 320^0C for an embedding temperature for further processing into multi-ply laminates investigated later in this project. Counter to this issue, UD specimens tended to show less of a tendency to split apart between UD fibers than those specimens embedded at 100^0C, 150^0C, and 200^0C due to the wetting of the fibers with the polymer matrix. This allowed the specimens to be handled without disturbing the UD ply and could prove to be useful for future consolidations of multiple plies.

Several key findings can be made from the results of the embedding. These finding for the embedding results, along with the respective temperature and pressure process parameters, will be used for further consolidation processes.

1) For both UD and fabric materials, with increasing temperature from 100^0C to 320^0C and pressures from 0.5 to 10 bar, there was a higher degree transfer from the substrate to the composite materials. This finding seems logical in that the viscosity of the PPS decreases and the *tackiness* of the PPS increases with increasing temperature allowing for a higher degree of VACNTs to become embedded.

2) As seen via SEM review of the post-embedded surfaces there seems to be a higher degree of matting or flattening out of the VACNTs with increasing pressures. Findings of other researchers using VACNTs with TS composites have found that matting of VACNTs at the interlaminar layer does not lead to a noted increase in interlaminar strength since the VACNTs cannot interdigitate with both composite plies on either side of the interlaminar region. With this finding in mind, it was chosen to use an embedding pressure of 1.0bar for further consolidation work within this thesis project. This pressure was selected over 0.5bar as 1.0bar was able to be easily produced with the available platen press without the added complexity of a vacuum bag setup that was needed for applying 0.5bar as described in section 4.3.1.

3) The embedding of ~50µm VACNTs with fabric materials leads to sporadic patches where no VACNTs are transferred, or areas of matting of the VACNTs occur. This is thought to be due to the undulations of the fibers in the fabric materials compared to the relatively flat nature of the UD materials.

4.3.5 Conclusions

Overall the hypothesis that VACNTs could be embedded into PPS TP/CF composite materials proved to be true. Embedding of VACNTs into UD materials proved to yield a higher qualitative degree of vertical alignment of the VACNTs due to the flat nature of the composite compared to that of fabric materials. Of the temperatures and pressures tested the process parameters of 200^0C and 1bar of pressure for embedding will be used for subsequent consolidation trials for both UD and fabric. This was chosen due to the high degree of transfer of VACNTs at this temperature and pressure and corresponding overall alignment of the VACNTs after embedding. Furthermore, the temperature was below that of the Tm of PPS and therefore left the composite materials still flexible and able to be easily handled compared to the fully consolidated nature of plies embedded at 320^0C.

At an embedding temperature of 320^0C and 0.5 and 1 bar of pressure a *skin* of PPS was shown to be on the surface of embedded VACNTs. While this set of parameters was not chosen for future consolidation work, it provides an interesting finding that the *skin* of PPS may protect the delicate nature of the VACNTs during subsequent consolidation and merits further investigation.

Lastly, while transfers of ~50µm VACNTs was shown to able to be accomplished at high degrees of transfer, the overall morphology of the VANCTs was seen to be highly matted and buckled at the higher pressures (3-10bar) needed to get a high degree of transfer. As such within this project, further in-depth work into the use of ~50µm VACNTs with PPS TP/CF fabric materials will not be studied outside of producing and constructing and testing mechanical specimens as described in section 5.

4.4 Consolidation

The process of consolidation consists fusing two plies of CF/TP composite materials with VACNTs pre-embedded on one side as shown previously in Figure 9 with the use of heat and pressure over a period of time. The consolidation process for this step was done to examine how the VACNTs at the interlaminar layer and their orientation react to the consolidation processes for PPS CF/TP composite UD and fabric materials. It is hypothesized that VACNTs, as embedded on one side of a composite ply, will be able to consolidated such that the VACNTs will have the majority of their vertical orientation intact and mimic that of consolidations seen by others with TS/CF composites. In total three specimens of each UD and fabric material were consolidated and examined for this qualitative assessment. An overview of the consolidation process which was performed is shown in Figure 31 for clarity.

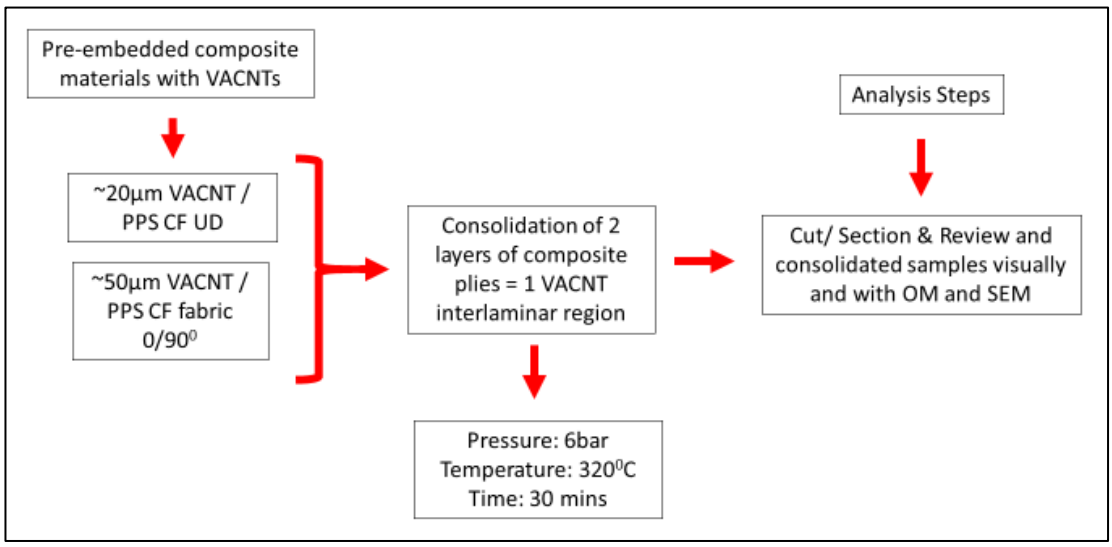

Figure 31 - Flow diagram - Consolidation of PPS composite materials

4.4.1 Specimen Preparation

The preparation of the test specimens used for the consolidating process consists of first embedding VANCT materials into PPS UD and fabric materials. Again, ~20µm and ~50µm VACNTs will be used respectively with the UD and fabric materials. The embedding parameters to be used for the specimens subsequently used for the consolidation process will be 200^{0}C, 1bar for 30 minutes as mentioned in section 4.3.4 and will follow the same temperature/pressure/time profile as indicated in Figure 18. UD and fabric specimens measuring 250mm x 250mm in size is used with 30mm x 30mm sections of embedded VACNTs in the center of the specimen.

The ply construction for the specimens is a three-ply (0/90/0) arrangement for UD materials and a two-ply $(0/90)_s$ for fabric materials to produce symmetric laminates. The layering of the composite plies was made with one ply having VACNTs embedded on the top side of the bottom-most ply to start with and the other layers placed on top. To keep the plies in place to prevent shearing during transit and the consolidation process they were spot-welded together in the four corners of the assembled plies using a Rinco RL35 hand-held ultrasonic welder.

4.4.2 Processing Procedure

The consolidation of the PPS CF/TP composite plies was performed on the same platen press and materials as used for the embedding process. The consolidation process was performed at 320^{0}C and 6bar for 30 minutes as mentioned previously in section 3.1 and follow the same temperature/pressure/time profile shown in Figure 18. A depiction of the consolidation process layout is shown for clarity in Figure 32. For detailed information about the materials and steps used for the consolidation processes reference Appendix A.

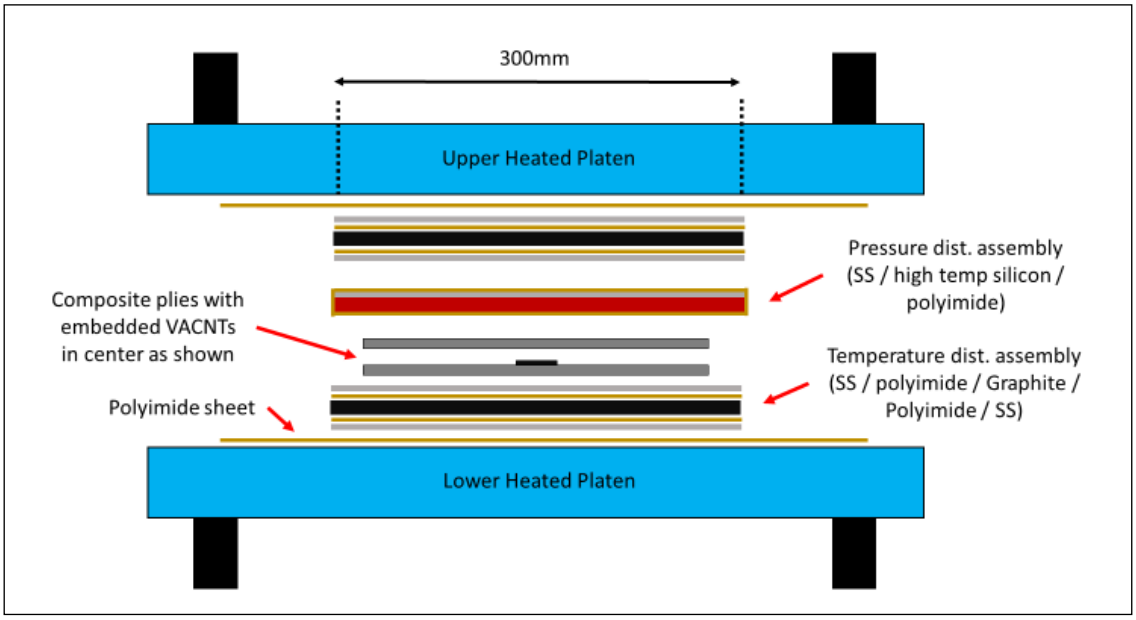

Figure 32 – Press layout for consolidation process 1-10bar

Upon removal from the press after consolidation, photographs and notes of the condition both sides of the specimen were taken. The 250mm x 250mm specimens were cut such that the center 100mm x 100mm area was retained for further analysis and the remaining material was discarded as indicated in Figure 33. This 100mm square specimen was further sectioned into specimens as shown to expose the cross-section of the composite material in the region where the VACNTs.

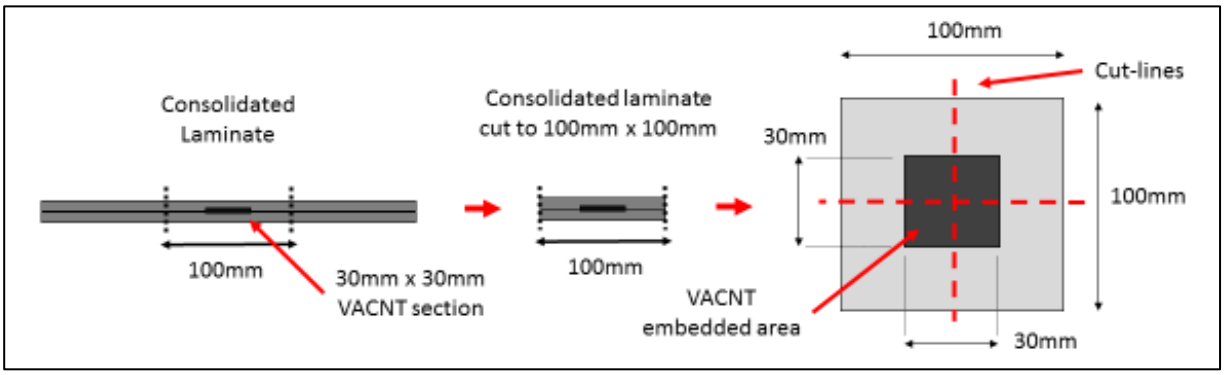

Figure 33 - Area to be cut from consolidated specimens for analysis

4.4.3 Analysis

The examination of the specimens following the consolidation process consists of several steps:

1) Mounting and polishing the cross-sectional specimens described in section 4.3.2. The specimens were polished to a 1µm finish using standard polishing equipment and procedures. Several etching techniques as noted in Appendix C were used as necessary to etch the polished surface with the goal of helping to visualize the VACNTs present.

2) A qualitative examination of the interlaminar region in areas with and without VACNTs using both a Keyence VHX-2000 digital microscope and the same JEOL SEM used previously. The location and morphology of the VACNTs was noted and recorded.

3) A quantitative measure of void and resin content of the observed specimens were taken using the same Keyence OM. The observed specimens were found not to have any noticeable voids. Using *ImageJ* processing software, for each of the three specimens three areas containing 0^0 fiber direction were analyzed for the percent of RC and recorded. This was checked to validate if the resulting consolidated materials have RC values on par with the manufacturer's recommended values listed in 4.1.

4.4.4 Results / Discussion

The results of the consolidation processes with VACNTs and PPS UD and fabric materials are discussed herein succession.

Shown in Figure 34 is a cross-section of a consolidated UD specimen observed with OM. Seen at 2000x magnification the initial ~20µm long VACNTs can be seen matted and buckled at the interlaminar layer between the 0/90 laminate interface as the darker grey area. These images are similar to other locations seen at the interfaces of the three specimens of UD consolidated specimens. While the orientation of the VACNTs is hard to make out their presence at the interlaminar layer can be seen with an average measure height of 10.2µm indicating matting and buckling of the VACNTs occurred.

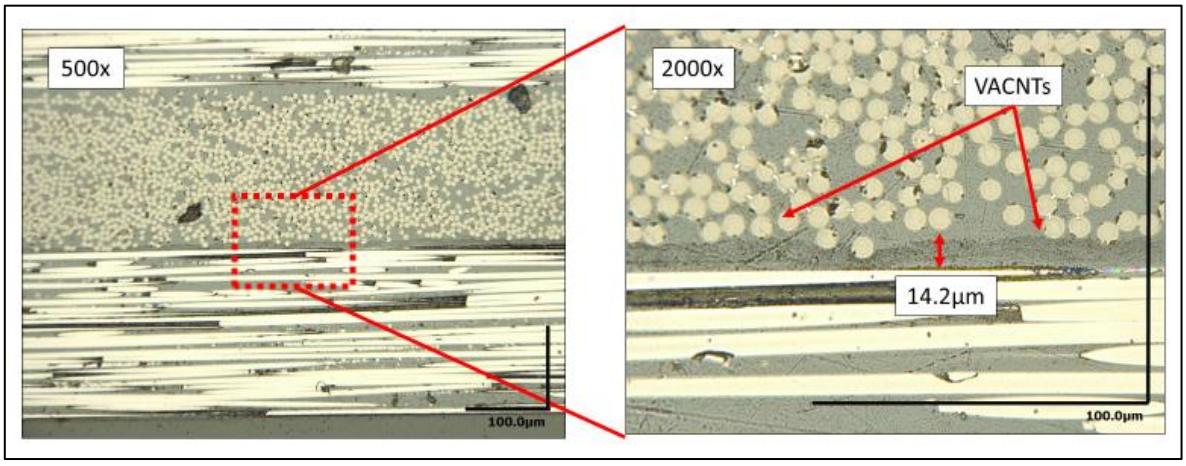

Figure 34 - VACNT interface region on UD - 320^0C at 6bar

Shown in Figure 35 is a representative cross-sections of a consolidated fabric specimen observed with OM showing the VACNTs both sandwiched between the tight fiber-to-fiber interface points as well as free-floating in the resin-rich areas. In resin-rich regions, shown in detail at 500x and 2000x magnification, the VACNTs can be seen to bunch and curl up with striations being able to be seen through the thickness of the VACNTs. The height of the VACNTs in this area was measured to range

from 15 to nearly 50µm, indicate that for the specimens, there is a range of matting or buckling of the VACNTs.

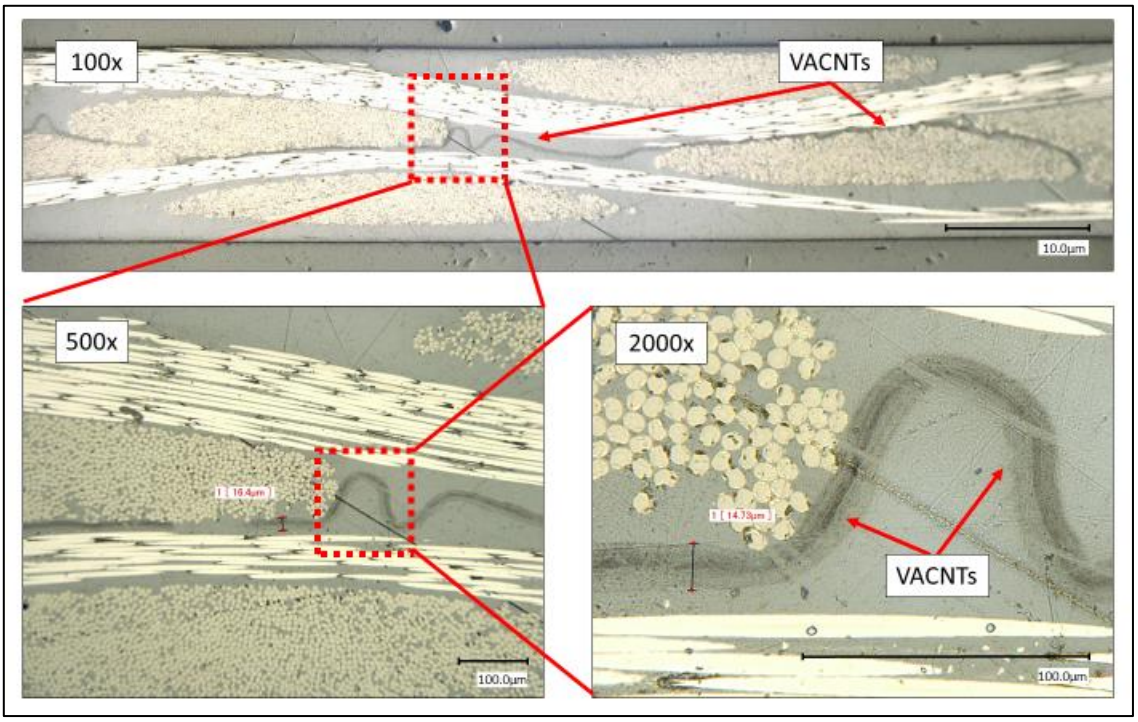

Figure 35 – OM images VACNT interface region on fabric - 320^{0}C at 6bar

The specimens of the consolidated fabric materials were further investigated with the SEM, and it was found, as shown in Figure 36, that the striations of VACNTS, similar to that seen in Figure 35, appear to be buckled VACNTs. When viewed with a SEM at a magnification of 50,000x and higher, the cut faces of the individual CNTs within these striations can be seen. This indicates that the striations seen in the majority of the OM reviewed UD and fabric specimens are indeed crushed, matted, or buckled VACNTs that have not retained the vertical orientation from their virgin state.

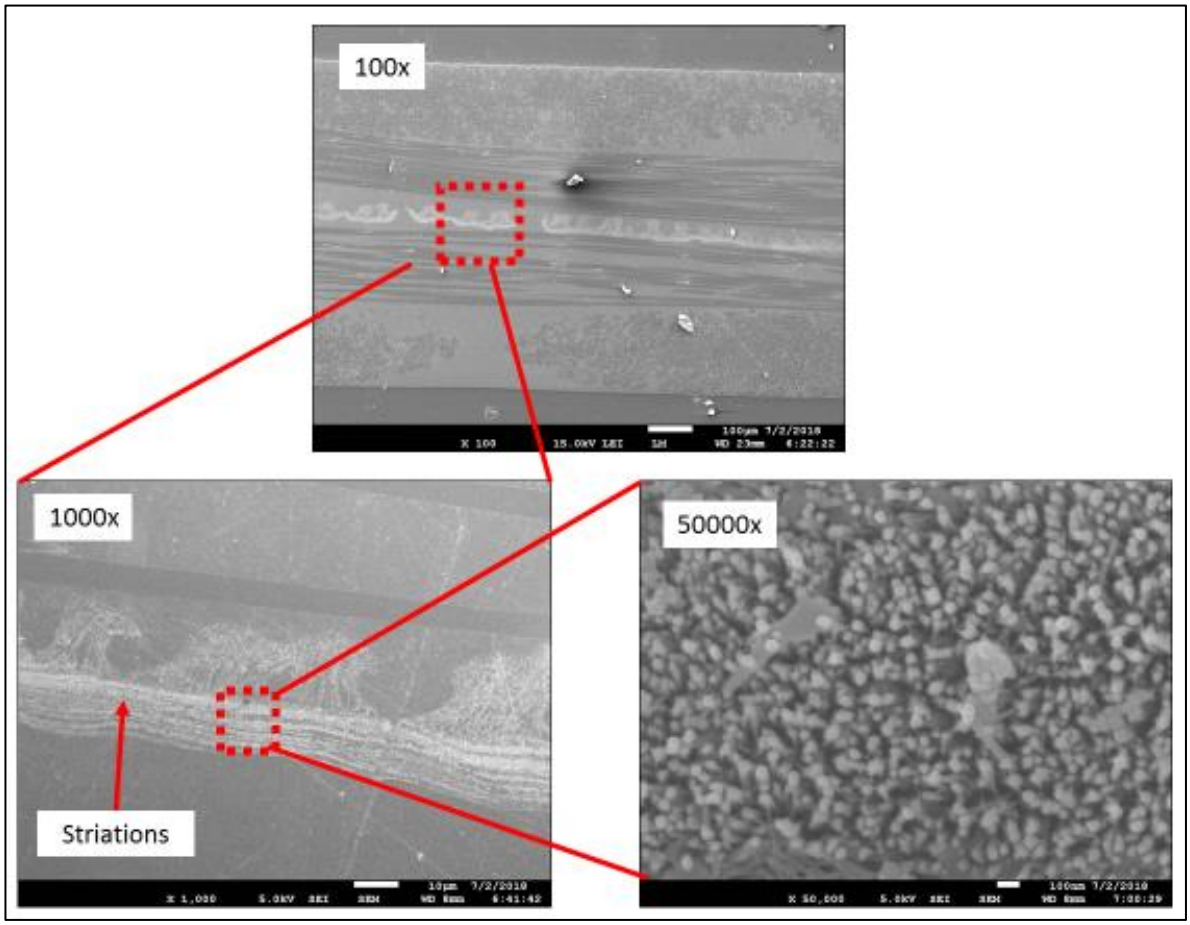

Figure 36 – SEM images of VACNT interface region on fabric - 320^0C at 6bar

From the photographs of the consolidated laminates, no discernable features could be seen on either the top or bottom surfaces. No abnormal squeeze-out of resin from either the UD or fabric materials was seen that would indicate that too high of pressure for the consolidation.

For both UD and fabric consolidation specimens, there were no visible voids observed within the consolidated specimens either the areas with or without VACNTs present. An averaged nominal value of the RC as a fraction of both types of materials was taken on areas of 0^0 fiber orientation similarly to that described in section 4.4.3. These results are listed in Table 1.

UD	Resin Content	Std. Dev		Fabric	Resin Content	Std. Dev
PPS w/ VACNTs	36.01%	2.56		PPS w/ VACNTs	47.64%	1.37
PPS w/o VACNTs	37.89%	2.96		PPS w/o VACNTs	45.16%	2.21
PEEK w/o VACNTs	35.83%	1.81		PEEK w/o VACNTs	42.67%	2.84

Table 1 - Resin Content values – Consolidation specimens

From the lack of voids present in the consolidated materials, it could be possibly concluded that the time spent at maximum temperature for consolidation is more than enough to permit adequate flowing of PPS resin. Possible shortening of that time or a combination of reducing the consolidation

pressures could result in VACNTs that retain some of their vertical orientation and would require further work to investigate properly.

In a review of the consolidated specimens for both UD and fabric materials, several key points can be observed. For UD materials the VACNTs were observed to able to be well placed along the interlaminar region, but do not mix well with the fibers of the composite materials. For fabric material, the VACNTs were observed to have floated away from their original embedded location and bunched up in the resin-rich zones of the consolidated fabric. In both UD and fabric material, where the VACNTs were seen coming in contact with fibers from the upper and lower plies (in most places for UD and at the bundle-to-bundle contact points for fabric) there was matting of buckling observed. These issues are thought to be caused by several possible reasons including the following.

1) The much higher viscosity of the PPS compared to the TS resins prevented good wetting of the polymer into the VACNTs. This may be an issue that is not able to be overcome and may be a barrier to similar embeddings with TP materials as seen with TS materials.

2) The application of light pressure in the initial part of the temperature and pressure profile as shown in Figure 18 while the resin was still at room temperature may have crushed or buckled the VACNTs. One solution to this would be to heat the composite materials to a higher temperature with no added pressure and then only once at the target 320^0C, additional pressure be applied.

3) Damage to the VACNTs between the embedding and consolidation processes may have occurred whereby the VACNTs were matted or crushed prior to being fully consolidated. While care was taken to eliminate any excessive touching of the embedded materials that were used to construct the consolidated specimens, further investigation of the processes would be needed to determine if this is a contributing factor to the matting and buckling.

4) The density of the VACNTs may not be sufficient to withstand the pressures needed for consolidation. Further work would be needed to determine if this is a contributing factor.

5) More time than necessary was used for the consolidation process. As noted previously, a shorter time at maximum temperature could be used, but would need to be investigated to confirm this.

6) The temperature and pressure of the consolidation may not have been properly paired to work with the VACNTs and the PPS composite materials to yield the hypothesized orientation of the VACNTs after consolidation. The process parameters used for the consolidation were based on the recommended parameters of the composite manufacturer. A further in-depth investigation

would be needed to examine if a lower range of pressures and temperatures would allow for consolidation with less matting, buckling, and shifting of the VACNTs as was observed.

4.4.5 Conclusions

Overall the hypothesis of if VACNTs could be consolidated was roughly half fulfilled. While the VACNTs did not appear to present a barrier to consolidation, in neither UD or fabric materials were the VACNTs observed to largely maintain their perpendicular orientation to the fibers of the composite plies tested. As mentioned, several reasons for this were listed from which one or more distinct or related factors be the cause of this.

Given that the scope of this project did not permit an in-depth investigation of the temperatures, pressures, and time spans of consolidation to be performed. The same process parameters used for the further consolidation of multi-ply laminates will be the same as used for the consolidation examination used in this section of the project. It is hypothesized that the similar matted and buckled condition of the VACNTs will be replicated in multi-ply laminates, which may have a detrimental impact on the mechanical properties of the to-be-tested specimens.

5 Mechanical testing

The second primary objective of this project was to investigate what, if any, influence VACNTs have at the interlaminar layer of PPS CF/TP composites. To evaluate this several mechanical tests were chosen for this project. As noted in section 3.2 the tests used will focus on measuring the ILSS, compressive strength, fracture toughness with the use of SBS, CLC and MPT tests respectively. All testing was performed at ambient room temperature and humidity. The SBS testing will be performed first and followed by CLC. Both of these tests will both be performed within the DASML at the Technical University of Delft. The MPT testing will be done last at the at the University of Twente.

Following each type of mechanical tests, analysis of the failed specimens was performed using, visual inspection as well as OM and SEM techniques to understand what impact the VACNTs have on the fracture mode of the specimens. Control specimens consisting of PPS and PEEK composite materials without VACNTs at the interlaminar layer were prepared and tested alongside the PPS with VACNT composite to compare against. The number of specimens tested for each type of material per each mechanical test are listed in Table 2. A workflow of the testing steps and procedures which were performed is shown in Figure 37 for clarity.

Test	Specimens tested per material type
SBS	25
CLC / MPT	5

Table 2 - Specimens to be tested

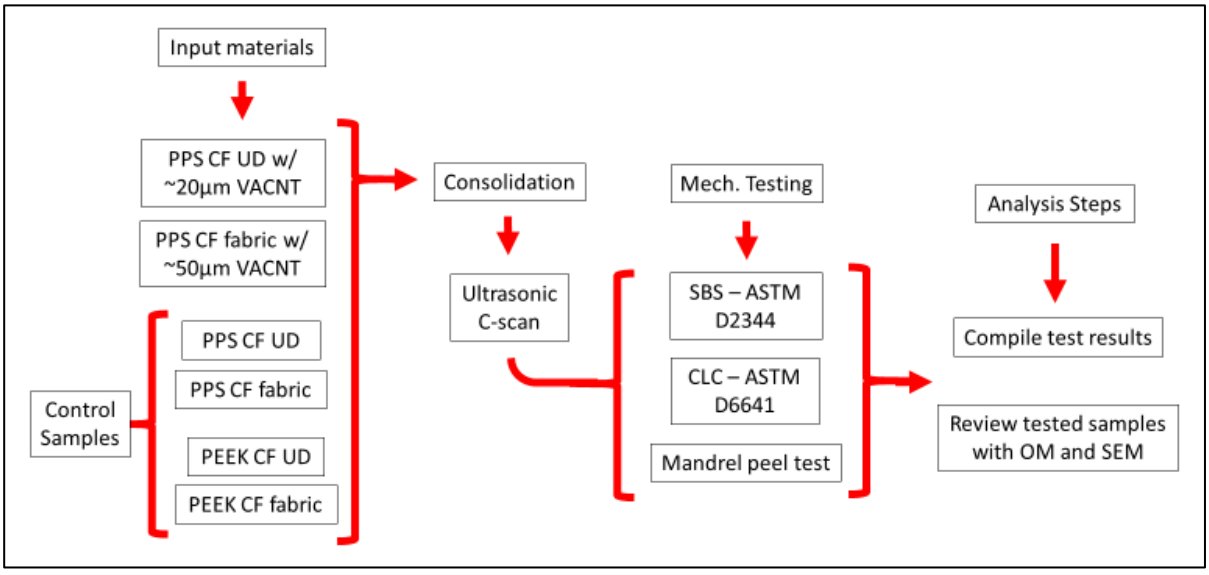

Figure 37 - Flow diagram – Construction and Testing of Specimens

Based on the observed matting, buckling, and flowing of the VACNTs in the UD and fabric consolidation specimens if a similar morphology is present in the constructed specimens, it is

hypothesized that there would be little to no impact on the mechanical properties since there would be no bulk orientation of the VACNTs across the interlaminar region. Alternatively, if a high level of vertical orientation of the VACNTs can be maintained at the interlaminar region of all or most of the plies with good interlocking of the VACNTs to the two adjacent plies than an expected increase in mechanical properties would be expected.

The following subsections within this section will discuss the details concerned with the materials and their respective preparation, testing procedures, analysis and examination of tested materials, and conclusions of any findings.

5.1 Materials

The VACNT and composite materials used in the composite laminates used for mechanical testing were the same as listed in section 4.1. For specimens produced for SBS and CLC testing utilized VACNT material in 30mm wide strips, while specimens utilized for MPT were cut from the wider 380mm substrate material. Further information about the materials used can be found in Appendix D.

5.2 Laminate Preparation and Construction

The test and control laminates constructed for mechanical testing share some similarities across the various types of mechanical tests such as orientation and number of plies per laminate. A detailed overview of the construction and details for the various materials that were constructed are presented here, and further information about the processing steps used can be referenced in Appendix D.

The ply orientations of the laminates to be tested was driven by the need for adequate laminate thickness which fit within the specifications of the respective test standards where applicable. The allowable material thicknesses and fiber orientations for SBS, CLC are similar such that they could be produced from same laminate, thus saving time and material. Laminates for MPT the laminates for a specific ply orientation along with a crack initiation layer and thus were constructed separately. A list of these orientations is along with an averaging of their resultant measured thicknesses is shown in Table 3.

Test	Material	Ply laminate	# of plies	PPS avg. thick. (mm)	PEEK avg. thick (mm)
SBS / CLC	fabric	$[(+45/-45)/(0/90)]_{3S}$	12	3.36	3.49
	UD	$[0/90/+45/-45]_{2S}$	16	2.69	2.23
MPT	fabric	$[(0/90)/(0/90)]_{3s}$	12	3.37	3.38
	UD	$[0_{13}/-5//+5/0]$	16	2.66	2.20

Table 3 - Laminate orientations and ply thicknesses

For PPS based UD and fabric specimens tested with VACNTs, the necessary composite plies were first embedded with the appropriate length VACNTs. For the embedding and consolidation processes, the same heated platen press used with previous embedding and consolidation trials listed in sections 4.3.1 and 4.4.1 was used. The embedding of the plies with VACNTs was completed in a manner

where up to six plies were embedded at the same time via a vertical stacking method. The percentages of VACNTs transferred from the substrate to the plies were calculated as described in section 4.3.3. The resulting percentages for all of the embedding cycles for both UD and fabric materials were found to be 94-100% and 69-82% respectively.

All of the composite plies, either with or without VACNTs were arranged as listed in Table 3 and spot-welded together in the corners of the laminates using a Rinco RL35 hand-held ultrasonic welder similar to the consolidation specimens described in section 4.4.1. The specific consolidation parameters of the PPS and PEEK are listed in Table 4 and follow the same temperature/pressure/time profile as indicated previously in Figure 18. A depiction of the press layout for the laminate consolidation process is shown in Figure 38.

Material	Max temp (C)	Pres. (bar)	Time at temp (min)
PPS	320	6	30
PEEK	380	6	30

Table 4 - Consolidation parameters

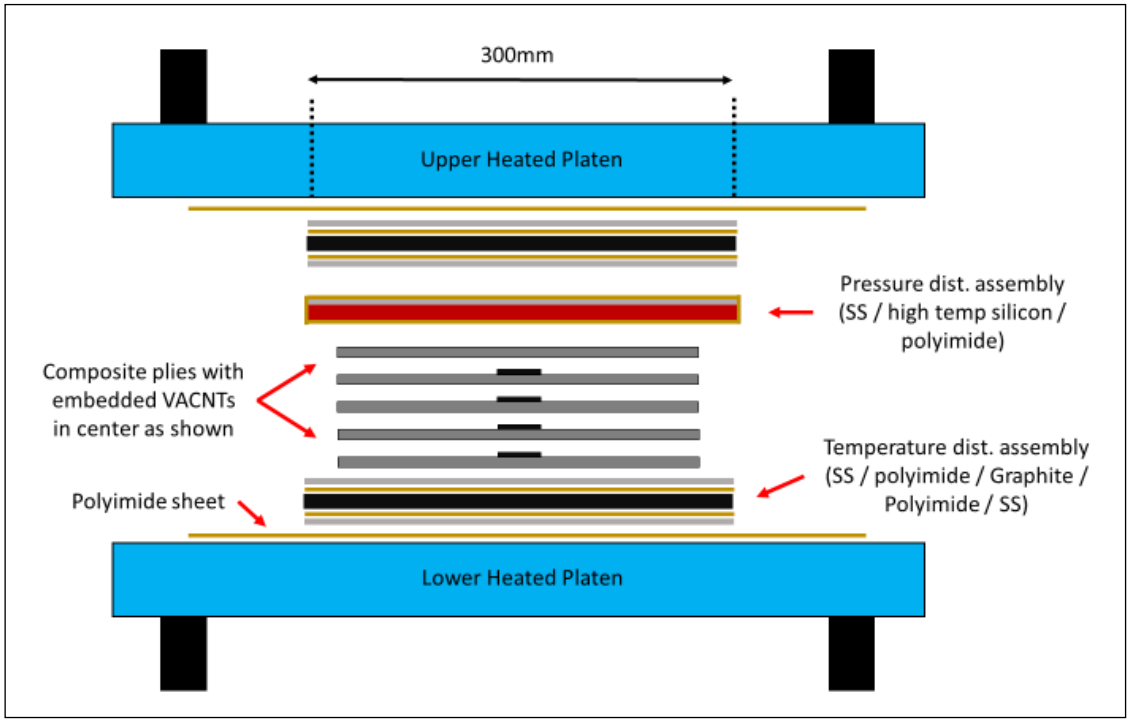

Figure 38 - Press layout for the consolidation process

Following consolidation, each of the consolidated laminates was scanned for voids. This was performed with a water-coupled ultrasonic scanner using a Staveley Instruments brand QC400 reflectoscope and Technisonic brand 10MHz ultrasonic probes, with a system resolution of roughly 1mm. From this scanning there were no confirmed voids in any of the UD or fabric laminates prepared for SBS or CLC testing. There were, however, significant noticed voids on the edges parallel to the fiber direction of the UD laminates produced for the MPT. These defects were marked on the laminates

and avoided when cutting the specimens from the laminates. All of the specimens for mechanical testing were machined from the appropriate laminates using a Proth PSGS-2250 automated wet-cutting machine with a diamond saw blade. Further details relevant to the specific sizes of the specimens for each of the mechanical tests are listed in the respective sections of this document.

5.3 Short Beam Shear (SBS)

To measure the impact of VACNTs at the interlaminar layer on the ILSS, ASTM D2344 – short-beam shear test was used. This test is a simple 3-point bending test, as seen in Figure 39, which induces stresses at the interlaminar sections of the specimens tested. Specimens were cut to size following the guidelines outlined in the ASTM specifications of a width and length for each specific laminate that was produced according to the predetermined ply orientations called out in Table 3. As mentioned, 25 specimens per sample set were tested using the SBS test arrangement with specimens labeled *A* to *Y* for their respective sample sets.

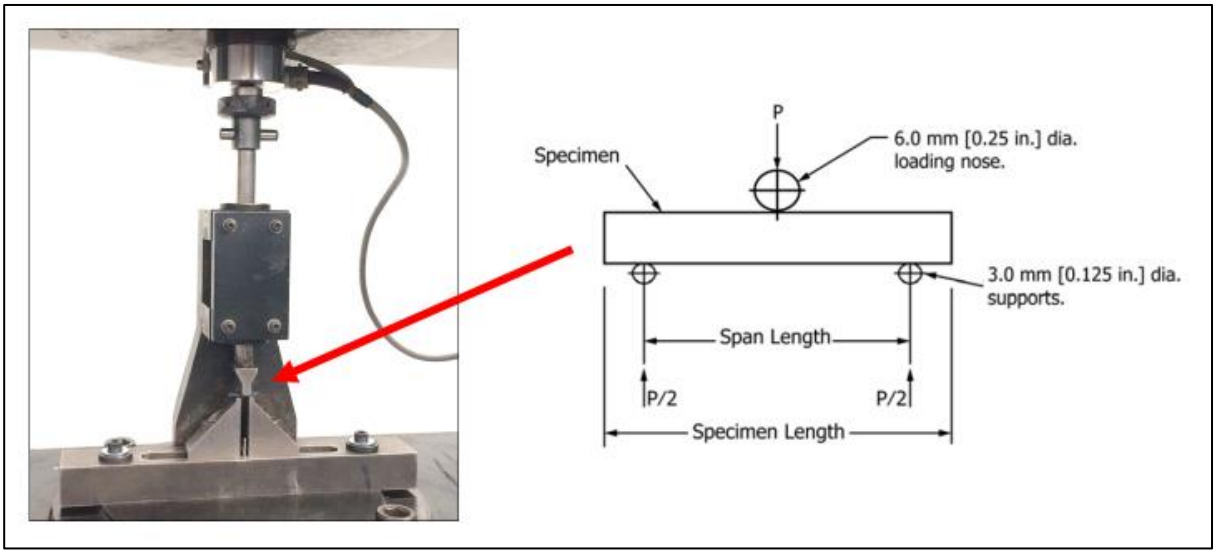

Figure 39 - SBS layout for flat specimens [78]

5.3.1 Preparation and Testing Procedure

The testing procedure follows the specifications laid out in ASTM D2344 standard with regards to flat specimen [78]. The tested specimens were cut such that the respective specimen widths and lengths were 2x and 6x the specimen thickness as measured before testing using a Mitutoyo 150mm digital caliper. The specimens were tested using a Zwick-Roell 1455 load-frame with a 10kN loadcell using in-house manufactured SBS fixture shown in Figure 39. The specimens were tested at 1.0mm/min and stopped once the recorded load had reached a 30% drop from its peak load.

It should be noted two sets of tests for PPS specimens without VACNTs were tested which will be discussed in section 5.3.3. The reason for this extra testing performed was due to the first set of PPS specimens without VACNTs being cut from a different but similarly prepared laminate as those specimens tested with VACNTs. The second set of specimens for PPS without VACNTs was cut from

the same laminate as that which contained the PPS specimens with VACNTs, but in a section where the VACNTs were not present.

5.3.2 Analysis

The examination of the SBS specimens consisted of the following steps:

1) Recording of the individual specimen dimensions before testing.

   Recording and saving of the force versus displacement data recorded through the Zwick software. The raw data was later exported to an excel spreadsheet for analysis and calculation of the short-beam strength values. These values were calculated utilizing equation (1) as denoted in the ASTM specifications, where F^{sbs}, P_m, b, and h are respectively, short-beam shear strength (MPa), max load observed (N), specimen width (mm) and specimen thickness (mm) [78].

$$F^{sbs} = 0.75 * \frac{P_m}{b * h} \tag{1}$$

3) Pictures were taken of the tested specimens after testing using a Coolpix P600 digital camera to note the deformed shape of the SBS specimens.

4) Several PPS tested specimens with VACNTs that exhibited visible fractures were examined in an SEM to visualize the fracture surfaces to observe if VACNTs could be seen.

5) Several PPS tested specimens with and without VACNTs were mounted, polished to a 1µm finish using standard polishing equipment and procedures and examined with OM techniques. This was done to qualify the overall morphology of the SBS specimens, the locations, and morphology of VACNTs, and the fractures to see how the VACNTs may play a role. Additionally, quantitative measurements for voids and resin content were taken.

5.3.3 Results / Discussion

As mentioned in the conclusions from the consolidation trials in section 4.4.5 only the PPS UD materials were tested to-date and the results are shown and discussed herein. The recorded short-beam strength values for each of the PPS UD SBS test specimens were averaged and are shown in Figure 40. As mentioned in section 5.3.1, the second set of tested PPS specimens without VACNTs is demarked with a red star. From these figures, it can be seen that the average short-beam strength values for PPS with VACNTs is roughly 10.6% less than that of values of PPS without VACNTs. Further, the scatter of the failure data points for PPS specimens with VACNTs is more than 3x as much than those withosut VACNTs.

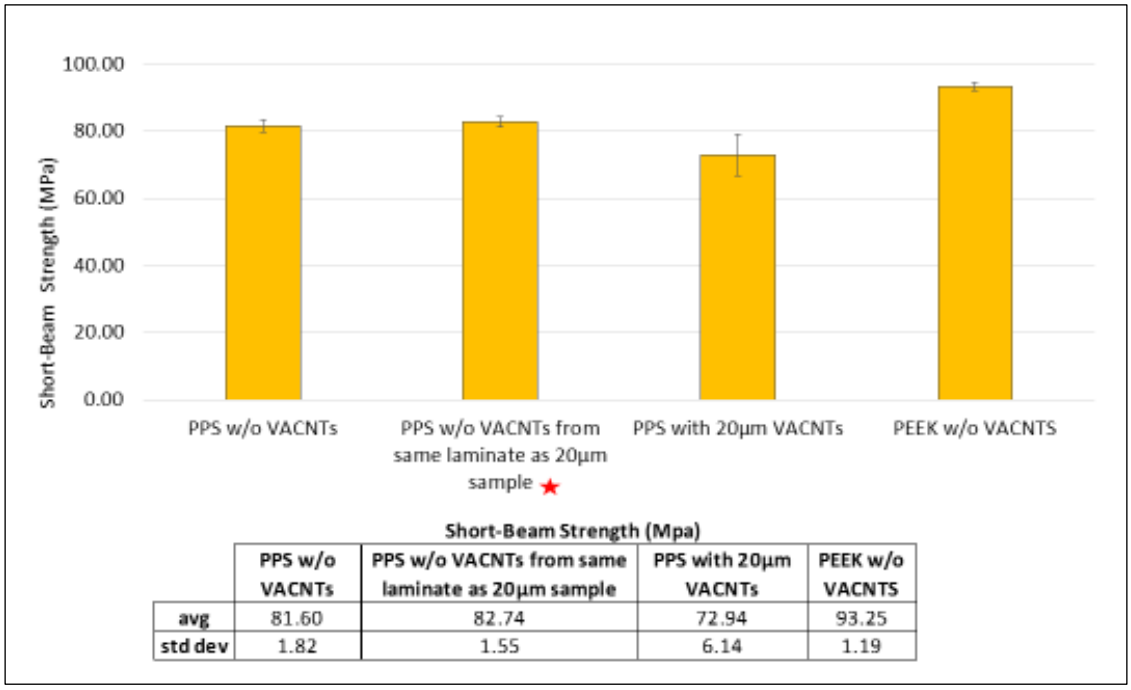

Short-Beam Strength (Mpa)

	PPS w/o VACNTs	PPS w/o VACNTs from same laminate as 20µm sample	PPS with 20µm VACNTs	PEEK w/o VACNTS
avg	81.60	82.74	72.94	93.25
std dev	1.82	1.55	6.14	1.19

Figure 40 – Short beam shear strength results – UD specimens

Overview images of several tested UD SBS specimens with and without VACNTS are shown in Figure 42. In this, the macro-level view the morphology of the post tested specimens can be seen, with more plastic deformation of the SBS specimens tested that did not contain VACNTs than those that did. This greater plasticity of specimens without VACNTs can also be seen in Figure 41. Here two representative force versus deflection curves of the two types of PPS SBS specimens, those with and without VACNTs are shown. The sharp drop-off of the force curve for the PPS with VACNT specimens indicates a fast fracture of the specimens rather than the more plastic deformation seen in non-VACNT specimens. The after tested morphology for the PEEK specimens without VACNTs was similar to those as the PPS specimens without VACNTs. It was observed both during testing and from visual inspection of the tested specimens that the majority of the PPS specimens with VACNTs had an interlaminar shear failure with fractures starting on one outer edge or another and leading to the middle of the specimens. However, the PPS and PEEK specimens without VACNTs had a combination of failures of interlaminar shear fractures, which were contained within the center section of the specimen and not leading out to the edges along the long axis of the specimen, and compression failure of the top plies of the specimens. These differences in fractures are shown in Figure 42 and Figure 44.

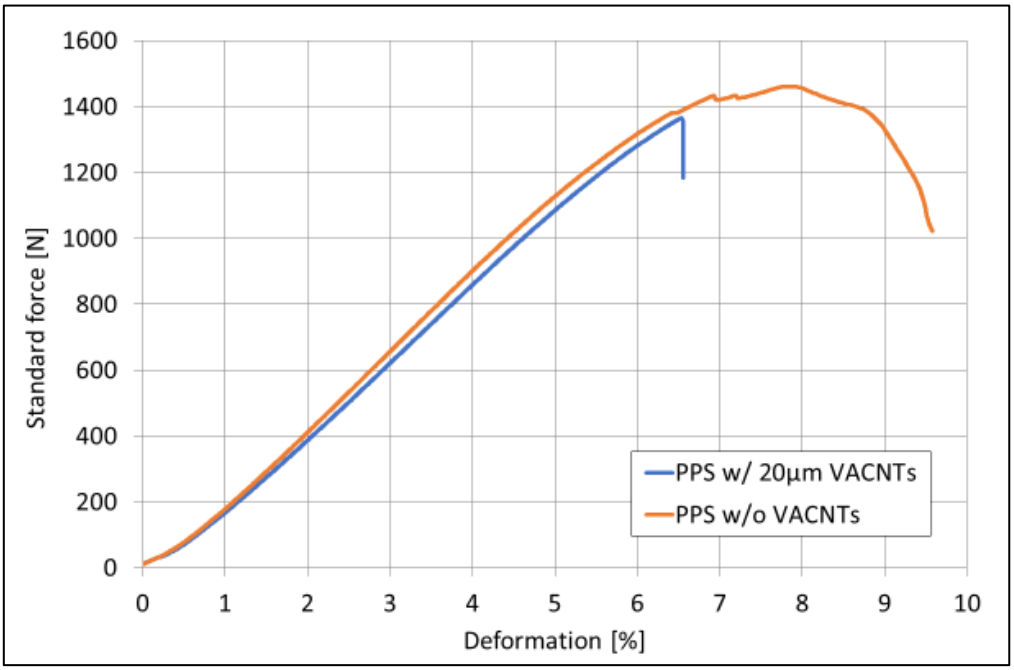

Figure 41 – Force vs. deflection curves – PPS w/ and w/o VACNTs

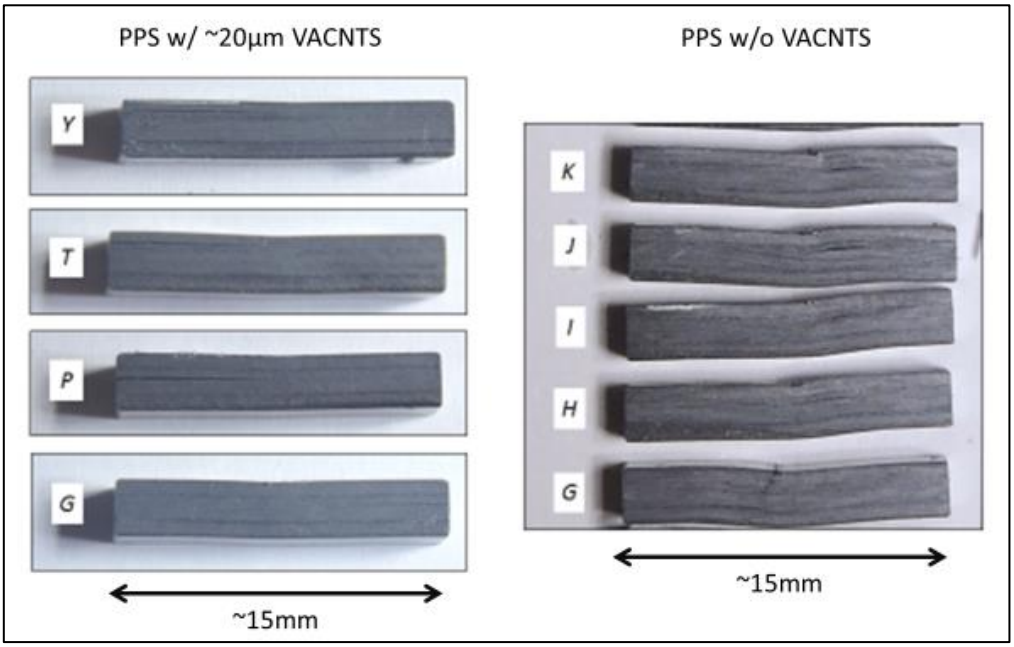

Figure 42 – Tested SBS specimens – UD with and without VACNTs

Several of the PPS with VACNTs SBS specimens were investigated with an SEM to observe if VACNTs could be seen at the fracture surfaces. Within the specimens observed, VACNTs could be discerned in a matted or compacted manner such that they are no longer perpendicular to the fibers of the composite plies as shown in Figure 43.

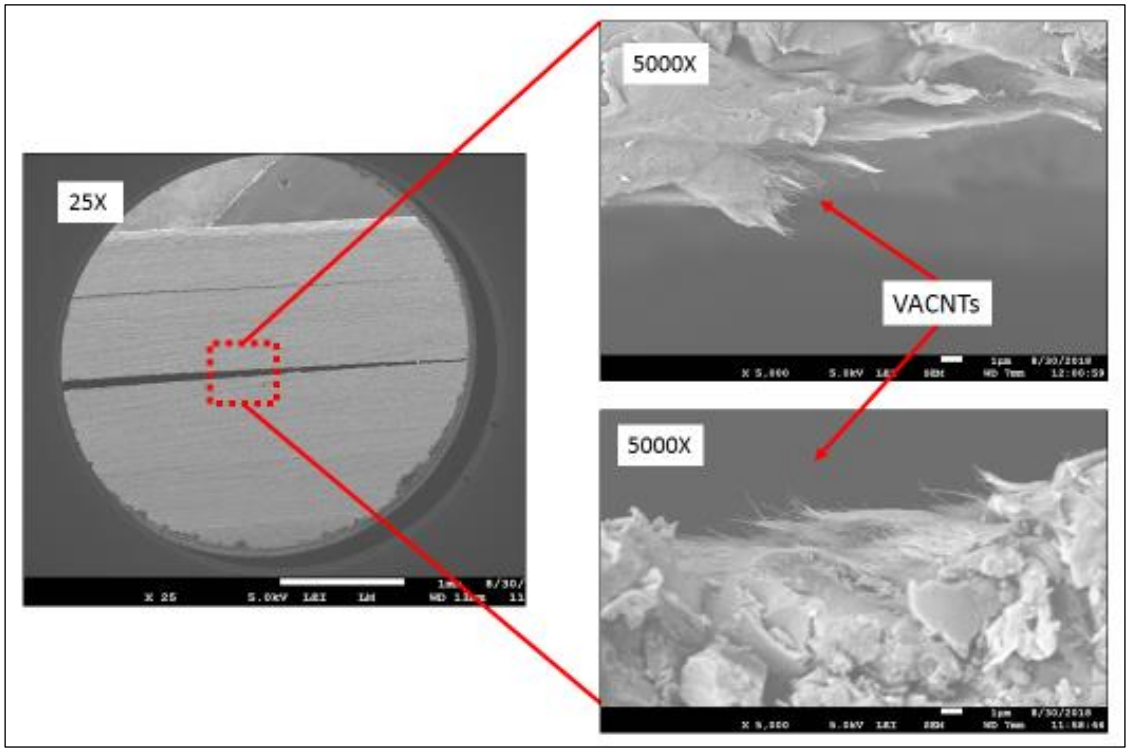

Figure 43 – SEM images – SBS PPS with VACNTs - Specimen *S*

Following the SEM investigations, the same specimens were mounted and polished using the same techniques mentioned in 4.4.3 and viewed with OM techniques and are shown in Figure 44. From this figure, the patterns of interlaminar fractures and morphology of the tested specimen discussed previously can be more clearly seen.

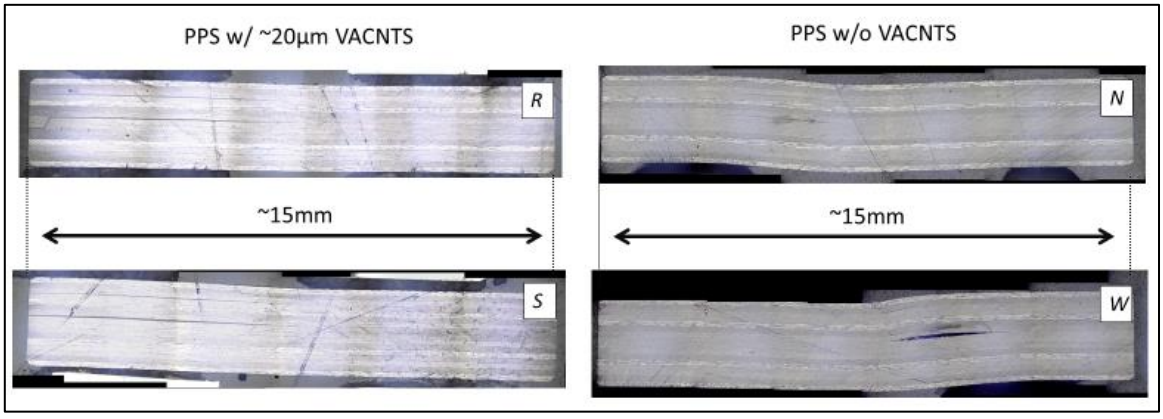

Figure 44 - Tested UD PPS SBS specimens – with and without VACNTs – 10x mag.

These specimens were further investigated, an example of which is shown as specimen *S* shown in Figure 44. In the 500x magnification section of this image, the VACNTs can be faintly seen as the black line on one side of the fracture. This feature of the VACNTs being on only one side of the fracture was seen in many areas of multiple specimens. In the 2000x magnification section of this image, the VACNTs can again be seen one side of the fracture as the dark grey line just below the fracture.

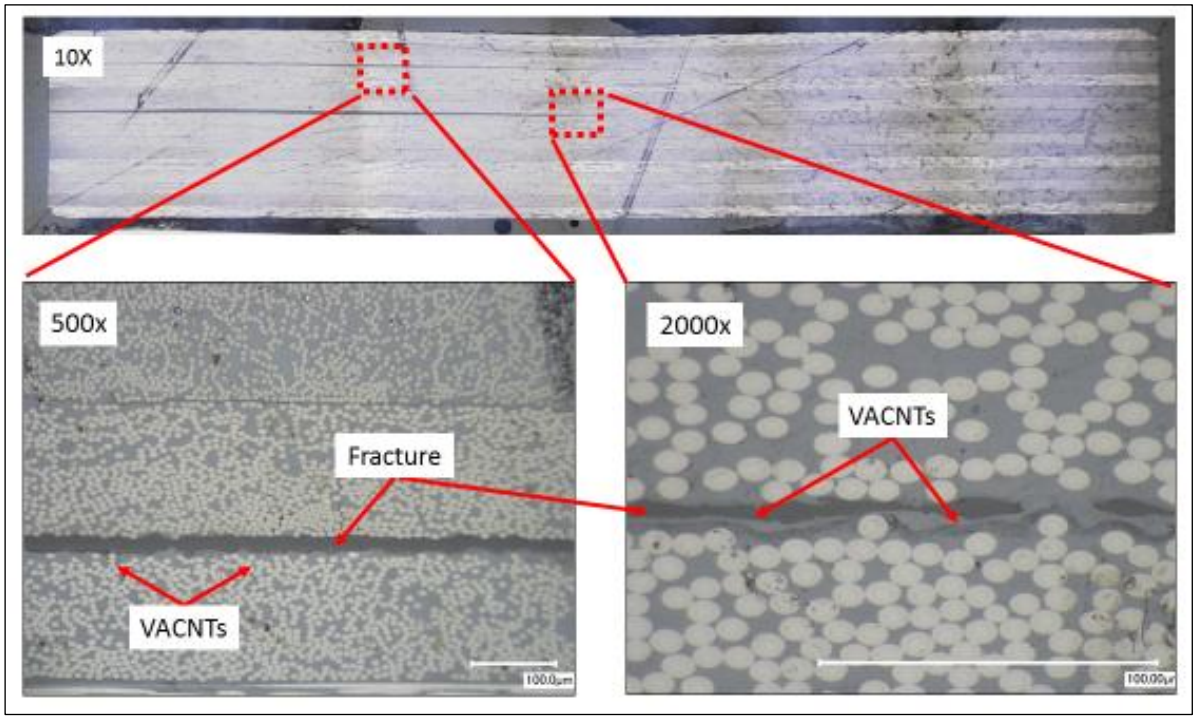

Figure 45 – OM images – SBS - PPS with VACNTs - Specimen *S*

While some VACNTs were seen on both the top and the bottom of the fracture surfaces at several locations as seen in Figure 43, the degree of embedding into the polymer at those points could be ascertained due to the unpolished cut surface of the specimen. As seen in subsequent examination of polished specimens, the bulk of the VACNTs are observed to be on one side of the fracture or another and the VACNTS seen in Figure 45. This similar pattern of crack propagation along one side of the VACNT layer was also seen in CF/TS SBS specimens tested for static and fatigue by D. Lewis [57]. This combination of observations helps lead to the conclusion that while the VACNTs are matted down when a fracture occurs on one side of them, there can be some residual VACNTs remain embedded in the opposite side of the fracture as seen in Figure 43.

A comparison of the fracture cross-sections of PPS with and without VACNTs is shown in Figure 46. There appears to be ductile tearing of the PPS matrix in the specimen without VACNTs, whereas the specimen with VACNTs does not show this ductile like behavior. This lack of ductile behavior of the specimens with VACNTs could lead to the possibility that the matted VACNTs act as a barrier for the resin to flow in and through the VACNTs. This barrier then acts as a stress concentration point leading to an overall lower short-beam shear strength.

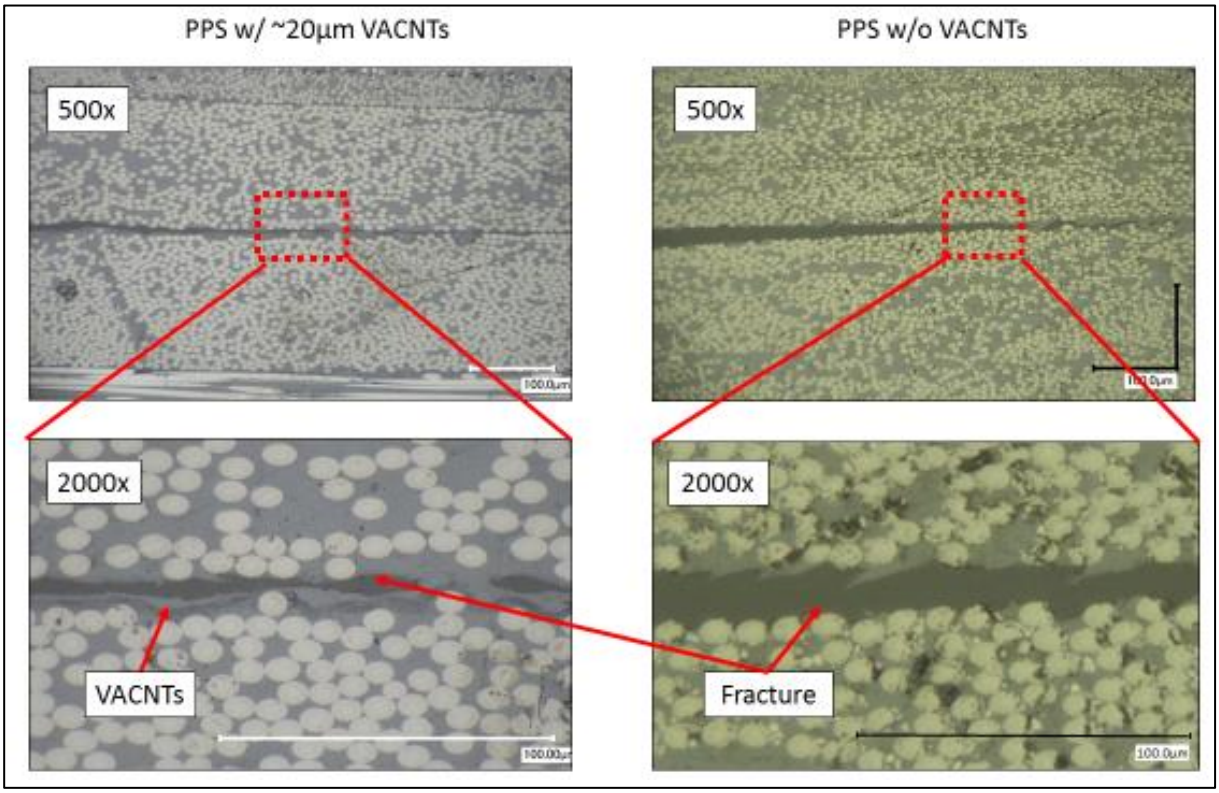

Figure 46 - OM images - SBS PPS with and without VACNTs

Overall all the observations of the as tested specimens show a similar matted or buckled behavior of the VACNTs as was seen in the consolidation section of this project as noted in section 4.4.4. Coupled with the resultant short-beam strength values, the impact of VACNTs at the interlaminar layer were detrimental to the short-beam strength. This was not as was anticipated, as it was thought that if there was matting and buckling of the VACNTS, then there would be little to no impact on the strength values.

A total of five specimens for each sample set were examined to check for visible voids observed, and none were found. An averaged nominal value of the RC as a fraction of the same specimens was recorded on areas of 0^0 fiber orientation and are in-line with the manufacturers suggest RC values. This indicates that composites were consolidated properly. The results are listed in Table 5.

UD	Mfg. stated RC	Measured RC	Std. Dev
PPS w/ VACNTs	34%	39.60%	2.37
PPS w/o VACNTs	34%	37.27%	1.94
PEEK w/o VACNTs	34%	35.72%	2.01

Table 5 – Resin Content values – SBS specimens

5.3.4 Conclusions

One primarily conclusion can be made from the results of the SBS testing and subsequent examinations and is that the as-tested specimens have a detrimental impact on the short-beam strength.

For the sample set for UD PPS specimens with VACNTs, there is a measured average decrease in the short-beam strength of roughly 10.6% compared to the average value for specimens without. Upon investigation with OM and SEM techniques, it was observed that the VACNTs do not seem to have their vertical orientation and interlocking with the carbon fibers of the laminates. The VACNTs which are seen seem to be matted or buckled similar to what was seen with the consolidation specimens examined section 4.3.5. The matted nature of the VACNTs seems to act as a crack initiator or propagator in the specimens where it is present.

It leaves the door open to further work, as mentioned previously in section 4.4.5, to investigate modification of the process parameters or density of the VACNTs and observe how those changes may impact the subsequent short-beam strength values.

Moving forward with CLC and MPT testing, the initial hypothesis of VACNTs having a little to no impact on the interlaminar related mechanical properties if the VACNTs are matted and buckled is now modified to expect a decrease in the respective measured mechanical properties.

5.4 Combined Loading Compression (CLC)

To measure the impact of VACNTs at the interlaminar layer on the compressive strength ASTM D6641 – combined loading compression testing was used. This was done to provide as a qualitative comparison tool to compare the compressive strengths of PPS specimens with VACNTs to specimens of PPS and PEEK without VACNTs. This accomplished by using test specimens which are held securely on two ends in a test fixture as shown in Figure 47. A gauge length of roughly 13mm is left open in the center of the fixtures while the entire fixture is compressed. Specimens were cut to size following the guidelines outlined in the ASTM specifications to be 140mm long and 13mm wide for each specific laminate that was produced according to the ply orientations called out in Table 3. For this test, five specimens per sample set were tested and were labeled *A* to *E* for their respective sample sets.

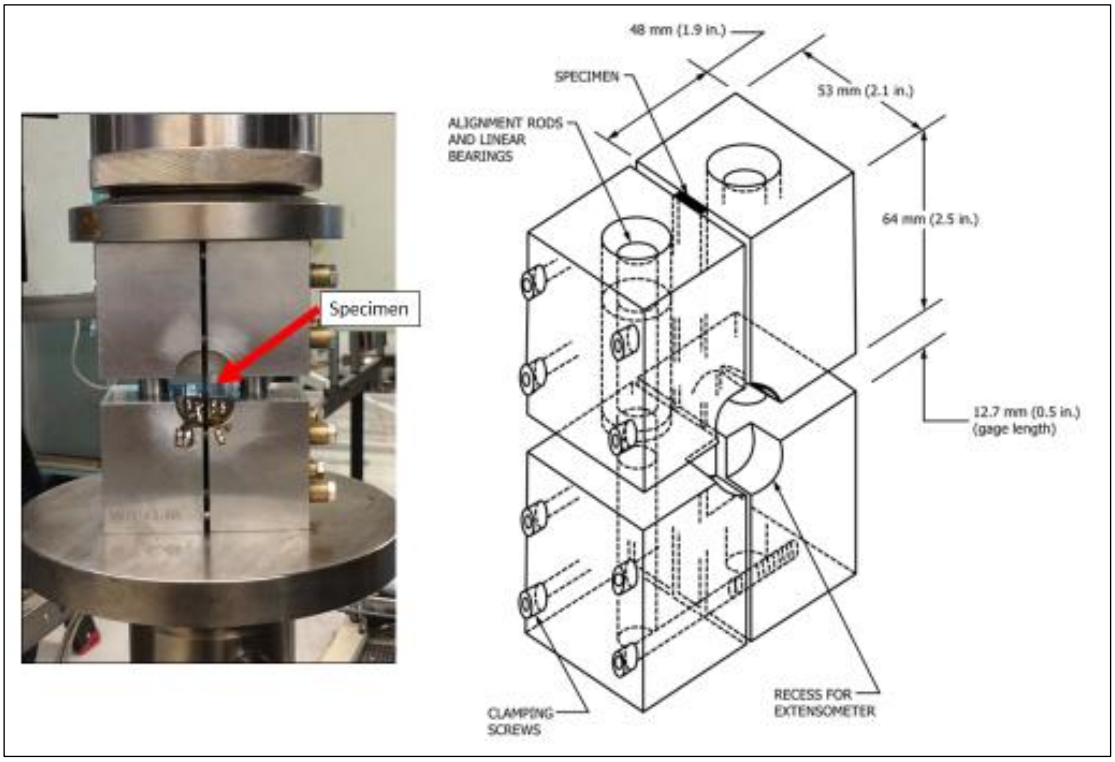

Figure 47 – Combined Loading Compression testing layout [79]

5.4.1 Preparation and Testing Procedure

The testing procedure follows the specifications laid out in ASTM D6641 standard in all regards except that the use of strain gauges was omitted [79]. This choice was made since only the laminate compressive strength was desired as a comparison to control specimens. The laminate compressive modulus of the laminate could be measured with the use of strain gauges to measure for buckling in the gauge section area, but was not desired for this testing. Tested specimens were cut as specified and measured using a Mitutoyo 150mm digital caliper. The use of tabs on the gripped ends of the specimens was not used since the laminates did not contain more than 25% 0^0 plies and was below the recommended 50% maximum threshold specified in the test standard. The specimens were tested using a Zwick-Roell 250kN load-frame with a 250kN loadcell using Wyoming Test Fixture brand WTF-EL test fixture. The specimens were tested at 1.3mm/min and stopped once the recorded load had reached a 30% drop from its peak load.

5.4.2 Analysis

The examination of the CLC specimens consisted of the following steps:

1) Recording of the individual specimen dimensions prior to testing.

2) Recording and saving of the force versus displacement data recorded through the Zwick software. The raw data was later exported to an excel spreadsheet for statistical analysis and calculation of the compressive strength values. These values were calculated utilizing

equation (2) as denoted in the ASTM specifications, where F^{cu}, P_f, w, and h are respectively laminate compressive strength (MPa), max load to failure (N), specimen gage width (mm) and specimen gage thickness (mm) [79].

$$F^{cu} = \frac{P_f}{w * h} \quad (2)$$

3) Pictures taken of the tested specimens after testing using a Coolpix P600 digital camera to note the shape and features of the tested CLC specimens.

4) One specimen each of the PPS with and without VACNTs were examined in an SEM to visualize the fracture surfaces to observe if VACNTs could be seen and understand how they may have played a role in the overall structure of the composite.

5) These same specimens were mounted, polished to a 1µm finish using standard polishing equipment and procedures and examined with OM techniques. This was done to qualify the overall morphology of the CLC specimens, the locations, and morphology of VACNTs, and the fractures to see how the VACNTs are exhibited in these regions of the tested specimens. Additionally, quantitative measurements for voids were taken.

5.4.3 Results / Discussion

For the CLC testing, both UD and fabric sample sets of PPS with appropriate length VACNTs and control specimens of PPS and PEEK without VACNTs were tested due to available time and materials. The results to that testing are shown and discussed herein. The average calculated compressive strength values for each of sample sets are shown in Figure 48. From this figure it can be seen that for UD materials there is a roughly 8.5% decrease in the compressive strength for PPS specimens with VACNTs than without. This lower average value for specimens with VACNTs is similar to that seen as seen with the SBS testing in section 5.3. For fabric materials, there appears to be only a 0.5% difference in the compressive strengths of the PPS specimens with VACNTs than without. The reason for this similar average compressive strength results between the different sample sets is unknown, but may be related to the similar matting and buckling at the contact points of the fibers and bunching up of VACNTs at the resin-rich areas of fabrics that were seen discussed in section 4.4.4.

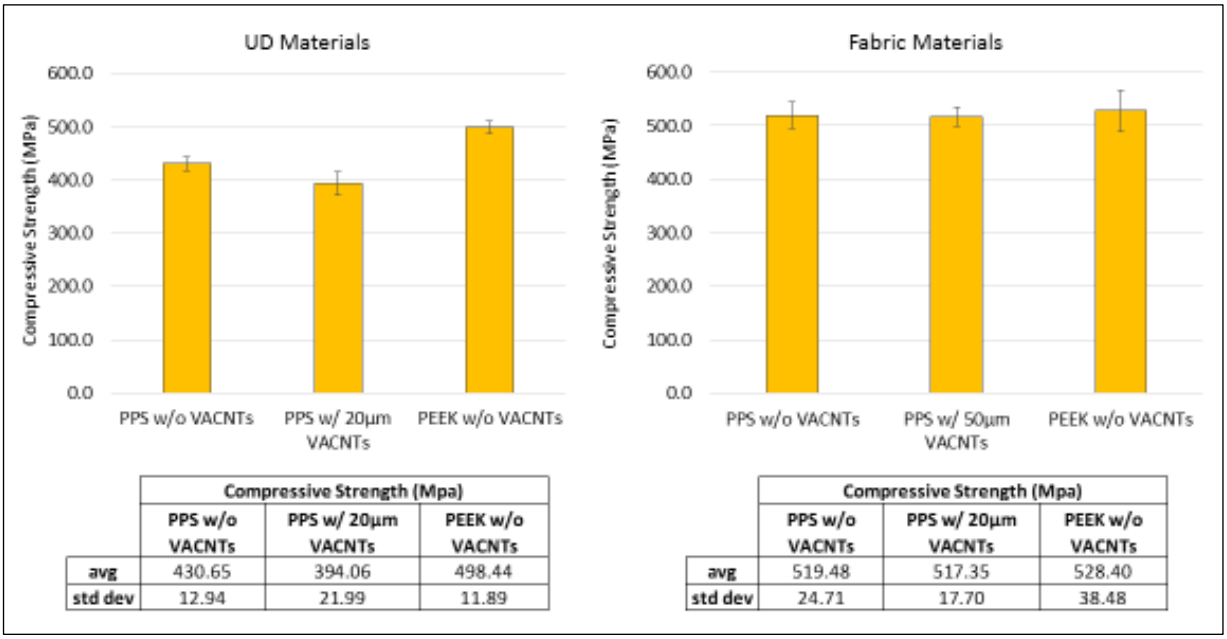

	Compressive Strength (Mpa)		
	PPS w/o VACNTs	PPS w/ 20µm VACNTs	PEEK w/o VACNTs
avg	430.65	394.06	498.44
std dev	12.94	21.99	11.89

	Compressive Strength (Mpa)		
	PPS w/o VACNTs	PPS w/ 20µm VACNTs	PEEK w/o VACNTs
avg	519.48	517.35	528.40
std dev	24.71	17.70	38.48

Figure 48 – Compressive strength results – UD and fabric specimens

Overview images of the central gage sections of PPS UD and fabric CLC specimens are shown in Figure 49. Note that PEEK UD and fabric regarded only as control sample sets for comparison compression values only, and were not investigated in detail further. In Figure 49, the macro-level view of the morphology of the UD specimens with VACNTs is unusual in that there seems to be more fracturing of the laminates within the central gage section than without. Specifically, two of the PPS UD specimens with VACNTs had outer layers of their laminates completely delaminate off the specimen during the testing, whereas no other specimens in other sample sets were observed to do so. For the fabric specimens tested, there was no discernable macro level visible difference in the fractured surfaces.

Further investigation of the tested fabric specimens was not taken forward. This was decided since the similarities in the compressive strengths across all of the fabric sample sets tested was thought to be caused by the similar matting and buckling of VACNTs at the contact points of the fibers and bunching up of VACNTs at the resin-rich areas as discussed in section 4.4.4. Further investigation at a micro level was thought to yield similar results for the location and morphology of the VACNTs. Secondly, the time needed to investigate these specimens was outside the available time resources of the project.

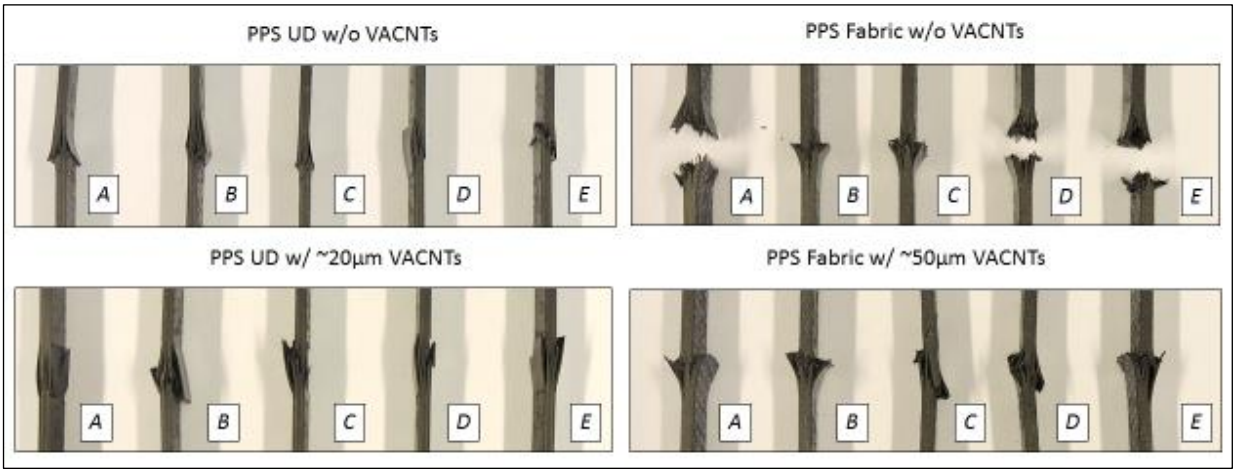

Figure 49 - Tested CLC specimens – UD and Fabric with and without VACNTs

The center 20mm section of the tested specimen *A* from the PPS with VACNTs sample set was cut out the larger specimen and investigated with an SEM. This was done to observe if the VACNTs could be seen at the fracture surfaces and is shown in Figure 50. Within each specimen, several fracture surfaces were examined, and it was observed that some presences of VACNTs were present at one side of the fracture surfaces, but were found to be matted down and compressed into the PPS matrix similar to what was seen in the tested SBS PPS specimens with VACNTs in section 5.3.3. From the morphology of the fracture surfaces and the abundance of the observations of matting of VACNTs within the PPS matrix materials, it is believed that the VACNTs were matted before the compression testing and not matted during or after the testing.

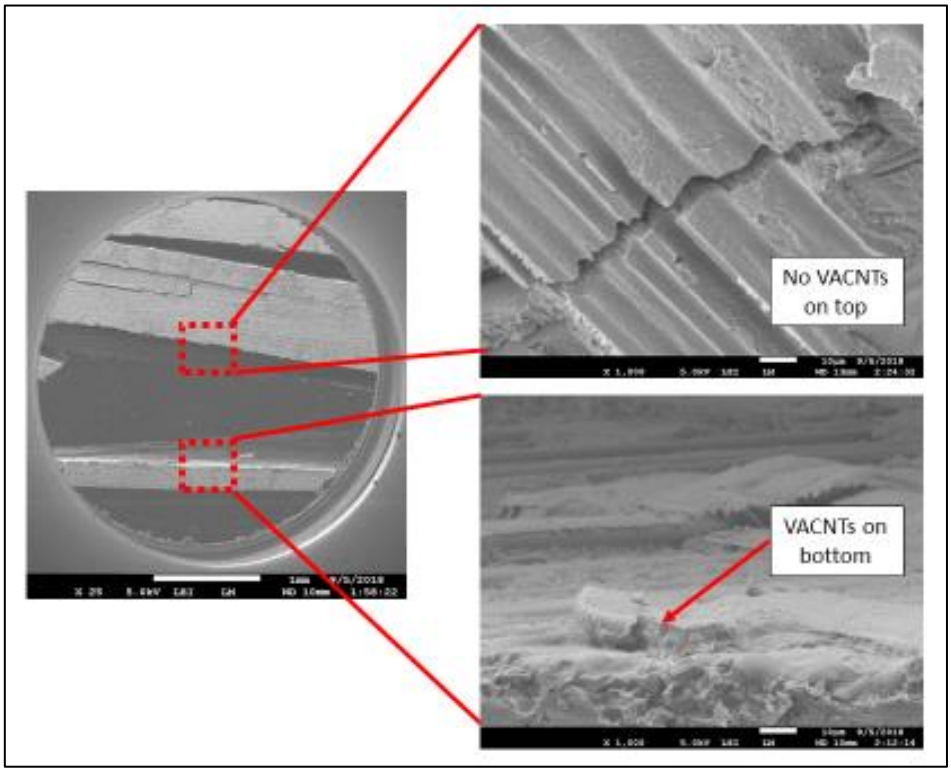

Figure 50 - SEM images – CLC PPS with VACNTs - Specimen *A*

Following the SEM investigation, the same specimen along with a specimen from the PPS without VACNTs were mounted and polished using the same techniques mentioned in 4.4.3 and viewed with OM techniques and are shown in Figure 51. From this figure, it is clear to see that the amount of delaminations present in the CLC specimen with VACNTs is much more numerous across the entire fracture zone with delaminations at nearly each ply interface and several plies at the lower portion of the specimen completely fractured off. By comparison, the specimen without VACNTs show much less inter-ply delaminations and the predominant failure mode is that of compression buckling.

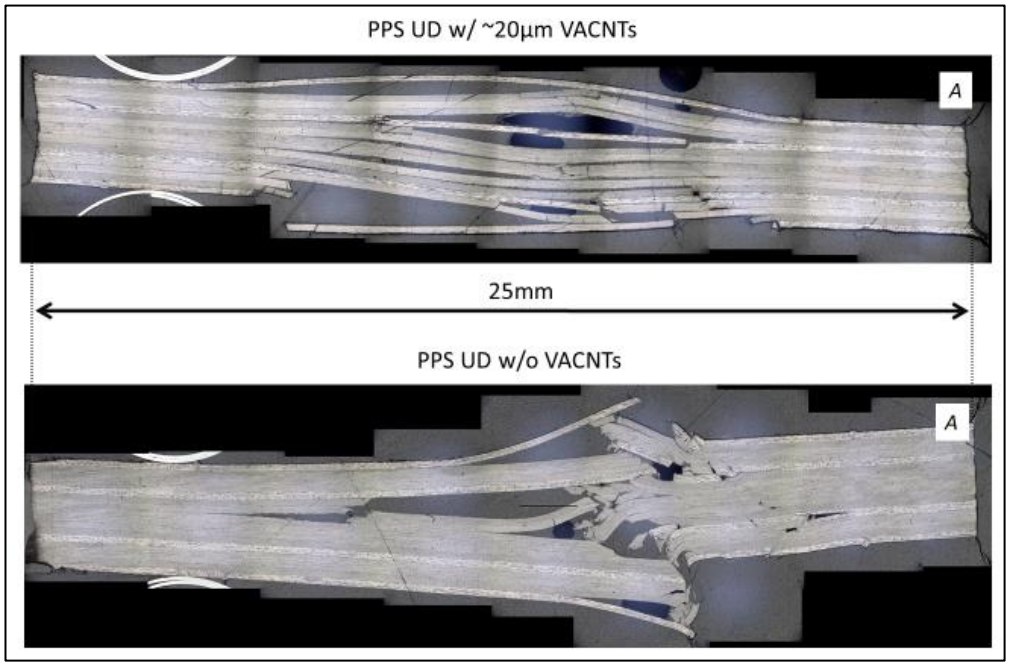

Figure 51 - Tested UD PPS CLC specimens – with and without VACNTs – 10x mag.

These specimens were further investigated to review the interlaminar fracture surfaces and are shown in Figure 52. This image shows fractures at two different locations where the VACNTs can be seen only present on one side of the fracture surface. This observation follows along with what was seen in the SEM images in Figure 50 where VACNTs were seen matted down on one side of the delaminations.

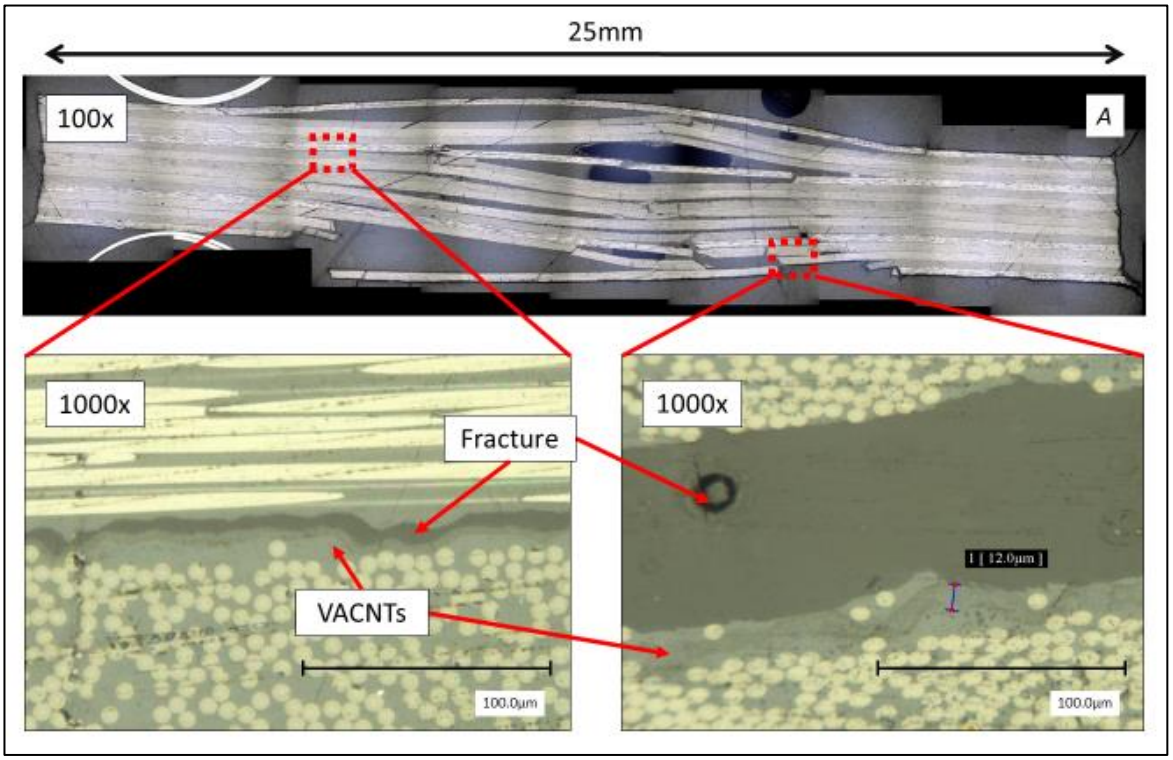

Figure 52 - OM images - CLC PPS with VACNTs - Specimen *A*

Overall all the observations of the as tested specimens show a similar matted or buckled behavior of the VACNTs as was seen in the consolidation section of this project as noted in section 4.4.4 and in the SBS testing performed prior to the CLC testing. Coupled with the resultant compression strength values, the impact of VACNTs at the interlaminar layer were observed to be detrimental overall to the compressive strength. This result was partially anticipated given that the tested CLC specimens were sourced from similarly produced and processed laminates as those used for SBS testing.

The non-fractured areas from each of the sample sets were examined to check for visible voids observed, and none were found. An averaged nominal value of the RC as a fraction of the same specimens were recorded on areas of 0^0 fiber orientation. The results are listed in Table 6.

UD	Resin Content	Std. Dev		Fabric	Resin Content	Std. Dev
PPS w/ VACNTs	33.45%	1.56		PPS w/ VACNTs	44.86%	2.41
PPS w/o VACNTs	35.64%	2.35		PPS w/o VACNTs	44.13%	1.21
PEEK w/o VACNTs	36.01%	2.87		PEEK w/o VACNTs	41.59%	1.78

Table 6 - Resin Content values – CLC specimens

5.4.4 Conclusions

Similar to that found in the SBS testing, one primary conclusion can be made from the results of the CLC testing and subsequent examinations and is that the as-tested specimens have a detrimental impact on the compression strength.

For the sample set PPS specimens with VACNTs there is an average decrease in compressive strength of 8.5% compared to the average value for specimens without. Upon investigation with OM and SEM techniques, similar to findings seen with similar SBS specimens, it was observed that the VACNTs at the interlaminar region do not have a vertical orientation and they are largely crushed, matted, or buckled. As witnessed in Figure 51, delaminations occurred much more readily in PPS specimens with VACNTs than without. These increased delaminations are thought to be caused by the matted and buckled VACNTs acting as barriers where the VACNTs do not readily interlock to the fibers of the adjacent laminate ply. Additionally, the matting of VACNTs may become an impervious barrier that prevents the PPS resin to wet the VACNTs fully and allow for unsaturated dry areas. This would be consistent with the observed dry VACNTs on both sides of the fractures in the SBS specimens shown in Figure 43.

Moving forward with MPT testing, the modified hypothesis of VACNTs having a detrimental on the interlaminar related mechanical properties values if the VACNTs are matted and buckled still stands.

5.5 Mandrel Peel Test (MPT)

To measure mixed Mode I and II fracture toughness of PPS composites with and without VACNTs the MPT, as described in section 2.4.3, was used. This is a test, as seen in Figure 53, which peels a top layer of composite laminate off of a consolidated base that is attached to a sliding table and measures the resultant alignment and peel force to calculate a fracture toughness value. Laminates, constructed in orientations indicated in Table 3 were made with 12.5μm thick PI film laminated at one end to allow for the top layer to be used as the peel arm as shown. Those PPS UD and fabric specimens with VACNTs at the intended interface surface with the same embedding process parameters as mentioned in section 4.3. Further details of this manufacturing process can be referenced in Appendix D. Ten specimens per sample set were prepared to be tested, labeled *A* to *J* for their respective sample sets, though only five specimens for each sample set were tested due to the tendency of the peel arms of specimens to break prematurely during testing. The specimens tested started alphabetically with *A* and continued alphabetically and only skipped a letter designation when a specimen(s) broke prematurely.

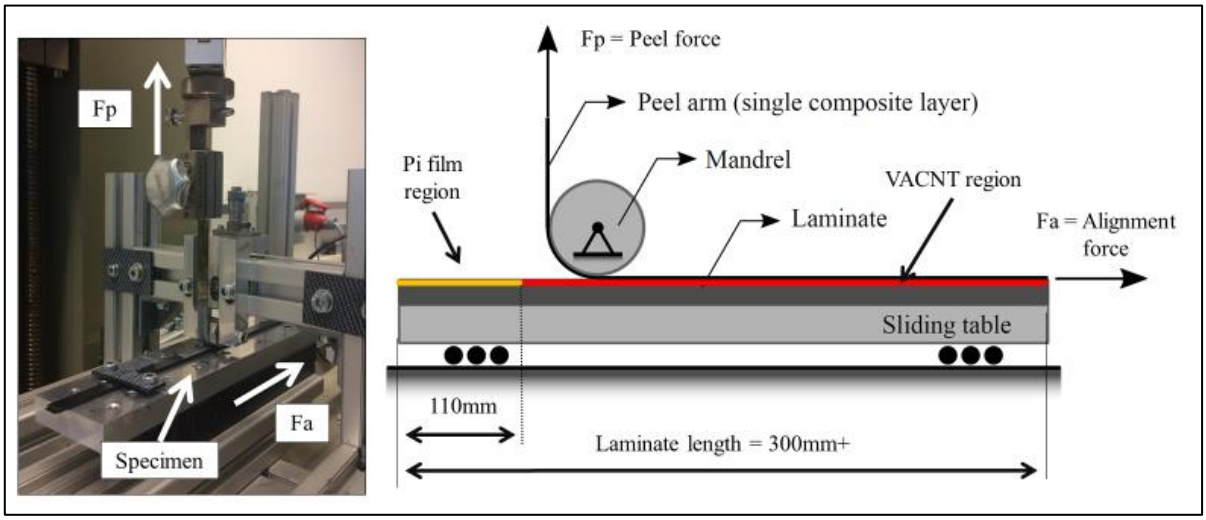

Figure 53 - MPT testing layout [69]

5.5.1 Preparation and Testing Procedure

The testing procedure for the MPT follows with previous work [69]–[71] with notes added here for clarity. The tested specimens were cut from consolidated laminates to widths of 10mm and measured in three places along the length before testing using a Mitutoyo 150mm digital caliper, upon which the average width value was used in the calculation of the fracture toughness. The specimens were tested on a Zwick universal testing machine located at the University of Twente. The load-frame used two HBN brand 200N loadcells for the reading of the peel and alignment forces. The MPT fixture for the test was provided by the University of Twente and was used with a 15mm diameter mandrel supported on a roller bearing. The specimens were tested at a speed 30 mm/min with a starting peel and alignment forces set at roughly 80N. In total, between 80-100mm of peeling distance was tested for each MPT specimen. Two tests were run for each specimen, the first where the top composite laminate strip was peeled off while measuring the peel force and alignment force. The second test consisted of a lowering and re-setting of the crosshead of the machine with the specimen still clamped in place and re-running of the test while measuring the same peel and alignment forces on the now de-bonded specimen which would have corresponding fracture toughness value of zero. This frictional force was later used for the calculation of the fracture toughness value.

5.5.2 Analysis

The examination of the MPT specimens consisted of the following steps:

1) Recording of the individual specimen width prior to testing. The average width from three measurements along the length of the specimen were used for later analysis of the fracture toughness

1) Recording and saving of the force versus displacement data for both as mentioned parts of the test were recorded through a custom LabVIEW program. The raw data was later exported to an

excel spreadsheet for statistical analysis and calculation of the resultant energy release rate G_c. These values were calculated utilizing equation (3), where G_c, F_p, F_a, w, and μ are respectively energy release rate (kJ/m^2), peel force (N), alignment force (N), width (m), and frictional force (N). The frictional force μ is calculated using equation (4).

$$G_c = \frac{1}{w}(F_p(1-\mu) - F_a) \tag{3}$$

$$\mu = (F_p - F_a)/F_p \tag{4}$$

Note that the μ used for the calculation of G_c is an averaging of the five tested specimens per sample set and is used for the calculation of the G_c for the respective sample set only. A full description with examples of these calculation are discussed in Appendix E.

2) Pictures were taken of the tested specimens after testing using a Coolpix P600 digital camera to note the shape and features of the tested MPT specimens.

3) One specimen each of the PPS with and without VACNTs were examined in an SEM to visualize the fracture surfaces to observe if VACNTs could be seen and understand how they may have played a role in the overall structure of the composite.

4) Sections from the same specimens containing the crack tip were mounted, polished to a 1µm finish using standard polishing equipment and procedures and examined with OM techniques. This was done to qualify the locations and morphology of VACNTs, and the fractures to see how the VACNTs are exhibited in these regions of the tested specimens.

5.5.3 Results / Discussion

MPT results for UD and fabric sample sets of PPS with appropriate length VACNTs and control specimens of PPS and PEEK without VACNTs are shown and discussed herein. The recorded values for each of sample sets were averaged and are shown in Figure 54.

From the displayed data it can be seen that there is an 18.6% decrease in the average G_c of the UD PPS specimens with VACNTs than those without. The reduced fracture toughness of the UD specimens with VACNTs would seem to follow those results for the SBS and CLC tests whereby the mating and buckling of VACNTs leads a more brittle interlaminar region. However, two interesting patterns can be seen from the data shown in Figure 54. First is that the average UD PEEK values were less than that of the PPS specimens without VACNTs, but not so for fabric materials. This was not as expected as it was understood that the fracture toughness of PEEK is higher than that of PPS. This is supported by findings of S.G. Ivanov et al. [80] who noted higher fracture toughness values of upwards of 60% for PEEK net resin versus PPS. While no direct comparison of fracture toughness data of PEEK

and PPS CF UD were discovered, it is reasoned that a similar pattern of higher fracture toughness of net resin for PEEK versus PPS would carry over to UD composites as well.

Secondly, the overall values for the fabric PEEK specimens were lower than that of the UD PEEK specimens. This is counterintuitive to what was hypothesized to occur in that UD materials were thought to have a lower fracture toughness than fabric materials. This is supported by findings from S.G. Ivanov et al. [80] who showed that fabric PEEK TP/CF materials showed a higher fracture toughness than that of PPS TP/CF materials. It is further supported by findings of F. Sacchetti [69] who noted that PEEK TP/CF fabric materials exhibited a 25% greater fracture toughness than corresponding PEEK TP/CF UD materials.

For fabric specimens tested, no significant difference in the fracture toughness was shown between the PPS specimens with and without VACNTs. This is thought to be due to the VACNTs bunching up in the resin-rich portion of the interlaminar region as discussed in section 4.4.4, but due to lack of resources, a detailed investigation as to why this occurred was not further investigated. As expected for the PEEK specimens, there as a 41% increase in the average fracture toughness over both types of PPS specimens which follows the convention of PEEK having a higher fracture toughness value than that of PPS as previously noted.

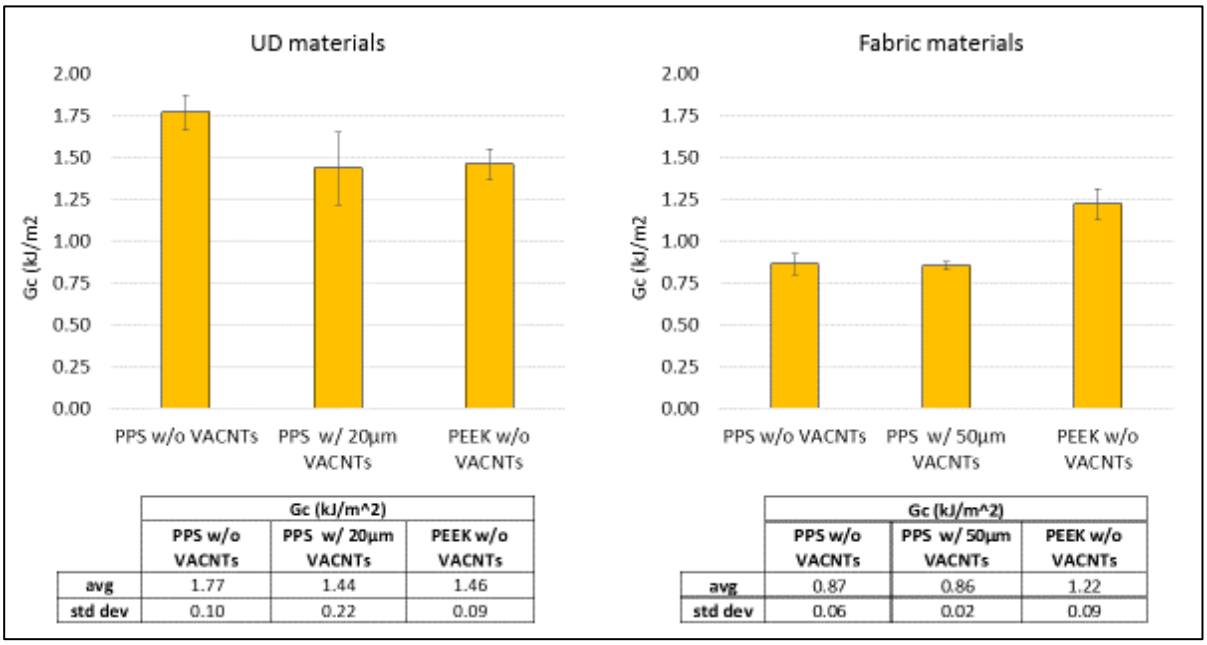

	Gc (kJ/m^2)		
	PPS w/o VACNTs	PPS w/ 20µm VACNTs	PEEK w/o VACNTs
avg	1.77	1.44	1.46
std dev	0.10	0.22	0.09

	Gc (kJ/m^2)		
	PPS w/o VACNTs	PPS w/ 50µm VACNTs	PEEK w/o VACNTs
avg	0.87	0.86	1.22
std dev	0.06	0.02	0.09

Figure 54 - G_c results – UD and fabric specimens

Sections from both UD PPS specimens with and without VACNTs were cut from the tested MPT specimens such that both the upper peel arm and the base of the composite could be viewed with an SEM as well as mounted specimens for the crack tip to be viewed with an OM as shown in Figure 55. This was done to see if VACNTs could be seen at the fracture surfaces of the specimen with VACNTs and how the fracture surface compares to that of the specimen without VACNTs.

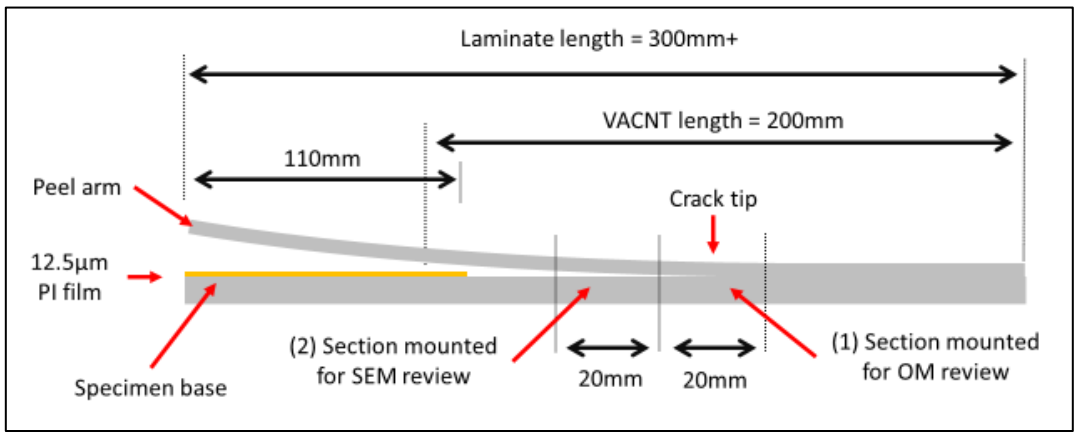

Figure 55 - MPT tested specimen side-view

In Figure 56 both sides of the MPT fracture surfaces of PPS specimens with and without VACNTs can be seen. The images shown are indicative of the majority of the specimens viewed. While there were no visible VACNTs seen in the specimen that was known to contain them, there was a marked difference in the contours of the fracture surfaces seen. The specimens without VACNTs, as seen on the right of Figure 56 has similar cupping and presence of shear lips on the PPS matrix material with roughly equal sections of bare carbon fiber, indicating a ductile fracture. However, the specimens with VACNTs have different surfaces with the base being largely covered in PPS polymer and the top having a clumped section of PPS, but with more uncovered carbon fibers than the base. This morphology along with the lower recorded fracture toughness values would lead to indicate a more brittle fracture occurred with these specimens.

Of note, during the running of the tests, there was a breakage of the peel arm on roughly 15% of the specimens.

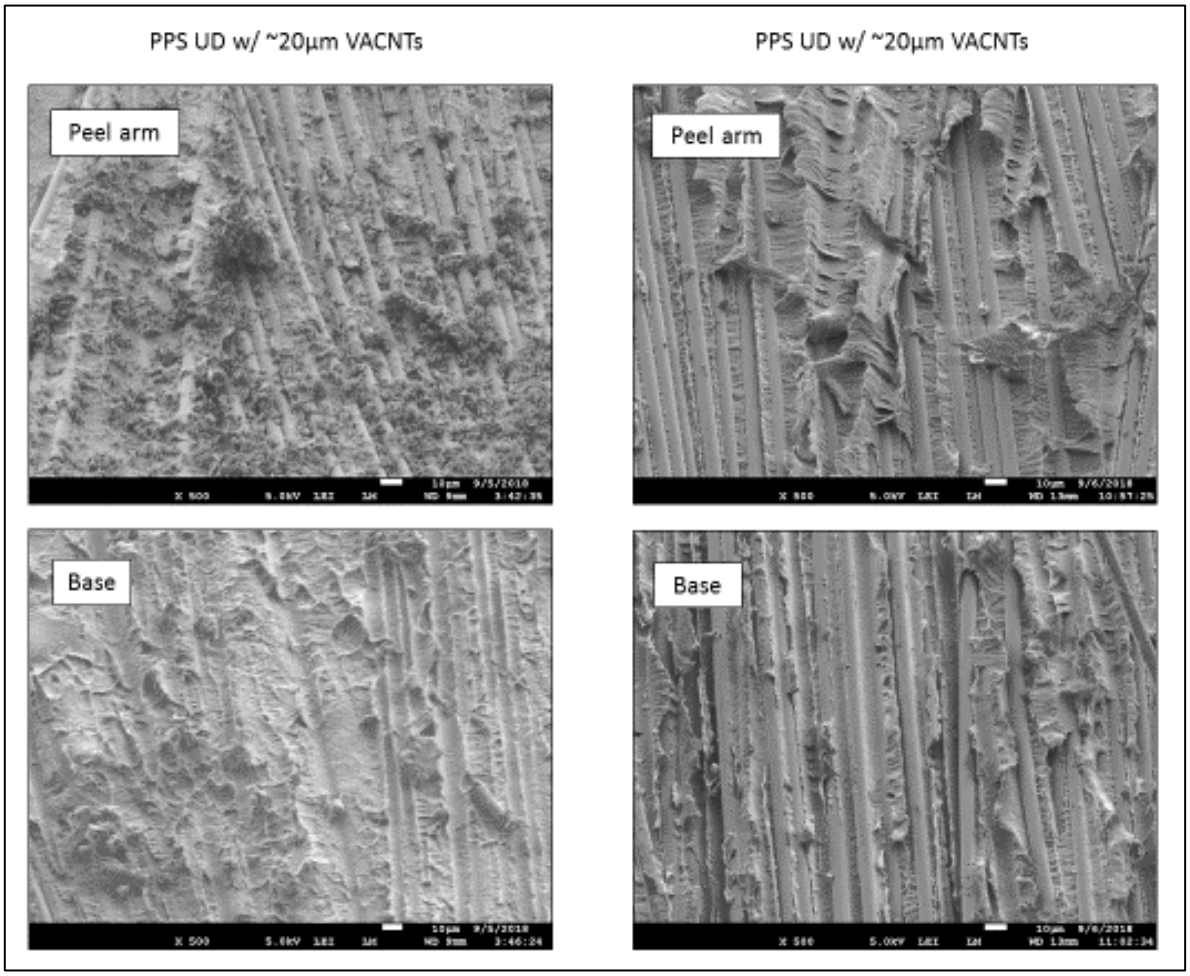

Figure 56- SEM images – MPT PPS with and without VACNTs – 500x mag.

The sections of two MPT specimens, both with and without VACNTs, containing the crack tip as shown in Figure 55 were reviewed using OM techniques to see if the VACNTs could be observed at the crack tip. One of each type of PPS MPT specimen, with and without VACNTs, is shown in Figure 57. From these images of the crack tip it was seen that for specimens with VACNTs, the crack through the specimens had not propagated through the interlaminar region with the VACNTs, but rather in the interlaminar region of the plies above or through the intralaminar region of a ply. For reference, as mentioned in Table 3, the laminates for the MPT specimens were constructed from a $[0_{13}/-5//+5/0]$ laminate where VACNTs were embedded to the -5^0 laminate layer and positioned in the final laminate such that they were present at the interlaminar region between the -5^0 and $+5^{0+}$ plies. This laminate construction was chosen since it had shown through testing by researchers familiar with the MPT development that a $\pm5^0$ scrim layer tends to propagate the crack at that interface better than a 0^0 interface between the layers where the intralaminar fracture is more observed to occur. The presence of VACNTs at the $\pm5^{0+}$ scrim layer was seen, but the orientation of the VACNTs was hard to determine due to the

largely unidirectional nature of the laminate fibers. It is believed that the VACNTs are matted and buckled in a similar nature to those observed in previously described SBS and CLC specimens.

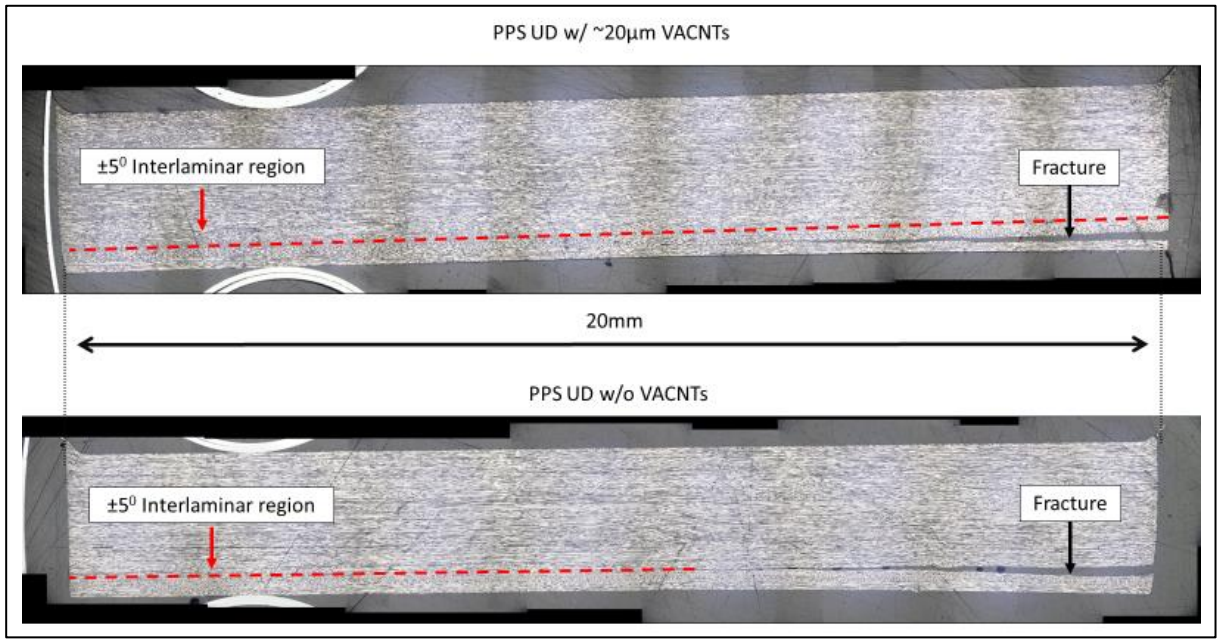

Figure 57 - Tested UD PPS MPT specimens at the crack tip – with and without VACNTs

5.5.4 Conclusions

Overall all the observations of the as tested MPT specimens show a degree of ambiguity as to how the results can be interpreted and what conclusions can be stated. For the use of ~20µm VACNTs with UD materials the data collected does not seem to match up to what was found in the cross-sectional images of the crack tips as shown in Figure 57. It is suggested that the findings of the UD testing be investigated further to more fully understand what is occurring before a clear conclusion can be made.

Similar to the SBS and CLC testing, the use of ~50µm VACNTs with fabric materials is not recommended to be taken further due to the bunching up of VACNTs at resin-rich areas of the interlaminar region.

The use of the MPT test was chosen specifically to avoid the issues with deviating crack fronts seen by other researchers working with analyzing fracture toughness of TS based composites with VACNTs at the interlaminar region. At first glance, it appears that VACNTs presents a similar issue with testing of MPT specimens and may not be an applicable test to use for accessing the fracture toughness of composite specimens (TP or TS) which incorporate VACNTs. However, the test in itself is considerably easier to prepare specimens for and faster to run than DCB testing. This positive attribute of the MPT test provides an opportunity for further research for use as a tool to test the fracture toughness of composite materials with VACNTs at the interlaminar region. A suggested next step would be to incorporate VACNTs at the topmost upper laminate plies and retest.

6 Conclusion and Recommendations

The ability to embed and consolidate VACNTs at the interlaminar layer of PPS TP composite UD and fabric materials along with their impact on several macro-level composite mechanical properties were investigated experimentally in this thesis project. From these findings, several significant conclusions can be drawn which add to the body of work in the field of material science related to composite materials. Furthermore, a number of key recommendations for future work with VACNTs and their use with TP composite materials can be made. The details of both of these points are discussed herein.

6.1 Thesis Conclusions

The use of VACNTs in lengths of ~20µm and ~50µm with PPS TP materials, in both UD and fabric woven formats, was investigated in this thesis project with two key research objectives in mind.

The first objective, to understand how a range of heat and pressures impacted the ability for VACNTs to be embedded and consolidated into PPS TP UD and fabric composites at the interlaminar region yielded several key findings and conclusions including:

1) There was an observed correlation between the percentages of VACNTs able to be transferred and the temperatures used for the embedding processes. At the tested temperatures of 100, 150, 200, and 320^{0}C, there was a noticed increase in the amount of VACNTs transferred with nearly 100% of VACNTs able to be transferred when embedded at the 320^{0}C which is above the 285^{0}C Tg of PPS. This correlates to the fact that the viscosity of the PPS decreased with temperature and becomes *tackier* and able to allow for VACNTs to be embedded into the PPS matrix of the composite materials.

2) There was a further observed correlation between the percentages of VACNTs able to be transferred and the pressures used for embedding. At the tested pressures of 0.5, 1, 3, 5, and 10bar there was a noted increase in the percentage of VACNTs transferred with increasing pressure at all tested temperatures. It was found that that the tested pressure of 0.5bar yielded the lowest transfer percentages for first tested temperatures of 100^{0}C and 320^{0}C and was subsequently was not repeated for 150^{0}C and 200^{0}C.

3) The use of ~20µm VACNTs was found to be more readily able to be embedded into UD materials while maintaining the overall vertical orientation of the VACNTs versus ~50µm VACNTs could be with fabric materials. The relative flatness of the UD materials compared to the periodic undulations of the fabric woven materials allowed for embedding of VACNTs without crushing or matting of the VACNTS at some pressures and temperatures. The use of VACNTs with fabric materials, while maintaining their orientation and location through embedding and consolidation processes presents a difficulty that warrants further study.

4) From the previously noted findings, the embedding parameters of 200^{0}C and 1bar of pressure were chosen for subsequent embedding steps used for consolidation process within this study. These were chosen since they were seen to correlate to a high average percentage of transfer for UD materials, 92.52%, and were seen to allow for a high degree of vertical orientation to be maintained. The same parameters were used for fabric materials, though these exhibited a lower average percentage of transfer, 82.27%, and came with sporadic transfer patterns the correlated to the high spots of the woven fabric materials.

5) For consolidation of both UD and fabric materials at 320^{0}C and 6bar, it was found that there was significant buckling and matting of VACNTs at the interlaminar region of the observed specimens. The same interlocking of VACNTs seen by others with TS based composite materials was not observed with the tested TP composite materials. This buckling is thought to be caused by shifting or buckling in handling for the consolidation process, the VACNTs having a relatively low areal weight and subsequent low compressive strength, or a combination of both.

Overall takeaways for embedding and consolidation studies performed are that UD materials are better suited than fabric materials for the use of VACNTs due to their flatter surface. During embedding high percentages of transfer and high degrees of vertical orientation can be maintained and could present opportunities for other uses of VACNTs and UD TP materials such as welding, heating, or other material structural enhancements. However, those same VACNTs that were embedded with their orientation intact were seen to be buckled or matted down during the follow-up consolidation process. It is this second process that warrants further work to see if the issues with loss of the original orientation can be resolved as it is thought that the interlocking of the VACNTs at the interlaminar region of both composite plies to be key increasing the overall interlaminar strength of the resulting composite materials.

The second objective, to understand and quantify the impact that the VACNTs at the interlaminar region in by way of testing for interlaminar shear, compressive and fracture toughness values was built on the foundation of the first objective. This testing yielded several key findings and conclusions including:

1) For SBS and CLC testing of PPS UD materials, there were respective decreases in short-beam and compressive strength of 10.6% and 8.5% for specimens with VACNTs compared to those without. This cause is thought to be because the VACNTs in the consolidated laminates were seen through OM and SEM observation to be buckled and matted over and not interlocked with the fibers of both composite plies that they were placed between. This matting seemingly acted as stress concentration zone at the interlaminar regions which provided a path of least resistance for fracture.

2) For the MPT results with PPS UD, the recorded fracture toughness values were seen to be 18.6% lower for those specimens with VACNTs than without. However, it was seen through inspection that the crack through the part was not through at the intended scrim interface of the laminate where the VACNTs were present, but through an adjoining interlaminar region, through the ply or a combination of both. While the VACNTs present at the intended interlaminar region were seen to be similarly buckled and matted as seen in SBS and CLC specimens, the VACNTs that are present may be providing a barrier for crack propagation and a true higher fracture toughness.

3) In all three tests the results with PPS fabric materials, with and without VACNTs, showed no significant impact on the resulting strength and toughness values. This is thought to due to the previously mentioned finding that the VACNTs in fabric materials become buckled, matted at the high points of the woven fabric and also tend to migrate into the resin-rich area of the fabric. This combination does not lead to an interlocking of the VACNTs between the fabric plies, which is the intended mechanism of the VACNTs to increase the interlaminar mechanical properties.

Overall takeaways for mechanical tests performed, on both UD and fabric PPS materials, show that the materials produced from the developed process for embedding and consolidation of VACNTs does not lead to the hypothesized increase in interlaminar structural properties of the PPS composite materials tested. A lack of interdigitating of VACNTs between the layers of the composites, as has been witnessed in TS composites by other researchers, is thought to be the reason for this lack of an increase in the interlaminar related mechanical properties. If a solution to these observed issues can be fashioned, the use of VACNTs with TP PPS composite materials may be a viable option for future applications.

6.2 Recommendations for future work

As with any research project, a list of *what if* questions arose throughout this thesis project that were left unanswered due to lack of time and resources or came about only as a conclusion from the observed findings. Included is a list of suggested recommendations for future work.

1) Perform a detailed study of the VACNT materials themselves to understand better what features of the bulk material (sizing, density, type and orientation of CNTS, electrical and thermal conductivity) with the goal of being able to utilize the unique proprieties of the material more fully.

2) Look to understand if parameters such as density of VACNTs, length, composite materials used, or process parameters can be modified or added to produce consolidated laminates with VACNTs that retain a majority of their vertical orientation and interlock with the composite materials bordering the interlaminar region. As noted elsewhere, this interlocking of CNTs

across the interlaminar layer is the primary driving mechanism behind increase the interlaminar strength of composite materials with VACNTs. Specifically, within the realm of VACNTs, look at re-testing the as described embedding and consolidation parameters with higher density VACNTs as it is thought that this density, and resulting bulk buckling strength of the VACNTs, plays an important role. Additionally, look to use different methods for transferring VACNTs to materials such as with heated vacuum tables or autoclaves for the reasoning that vacuum pressures may provide for more evenly distributed application of pressure of the VACNTs into the composite materials.

3) Look to embed VACNTs into TP films following the procedures laid out in this work or those of other researchers [7], [66], [67]. Some ancillary work with embedding ~50µm VACNTs into 250µm PPS films were investigated which yielded orientations of VACNTs that were largely vertical and fully wetted with PPS polymer. The details of this work are noted in Appendix F as a reference. Films embedded fully or partially with VACNTs could provide a vehicle for placing VACNTs at the interlaminar region of TP composites well be used for focusing elements TP welding techniques.

4) Review the surface and through-thickness morphology of the VACNTs after embedding to better understand the changes in orientation of VACNTs before and after consolidation.

5) Work at embedding and consolidating specimens of VACNTs larger than that of the 200mm x 300m format sized specimens tested in this work. While it is reasoned that the same process parameters used in this thesis project would work for larger sizes, some unforeseen benefits or issues may come about from the use of larger format sizes of VACNTs.

6) Look at the use of microwave and RF-based plasma etching with PPS materials to help to aid in the etching of the polished surfaces with the goal being better able to distinguish the morphology of the VACNTs embedded in the polymer materials.

7 Appendices

A) Embedding / Consolidation material and process details

The materials and procedures used for the embedding and consolidation portions of this project are detailed herein. All raw materials used as the tested materials, those used for setup or as consumables, and arrangements of those materials are noted. The tested materials used are the same as noted in section 4.1 and are listed again here in Table 7 This table also includes the consumables and will be referenced through the process steps.

The embedding process consisted of the following steps:

1) Cut composite materials into 250mm x 250mm squares. These would be used as the base material to embed 30mm x 30mm VACNT substrate material for the embedding process. This was done for both UD and fabric materials (items 2 and three respectively in Table 7). For the fabric material, the cutting was performed on a Gerber brand industrial plotter for the fabric materials from a larger role. For the UD materials, an aluminum sheet measuring 250mm x 250mm x 2mm thick was used as a cutting template and the UD materials were cut with a sharp razorblade by hand.
2) The composite plies were placed onto the center of a 300mm x 300mm x 2mm aluminum sheet and taped with sections of PI tape to 2 corners. This was done to hold the composite ply in place during attachment of the VACNT substrate and allow for safe handling of the composite ply.
3) The center 30mm x 30mm area was marked with a magic marker by hand to facilitate the location of the 30mm x 30mm VACNT substrate materials.
4) The VACNT materials were cut from their respective 30mm wide strips in lengths of 30mm using fresh industrial hand scissors to allow for a clean cut of the SS substrate. To two corners of the back side (non-VACNT side) of the substrate, small sections of PI tape were placed. This would be used to hold the substrate in place and to prevent it from shifting laterally in relation to the composite ply. To the pre-marked composite ply the substrate with VACNTs was placed by hand such that the VACNTs were facing down towards the composite ply. Care was taken to only hold the substrate by the edges which permitted the bulk of the VACNTs not to be disturbed. Light pressure was used to press the two PI tape sections on the corners of the VACNT substrate to hold the substrate to the composite ply. This entire step was performed inside an enclosed glovebox and while wearing latex gloves and an N100 dust mask. The prepared materials can be seen in Figure 14.

Tested materials			
Item Number	**Description**	**Manufacturer / Supplier**	**Notes / Qty. / Misc.**
1	VACNT materials	N12 Technologies	~20µm and ~50µm VACNT lengths. ~20µm on 30mm and 380mm wide subrate, ~50µm on 30mm substrate only
2	Cetex® TC1100 AS4D 12K UD	TenCate	221 g/m2 / 34% RC. Presented in 305mm (12 inch) wide roll form
3	Cetex® TC1100 T300 3K 5HS satin weave fabric	TenCate	280 g/m2 / 43% RC. Presented in 1.21 m (48 inch) wide roll form
4	Cetex® TC1200 AS4 12K UD	TenCate	146 g/m2 / 34% RC. Presented in 305mm (12 inch) wide roll form
5	Cetex® TC1100 T300 3K 5HS satin weave fabric	TenCate	280 g/m2 / 43% RC. Presented in 1.21 m (48 inch) wide roll form
Setup or consumable materials			
6	Polyimide film - 125µm thick	Dupont	Presented in 1.21m (48 inch) wide roll form
7	Polyimide film - 25µm thick	Dupont	Presented in 1.21m (48 inch) wide roll form
8	Polyimide film - 12.5µm thick	Upilex	Presented in 0.5m (20 inch) wide roll form
9	Polyimide tape - 25mm wide	n/a	Used for holding various items in place
10	High temperature tacky tape - 20mm wide	ITW Polymers	SM5150 high temp vacuum sealant tape
11	Graphite sheet - 3mm thick	n/a	Graphite sheet with SS mesh in center - used for temperature distribution assembly
12	Silicion sheet material - 1.5mm thick	Rogers Corp.	UltraPad MR - fiberglass reinforced high temperature silicon sheeting (fiberglass in center of sheet)
13	Aluminum oxide indulation - 50mm thick	n/a	Presented in 0.5m (20 inch) wide roll form
14	Aluminum foil - 0.07mm thick	n/a	Presented in 0.5m (20 inch) wide roll form
15	Stainless steel tube	n/a	1mm long x 2.5mm OD x 0.5mm wall - full soft condition
16	Stainlee Steel (SS) sheets - 1mm thick	n/a	Various uses
17	Mold Release	Marbocote	Marbocote - 227-CEE liquid mold release
18	Twill 2x2 fiberglass woven fabric	FiberMax Composites	162 g/m2. Presented in 1.21 m (48 inch) wide roll form
19	50mm Aluminum adhesive tape	n/a	Used on fabric laminates for consolidatoin

Table 7 - List of tested materials and consumables

5) The prepared VACNT and composite ply specimens were next be placed into the heated platen press. Each ply was embedded one at a time, and the layout of the materials to apply pressure was different based on if the embedding was at 0.5bar or between 1-10bar. The two different types of layouts are shown in Figure 15 and Figure 16 respectively. The arrangement of the materials is described here.

   a. The temperature distribution assembly consists of materials that all measure 300mm x 300mm in area. Within the assembly, a 3mm thick graphite sheet (item # 11 of Table 7) forms the center of the assembly. On both sides of graphite, 25µm thick PI films are placed (item 7 in Table 7) along with 1mm thick SS sheets (item 15 in Table 7).

   b. The pressure distribution assembly consists of materials that all measure 300mm x 300mm in area. Within the assembly, a high-temperature silicon rubber sheet is placed on a 1mm SS sheet, and both of the materials are wrapped in 25µm or 50µm PI film. The film thickness depends on the type and thickness of the silicon sheet used. For embeddings under 250^0C the UltrapPad MR materials are used (item 12 in Table 7) and wrapped in 25µm thick PI film. For embeddings above 250^0C a custom-made silicon rubber caul plate, as constructed using the following process and materials and is shown in Figure 58, is wrapped in 125µm thick PI film (item 6 in Table 7). This custom produced press-pad consists of a 1mm thick SS sheet which acts as a backing plate. To one side of this sheet, a layer of 3mm thick x 20mm wide strips of SM5150 high temp vacuum sealant tape (item # 10 in Table 7) was applied next to one another to cover the entire SS sheet surface. A single layer of $0/90^0$ fiberglass woven fabric is applied and pressed down into this first layer, and an additional layer of sealant tape is applied in a perpendicular direction to the first layer. To the top of this is applied a 125µm thick PI that is then wrapped tightly around the entire sandwich and taped on the backside. The surface of the assembly is then cured at 350^0C for 2 hours at 2bar of applied pressure to solidify the silicon rubber strips together into one homogenous piece. The resultant assembly has proven capable of being able to handle the 320^0C embedding cycles much more readily than the UltraPad MR material. In total it was shown to last nearly 40-50 cycles before the silicon was observed to start to break down and crack compared to the 1-2 cycles for the UltraPad MR materials. Note that the use of a PI film to wrap the silicon sheet is critical to help contain any silicon oil that may weep out of the silicon sheet. The use of silicon sheets with a fiberglass layer was found to be beneficial over similar rubber materials that did not contain any fiberglass structure. The fiberglass was discovered through testing to add considerable structure to the silicon preventing

squeeze out during pressings and helped to increase the total usable life of the silicon materials.

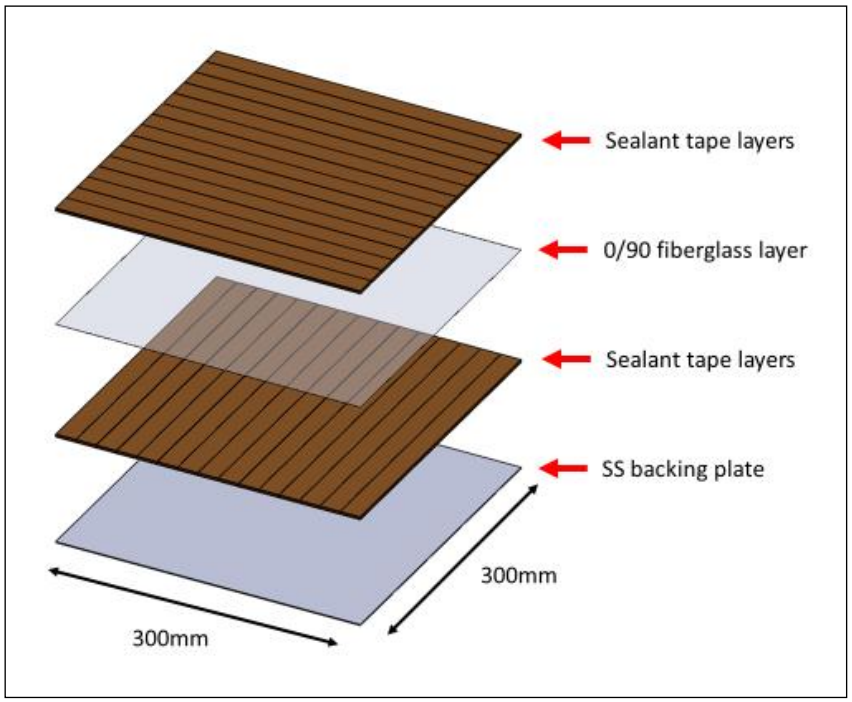

Figure 58 - Custom high-temperature press-pad

c. The vacuum bag consists of 125µm PI film and is sealed with SM5150 high temp vacuum sealant tape. The bag was made such that it was constructed of a single section of film cut to a size of roughly 120cm x 40cm as shown in Figure 59. This allowed the complete bag to made long enough to all for part of the bag to be placed off of the heated portion of the platen press and therefore not hardened and cure fully and remain re-useable for multiple sessions. Five sheets of woven fiberglass fabric (item # 18 in Table 7) were placed between the composite sheets and the opening end where the suction hose would be added to act as a high-temperature breather layer. Figure 60 shows the vacuum bag assembly installed with a vacuum hose installed. Note that a small section of the same fiberglass woven material was put over the opening of the hose input to prevent ripping of the vacuum bag.

d. The insulation layer shown in Figure 60 was constructed from 50mm thick aluminum oxide insulation (item # 13 in Table 7) and wrapped with 0.07mm aluminum foil (item # 14 in Table 7) and has an approximate size of roughly 500mm x 500mm. This assembly was only used for when the lower side of the platen press was used to help keep heat contained within the composite specimen. Trials were performed with thermocouples to ensure that this insulation was able to adequately limit heat loss.

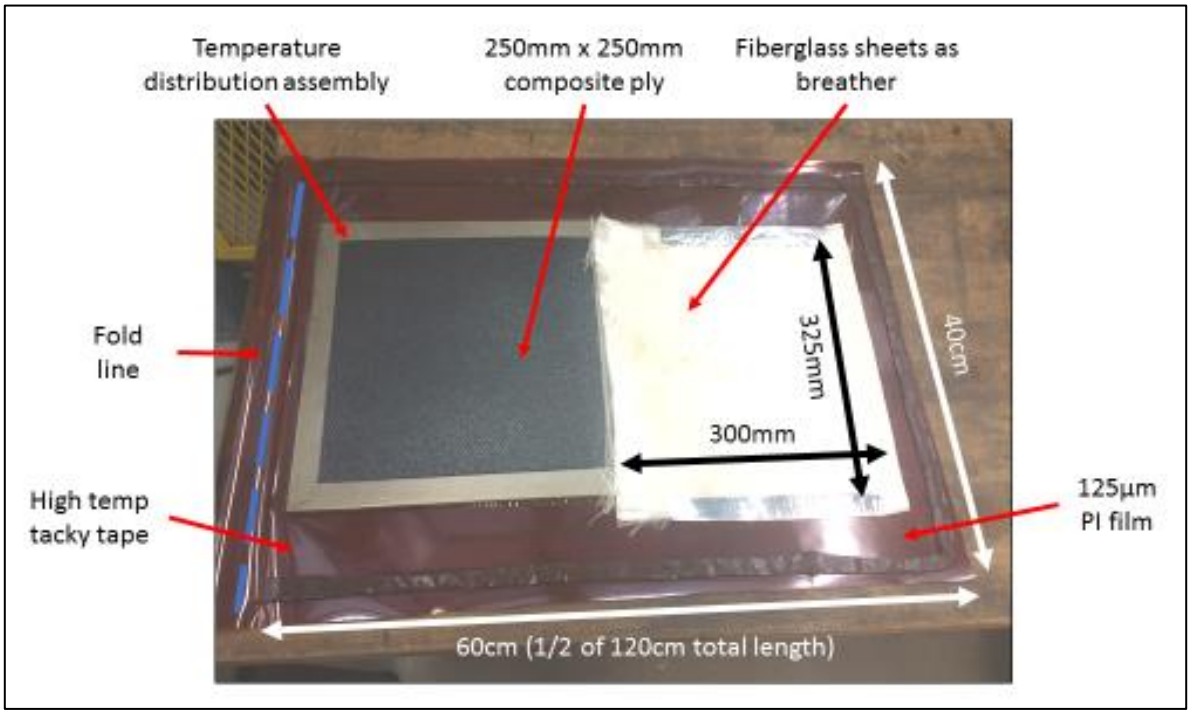

Figure 59 - Vacuum bag assembly – 0.5bar embedding

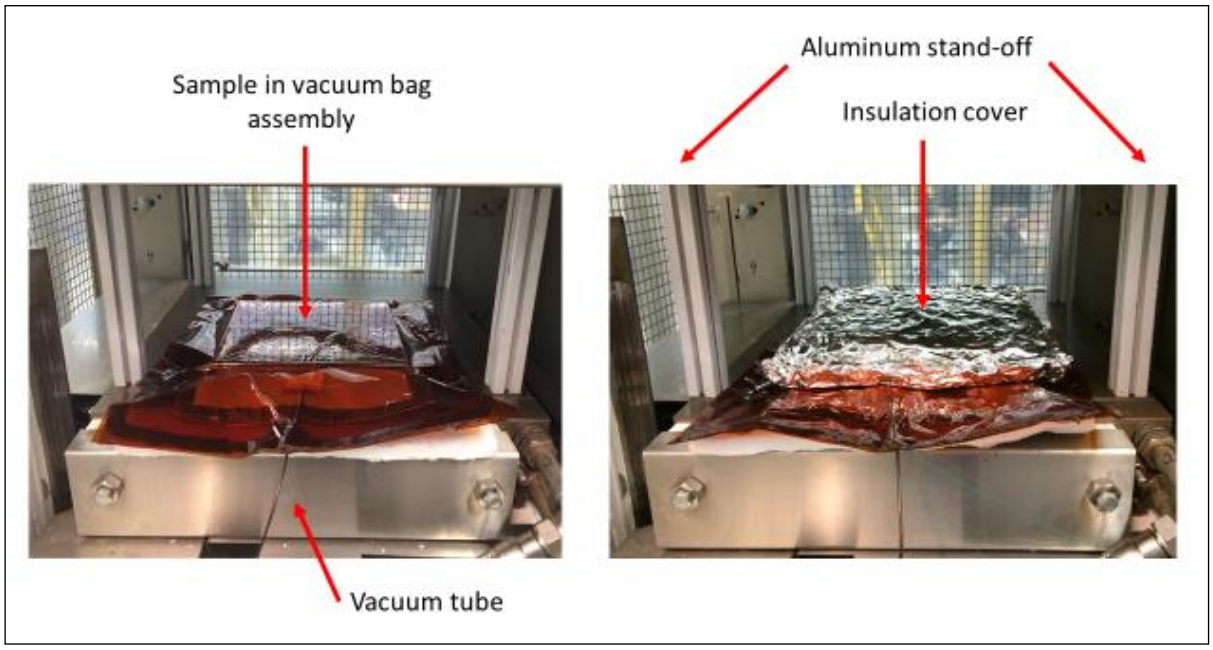

Figure 60 - Lower platen vacuum bag assembly with and without insulation cover

6) The prepared materials were placed into the platen press which was subsequently programmed to follow the temperature and heating cycle shown in Figure 18. Note should be made that the press used had limits of 7^0C/min heating and 10^0C/min cooling. The resultant heating (as measured by an array of thermocouples located in both the upper and lower platens and averaged) was nearly identical to the requested heating. The resultant cooling rate was nearly

identical to the requested rate until roughly 50^0C of room temperature upon which the resultant cooling rate would taper off and slow down.

7) Once the embedded specimens were cooled to within 20^0C of room temperature (usually 17-22^0C) the press the specimens were removed from the press. The 250mm x 250mm specimens were cut down to roughly 100mm x 100mm centered about the VACNT substrate to enable for easier handling.

8) For this step latex gloves were worn to prevent contamination of the specimens and limit CNT exposure. The VACNT substrate was removed by first peeling back one of the sections of the PI tape used to hold it in place and then carefully by hand peeling the SS substrate as shown in Figure 61.

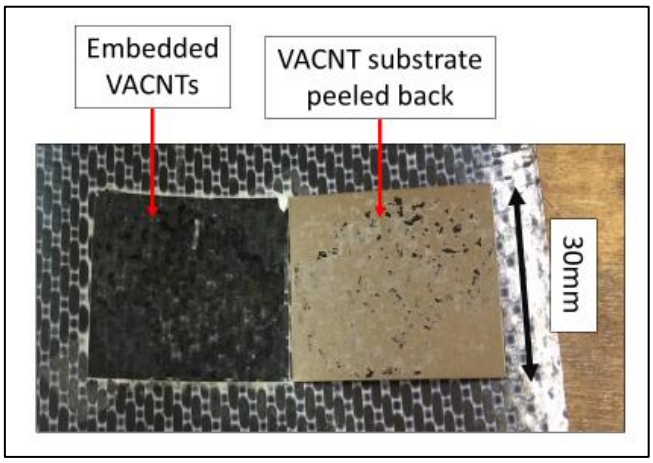

Figure 61 - VACNT and removed substrate after embedding

9) The surface of the now removed substrate that previously fully contained VACNTs had high-quality digital photographs taken of their surfaces using a Coolpix brand P600 camera and the images were processed using *ImageJ* software to calculate a percentage of VACNTs remaining on the substrate. This process is described in Appendix B.

The consolidation process as indicated in section 4.4 consisted of the following steps:

1) Composite plies of UD and fabric were first embedded respectively with ~20µm and ~50µm VACNTs at 200^0C and 1 bar of pressure following the above-noted processes.

2) As noted in section 4.4.1, two different laminate configurations were used for UD and Fabric materials. For UD materials a three-ply (0/90/0) arrangement was used and a two-ply $(0/90)_s$ for fabric materials to produce symmetric laminates. The plies with VACNTs were located at the bottom most of those respective laminate arrangements and spot-welded together in the four corners using a Rinco RL35 hand-held ultrasonic welder as indicated in Figure 62.

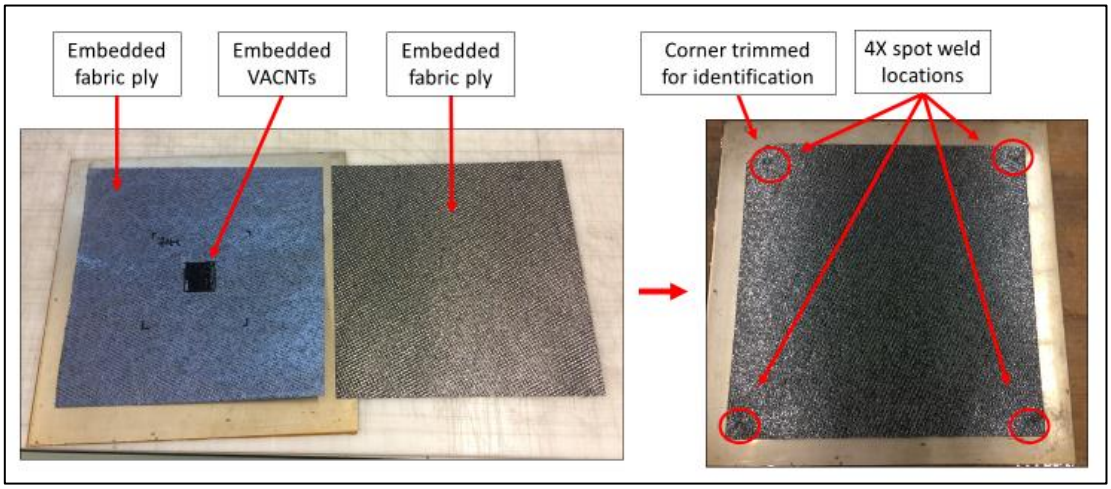

Figure 62 - Embedded fabric specimen for consolidation and spot-welding locations

3) The spot-welded assemblies were then put into the platen press with the configuration of components and materials as shown in Figure 63. The temperature and heating cycle shown in Figure 18 was used with requested temperatures of 320^{0}C and 6bar of pressure.

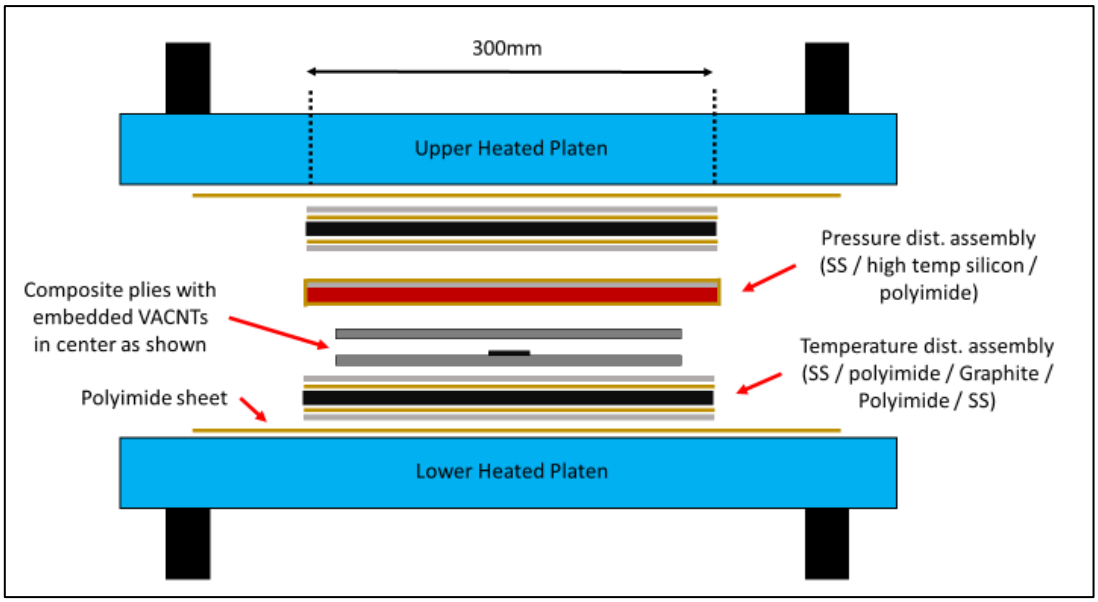

Figure 63 - Press layout for consolidation process

4) Once the embedded specimens were cooled to within 20^{0}C of room temperature (usually 17-22^{0}C) the press the specimens were removed from the press. The 250mm x 250mm specimens were cut down to roughly 100mm x 100mm centered about the VACNT substrate to enable for easier handling. Each consolidated specimen was further section as indicated in Figure 20 for further investigation with OM and SEM techniques.

B) Image Processing Techniques with *ImageJ*

The steps for using *ImageJ*, as used in this project, are described herein. The version of the software that was used for this project is 1.52b(fuji) and is an open source software that can be downloaded online. While there are many features that this software can accomplish, the steps used to process and analyze the pictures of the VACNT substrate materials after embedding will only be described.

1) Open a picture of a VACNT substrate and first duplicate it and use the original as a file to come back to if any issues arise. Use the ***Image -> Duplicate*** (Ctrl+Shift+D) feature as shown in Figure 64.

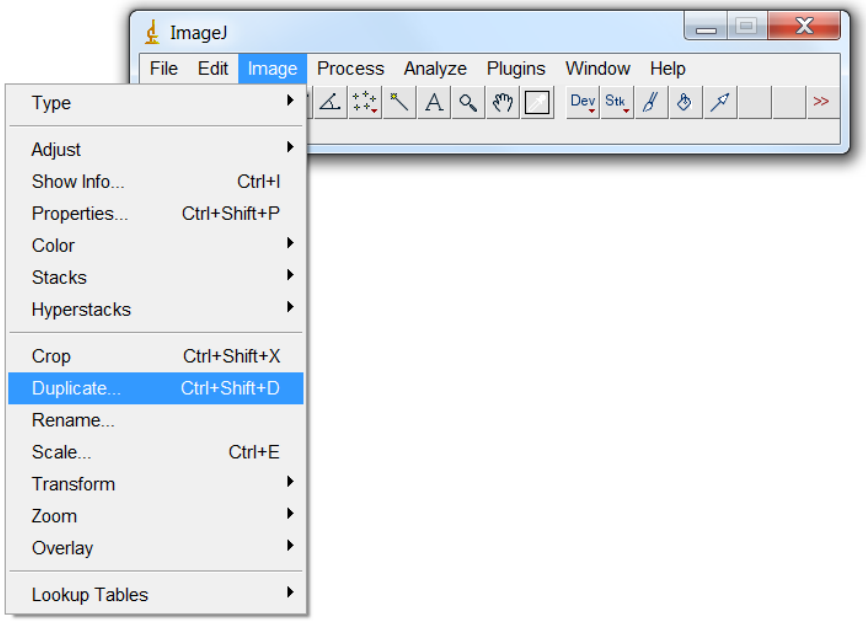

Figure 64 - *ImageJ* Processing - Step 1

2) Crop out the portion of the image that is not part of the VACNT substrate. Use ***Image -> Crop*** (Ctrl+Shift+X) to crop out just needed area as shown in Figure 65 .

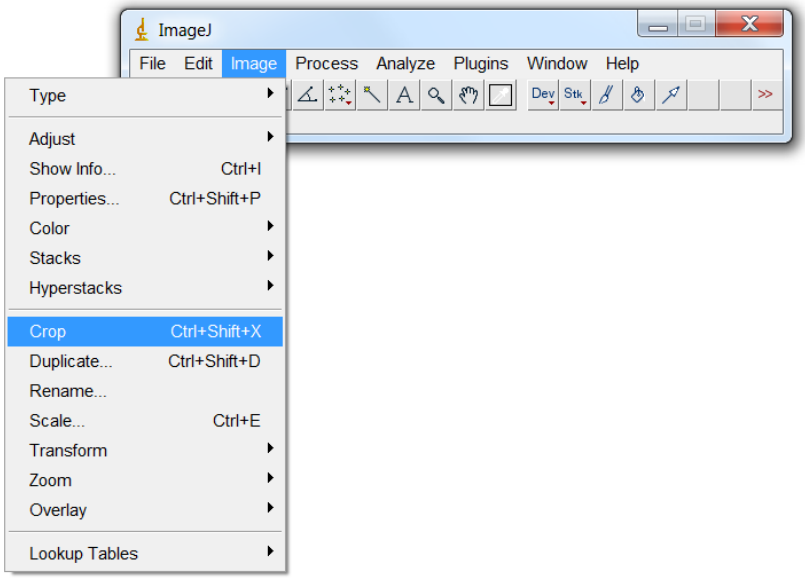

Figure 65 - *ImageJ* Processing - Step 2

3) Change the image to an 8-bit black and white image to allow for further processing. Use ***Image-> Type -> 8-bit*** as shown in Figure 66.

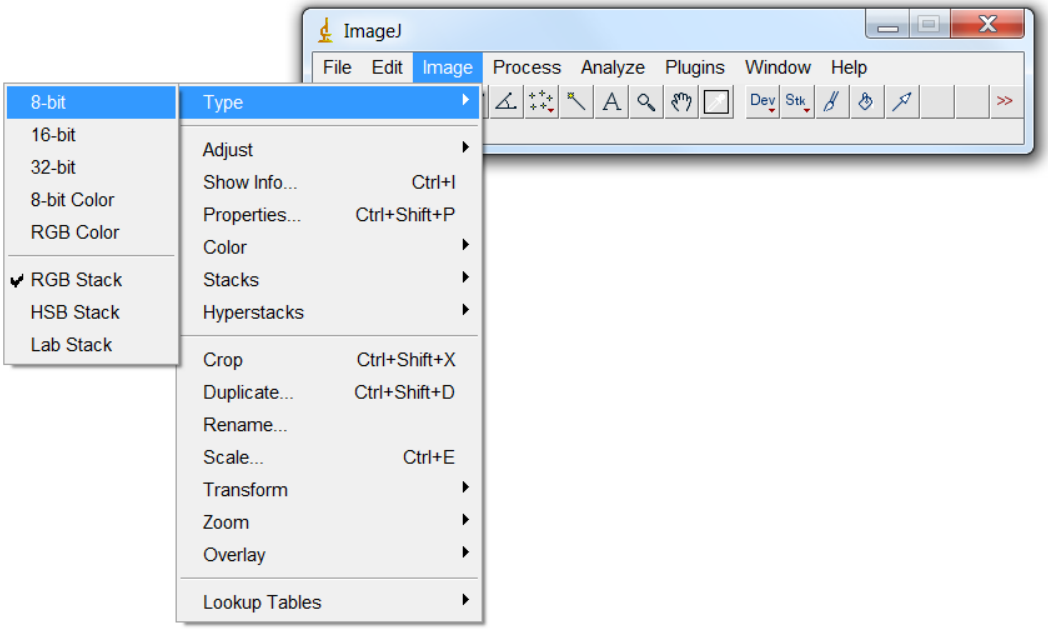

Figure 66 - *ImageJ* Processing - Step 3

4) Chose the threshold at which corresponds to the amount of VACNTs show in the image with what is on the substrate. It is advisable to have the original picture to relate back to. Use ***Image -> Adjust -> Threshold*** (Ctrl+Shift+T) and adjust the upper and lower adjustment bars to change the threshold of contrast as shown in Figure 67.

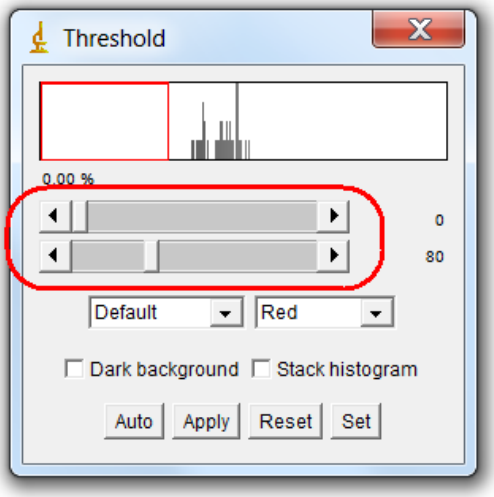

Figure 67 - *ImageJ* Processing - Step 4

5) If needed, one can **Fill** or **Clear** portions of the picture that were picked up by the threshold calculation that are or is not part of the area you want to be included in the area percent calculation. To do this, use the selection tools to enclose the area in question as shown in Figure 68. Use the ***Edit*** -> ***Clear*** or ***Edit*** -> ***Fill*** functions to remove (Fill) or add (Clear) areas of black as shown in Figure 69.

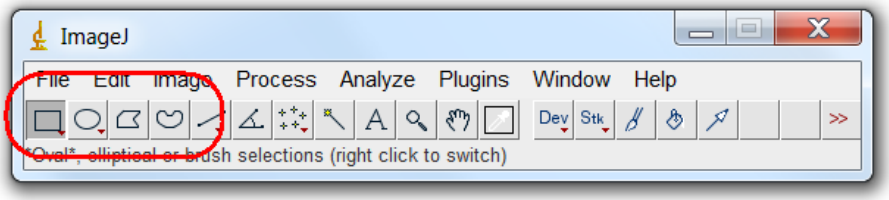

Figure 68 - *ImageJ* Processing - Step 5

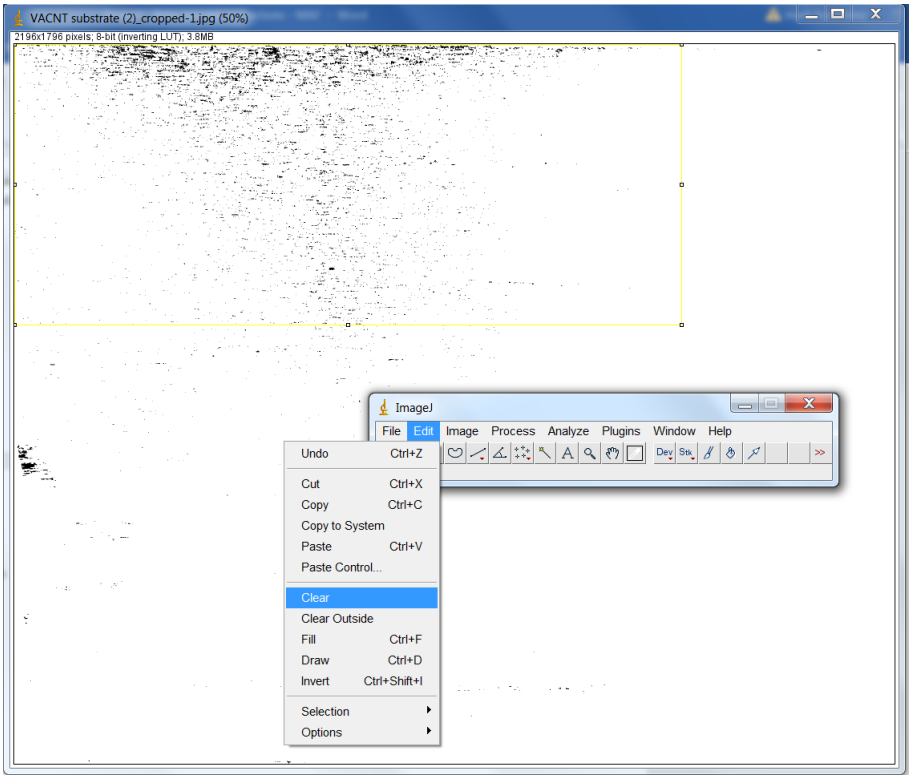

Figure 69 - *ImageJ* Processing - Step 6

6) Use the ***Analyze -> Set Measurements*** tool and click on just the ***Area fraction*** button as shown in Figure 70.

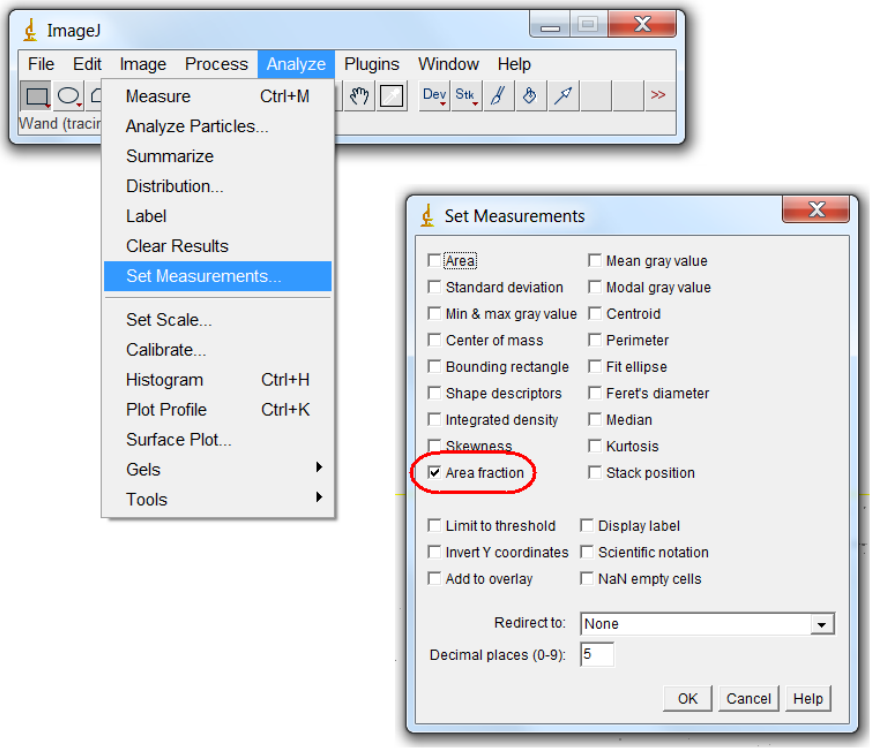

Figure 70 - *ImageJ* Processing - Step 7

7) Use the ***Analyze - > Measure*** (Ctrl+M) to measure all of the measurements that were set in the previous step. As shown in Figure 71 a window will open with the percent area of black that is in your picture.

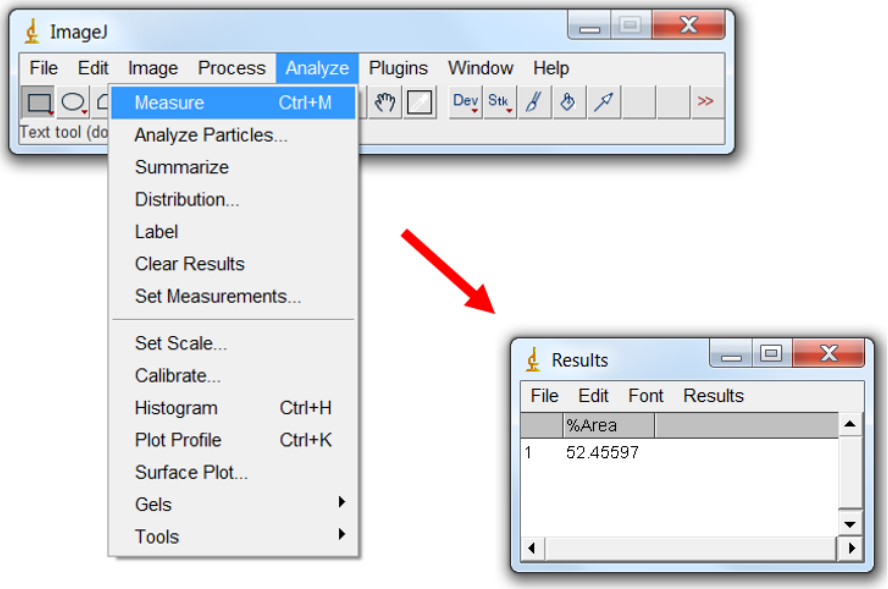

Figure 71 - *ImageJ* Processing - Step 8

8) Save the image you analyzed along with recording the percent area that was calculated.

C) Etching techniques

It was found through initial testing of PPS TP materials and VACNTs that, when fully embedded, the VACNTs can be extremely hard to distinguish from the PPS matrix unless at a fracture surface where the VACNTs can be pulled out or broken apart. Later use of high-quality polishing of mounted specimens to a 1µm surface finish and the use of OM and SEM techniques was shown to provide a macro-level indication of VACNT locations as shown in section 4.4.4. However, for finer level viewing of VACNTs and their possible orientation, such as that shown in Figure 6, three different etching techniques were trialed in the course of this project. This was done for the explicit reason to etch PPS CF/TP specimens with the goal of making the VACNTs present at the interlaminar region readably visible with OM and SEM techniques. These techniques were trialed on mounted and polished specimens of PPS that had been consolidated as described in sections 4.4 and 5.2

The first technique trialed was an alumina-chloride solution which has been shown by others [82] to be able to etch away amorphous PPS polymer materials. The solution was prepared as indicated in the reference literature and the solution was used to etch the surfaces for 30 and 60 seconds. It was found to not change the surface topology of the PPS specimens significantly.

The second technique trialed was the use of a plasma technique using a Tigres brand open-air three-headed plasma machine as shown in Figure 72. The vertical distance from the plasma nozzles was varied between 20 and 100mm and trails were tested for a range of 10-120 seconds in 10-second intervals to see the impact on the surface topology of consolidated PPS CF/TP specimens. The degree of change was qualitatively reviewed via OM techniques. It was found that for durations longer than 30 seconds and vertical distances of less than 40mm, burning or melting of the PPS polymer could be seen on the surface of the specimens and no clear indication of the location of VACNTs was able to be seen.

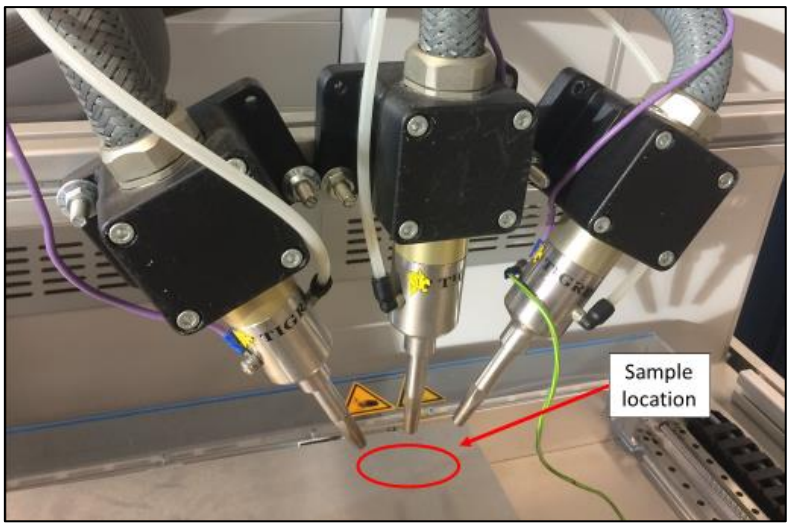

Figure 72 - Tigres plasma etching arrangement

The third technique trialed was a vacuum argon and oxygen plasma etching technique using a Tepla 300 microwave argon plasma machine which is located in the Kavli lab of the Applied Physics

department at TU Delft. This was chosen based similar use of plasma etching with TS/CF specimens in the works of Lewis [57] as well as from suggestions from individuals at N12 Technologies using similar etching techniques. In these cases, application of plasma to the polished face of TS/CF composite materials with VACNTs at the interlaminar layer was sufficient to etch of the organic TS polymer matrix material leaving VACNTs to be visible with OM and SEM techniques as seen in Figure 6. One difference though between those other researchers and these trials is that they used an RF powered plasma machine was utilized rather than the microwave powered one trialed here.

Specimens were trialed in both oxygen and argon environments for a range of 30-120 seconds in 30-second intervals. The gas flow rates were set at 225ml/min under a vacuum pressure of roughly 450 to 500mbar. Power settings of 300 and 600 watts were used. Mounted and polished PPS TP/CF specimens were placed on the top side of a glass beaker inside the Tepla 300 etching machine as shown in Figure 73. The inner Faraday cage was not used for these trails as it was understood to allow more activation of the surface of the specimen.

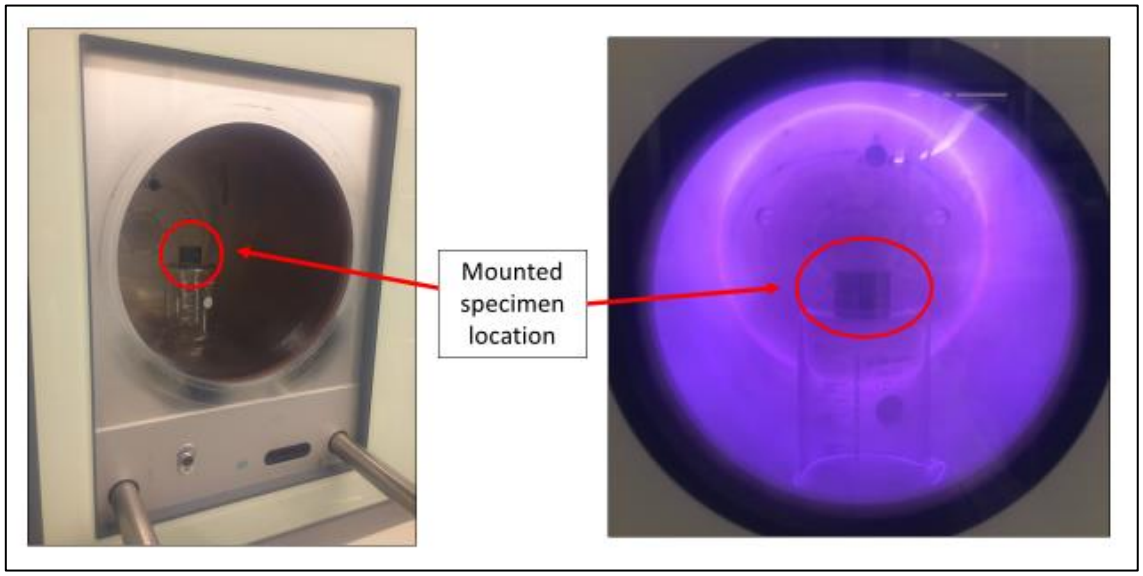

Figure 73 - Plasma Etching Specimen Arrangement

The results of the trials with plasma etching were deemed to be better than that of the two previously mentioned methods. Of the settings used, the highest quality view of VACNTs was judged to be with specimens processed in an oxygen environment for 60 to 120 seconds and at a power setting of 600 watts. In these specimens, the clarity of the VACNTs was somewhat crisper and easier to see than un-etched specimen and seems like a promising avenue for etching PPS composite materials.

Due to the location of the Tepla 300 machine inside a dedicated clean room the logistics to use it were time-consuming and it was decided to use standard high-quality polishing for the majority of specimens investigated in this project. It was found that polishing was able to produce a good macro-level view of VACNTs with OM techniques in a time efficient manner.

D) Laminate production techniques

The materials and procedures used for the production of the laminates used for this project are detailed herein. All raw materials used as the tested materials, those used for setup or as consumables, and arrangements of those materials are noted. The procedures developed and used are spelled out, and notes are given for what procedures were tested not used in the final full processes. The tested materials used are the same as noted in section 4.1 and are listed again in Table 7. This table also includes the consumables and will be referenced through the process steps.

The production of the laminates for testing with VACNTs consisted of first embedding plies of UD and fabric TP/CF materials with appropriate length VACNTs. This embedding process follows the same rough procedures used in Appendix A with some differences due to the differences in size of and format of the VACNT substrate materials.

The embedding process for materials used for SBS and CLC specimens consisted of the following steps:

1) UD and fabric composite materials (items 2 and three respectively in Table 7) were cut into 250mm octagons as shown in Figure 74. This was done to allow for the embedding of VACNTs in the center and easy stacking of the subsequently embedded materials in the variously prescribed laminates listed in Table 3. Centerline marks were made on the face of the composite plies with a black magic marker to aid in centering of the VACNT substrate materials.

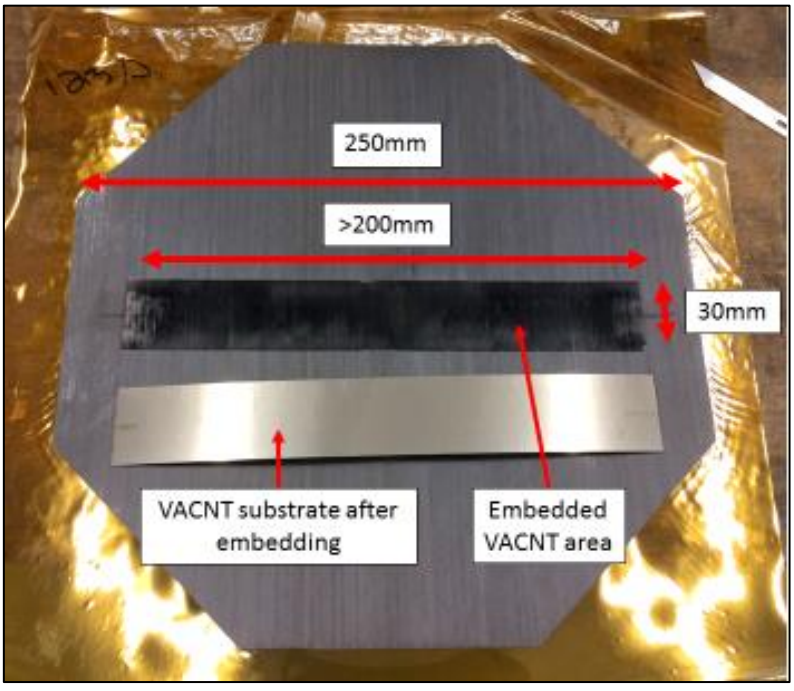

Figure 74 - 250mm Octagon layout with the substrate

2) The VACNT materials were cut from their respective 30mm wide strips in lengths of 30mm using sharp industrial hand scissors to allow for a clean cut of the SS substrate. To two corners

of the back side (non-VACNT side) of the substrate, small sections of PI tape were placed. This would be used to hold the substrate in place and to prevent it from shifting laterally in relation to the composite ply. To the pre-marked composite ply the substrate with VACNTs was placed by hand such that the VACNTs were facing down towards the composite ply. Care was taken to only hold the substrate by the edges which permitted the bulk of the VACNTs not to be disturbed. Light pressure was used to press the two PI tape sections on the corners of the VACNT substrate to hold the substrate to the composite ply. This entire step was performed inside an enclosed glovebox and while wearing latex gloves and an N100 dust mask. The prepared materials can be seen in Figure 75.

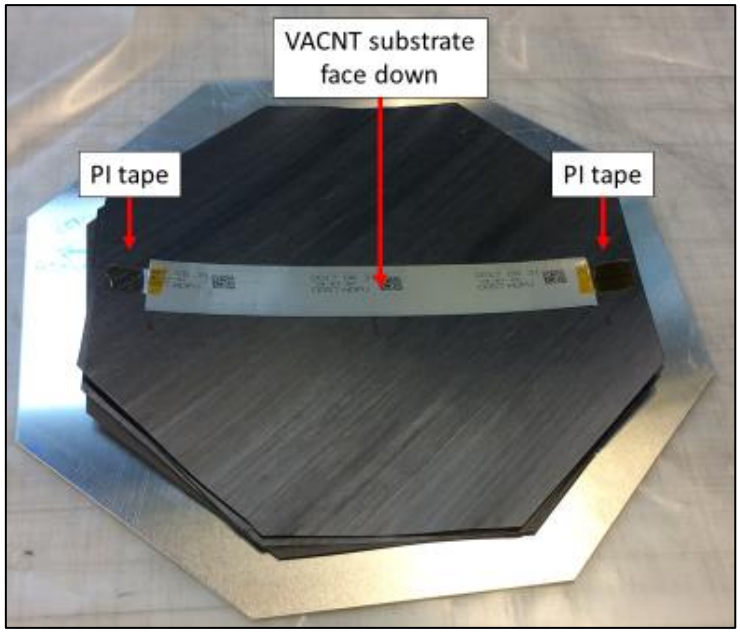

Figure 75 - VACNT substrate on Octagon composite ply

3) The plies were arranged and embedded using a process whereby six plies could be embedded at once in the platen press. This was chosen to save time rather than doing each embedding individually. The arrangement for this multiple ply embedding process is shown in Figure 76. The prepared materials were embedded in the press by use of a programmed temperature and heating cycle similar to that shown in Figure 18 with target max temperature and pressure of 200^0C and 1bar respectively.

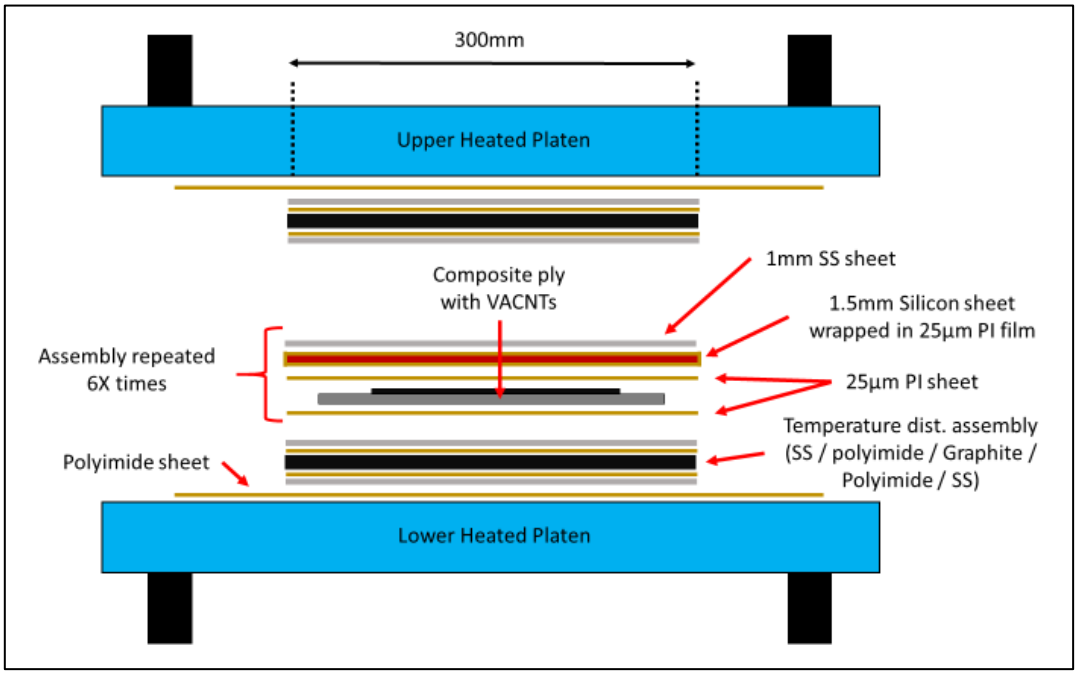

Figure 76 - Press layout for embedding multiple plies

4) Once the embedded specimens were cooled to within 20^0C of room temperature (usually 17-22^0C) the press the specimens were removed from the press.

5) For this step latex gloves were worn to prevent contamination of the specimens and limit CNT exposure. The VACNT substrate was removed by first peeling back one of the sections of the PI tape used to hold it in place and then carefully by hand peeling the SS substrate as shown in Figure 74

6) The surface of the now removed substrate that previously fully contained VACNTs had high-quality digital photographs taken of their surfaces using a Coolpix brand P600 camera and the images were processed using *ImageJ* software to calculate a percentage of VACNTs remaining on the substrate. This process is described in Appendix B.

The embedding process for materials used for MPT specimens consisted of the following steps:

1) Squares of 305mm x 305mm UD and fabric materials were cut UD and fabric composite materials (items 2 and three respectively in Table 7) were cut into 305mm x 305mm squares while material to be used for the $\pm5^0$ scrim layer were cut as indicated in Figure 81.

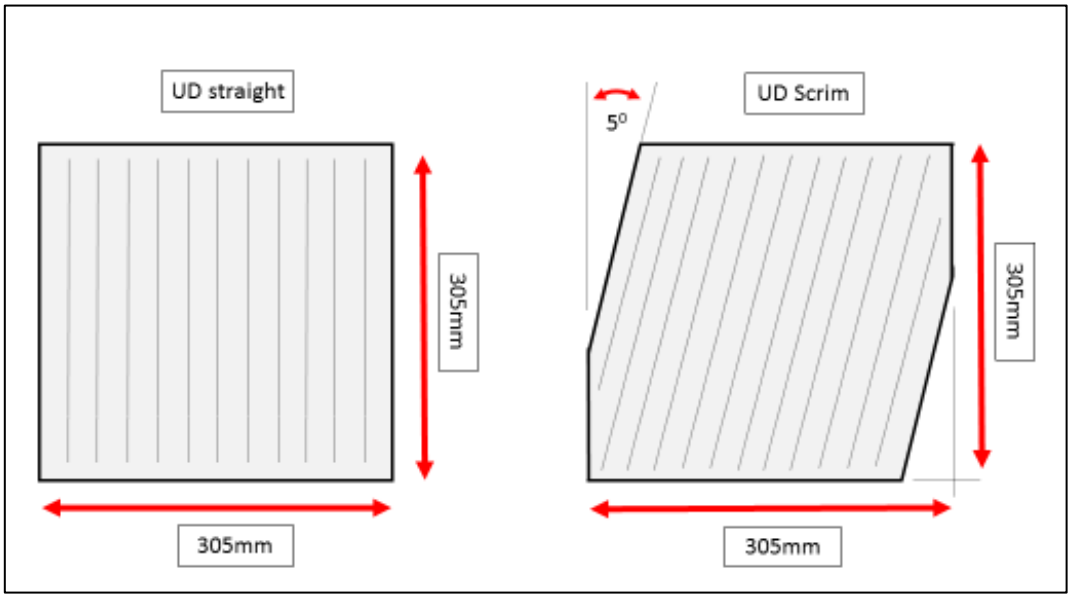

Figure 77 - Mandrel peel test UD material cut pattern

1) The VACNT materials used for this step were either from 30mm wide substrate material for ~50µm VACNTs or 380mm wide substrate material for ~20µm VACNTs. They were cut using sharp industrial hand scissors for the 30mm wide substrate, or an industrial paper/cutting shear as shown in Figure 78 for the 380mm wide substrate. For UD materials, 300mm x 200mm sections of VACNT substrate were cut, while for fabric materials nine sections of 30mm wide VACNT sections measuring 200mm long each were cut.

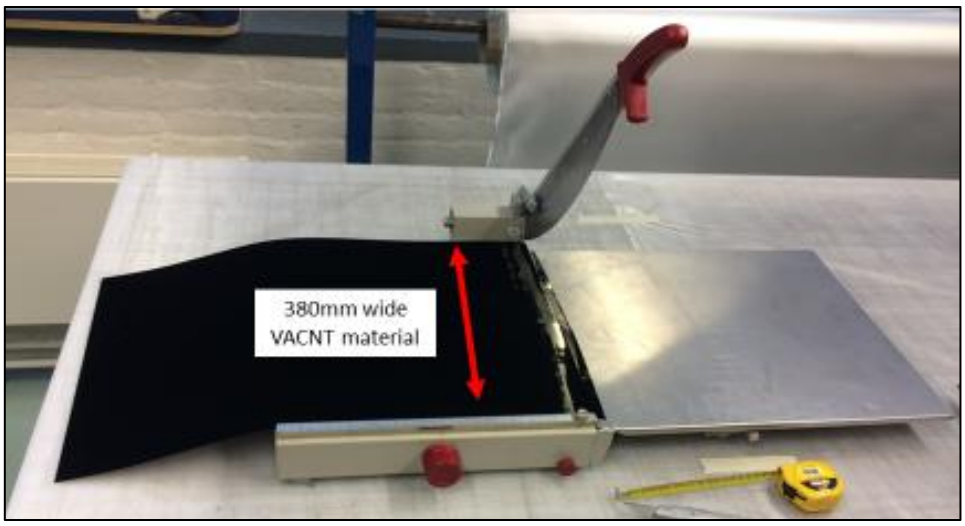

Figure 78 - 380mm wide VACNT substrate cutting shear

To the corners of the back side (non-VACNT side) of the substrate, small sections of PI tape were placed. This would be used to hold the substrate in place and to prevent it from shifting laterally in relation to the composite ply. To the pre-marked composite ply, the substrate with VACNTs was placed by hand such that the VACNTs were facing down towards the composite

ply. Care was taken to only hold the substrate by the edges which permitted the bulk of the VACNTs not to be disturbed. Light pressure was used to press the two PI tape sections on the corners of the VACNT substrate to hold the substrate to the composite ply. This entire step was performed while wearing latex gloves and an N100 dust mask. The prepared materials can be seen in Figure 79.

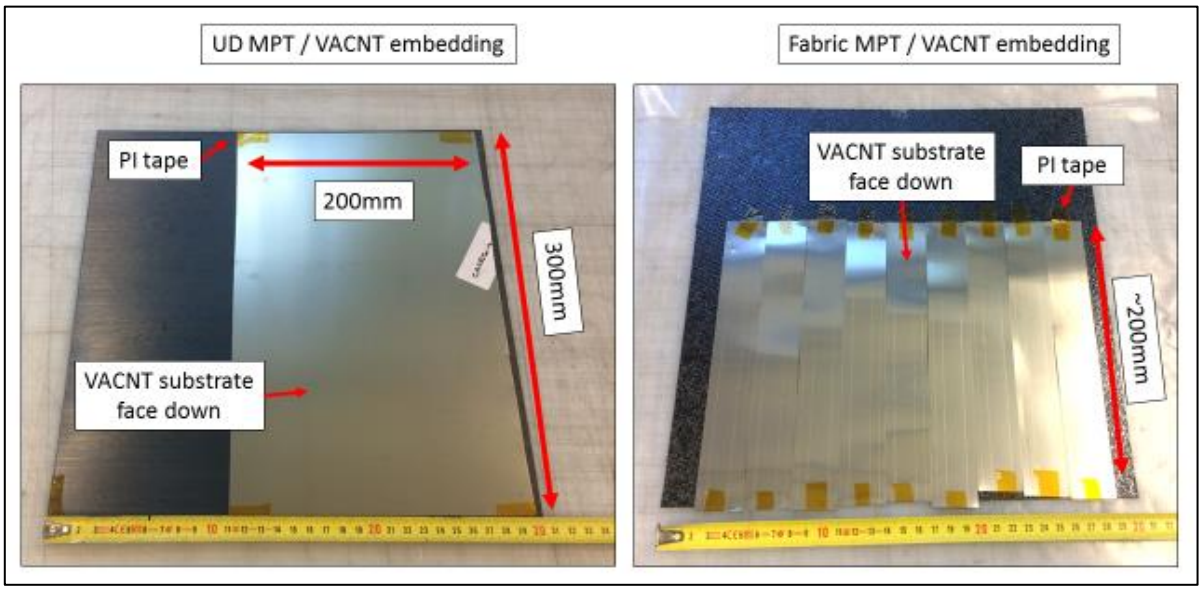

Figure 79 - UD and fabric MPT embedding layout

2) The prepared materials were embedded in the press by use of a programmed temperature and heating cycle similar to that shown in Figure 18 with target max temperature and pressure of 200^0C and 1bar respectively. The arrangement for this multiple ply embedding process is similar to that shown in Figure 16 and Figure 76.

3) Once the embedded specimens were cooled to within 20^0C of room temperature (usually 17-22^0C) the press the specimens were removed from the press.

4) For this step latex gloves were worn to prevent contamination of the specimens and limit CNT exposure. The VACNT substrate was removed by first peeling back one of the sections of the PI tape used to hold it in place and then carefully by hand peeling the SS substrate as shown in Figure 80.

5) The surface of the now removed substrate that previously fully contained VACNTs had high-quality digital photographs taken of their surfaces using a Coolpix brand P600 camera and the images were processed using *ImageJ* software to calculate a percentage of VACNTs remaining on the substrate. This process is described in Appendix B.

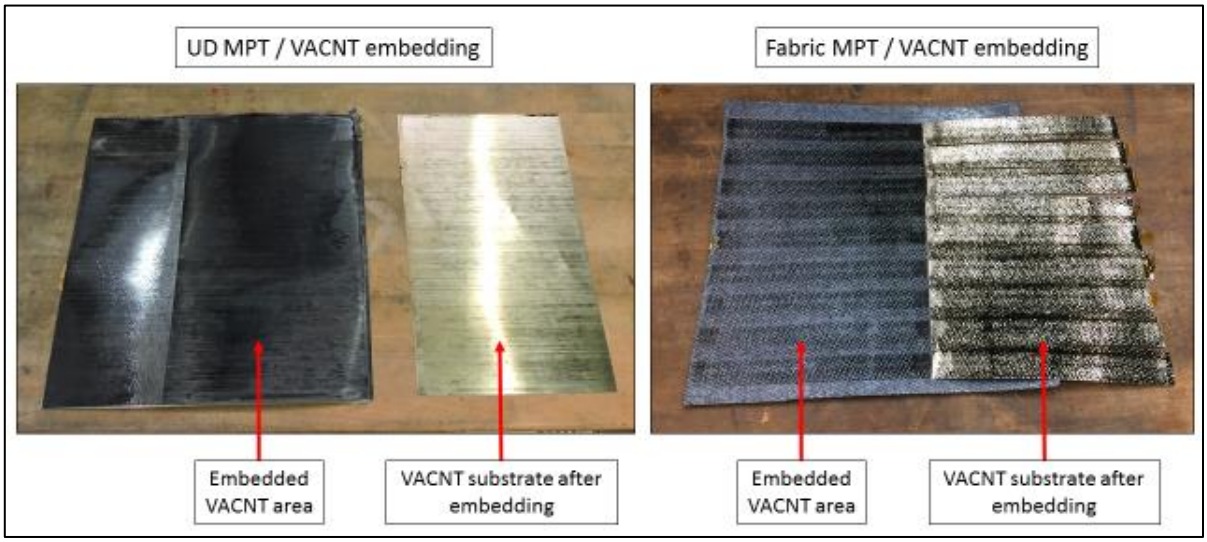

Figure 80 - UD and fabric MPT embedding layout – post-embedding

The consolidation process of the laminates used for SBS, CLC and MPT specimens consists of the following steps. Note that the consolidation process for laminates with and without VACNTs is mostly the same except where noted for the laminates with VACNTs. The consolidation process for laminates used for SBS and CLC specimens is different than that of the MPT laminates and consists of the following steps:

1) Composite plies of UD and fabric were first embedded respectively with ~20µm and ~50µm VACNTs at 200^0C and 1 bar of pressure following the above-noted processes.

2) For plies embedded with VACNTs, a small "V" shaped notch was cut along the centerline of the VACNT patch as shown in Figure 81. This was done before stacking each ply to allow the orientation of the VACNTs to be noted after consolidation.

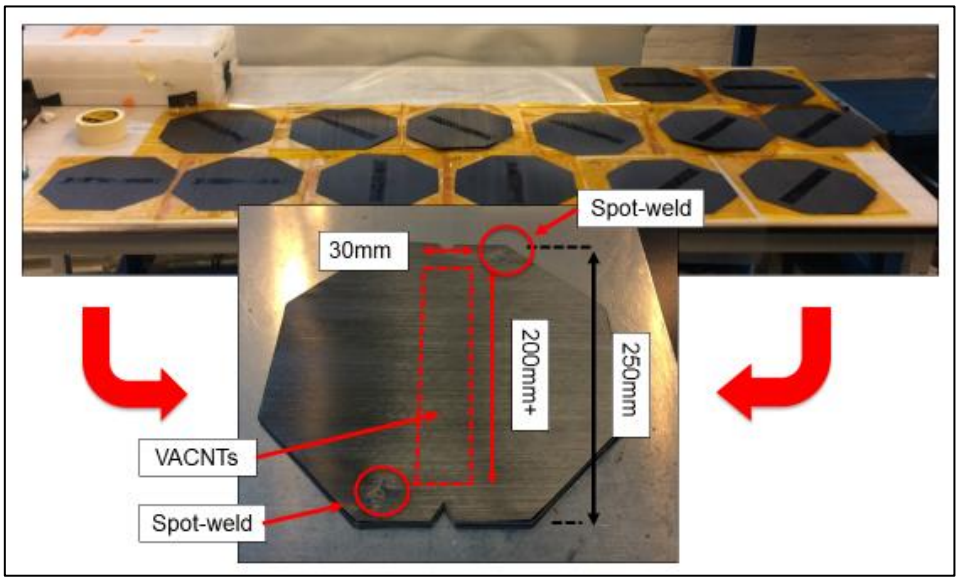

Figure 81 - Stacking of embedded plies and notch cut for VACNT identification

3) The embedded composite plies were stacked in the orientation as called in Table 3. For the specimens with VACNTs at the interlaminar region, the bottom-most 15 plies contained VACNTs embedded on the surface of each ply and was covered by a non-VACNT embedded ply to complete the laminate. The embedded plies are carefully stacked as not to shear or shift the surfaces of the VACNTs. Occasionally some shifting would occur due to the nature of the handling. The fully stacked plies were then spot-welded in two opposing corners using a Rinco RL35 hand-held ultrasonic welder as indicated in Figure 81. For UD materials this process of spot-welding was difficult to accomplish, and local downward pressure around the spot-welded area was needed to hold the plies in place during welding. For fabric materials, the spot-welding process did not present any issues. For each spot-weld, a dwell time of 2 seconds was used for the welding, and the downward pressure was held on the weld for roughly 30 seconds after the welding impulse to allow the weld to cool sufficiently.

The stacked and welded plies were prepared for consolidation depending on the composite material.

a. For UD materials the spot-welded plies were placed in a sandwich of materials consisting of 1mm thick SS plates cut to the same 250mm octagon shape shown in Figure 81. These plates were coated with Marbocote 227-CEE mold release (item 17 in Table 7) as per the instructions. Around the sandwich of materials, an eight-pointed star shape of 125µm PI film was cut on an automated plotter and tightly wrapped around the assembly to help physically constrain the UD plies during consolidation. A depiction of the steps is shown in Figure 82.

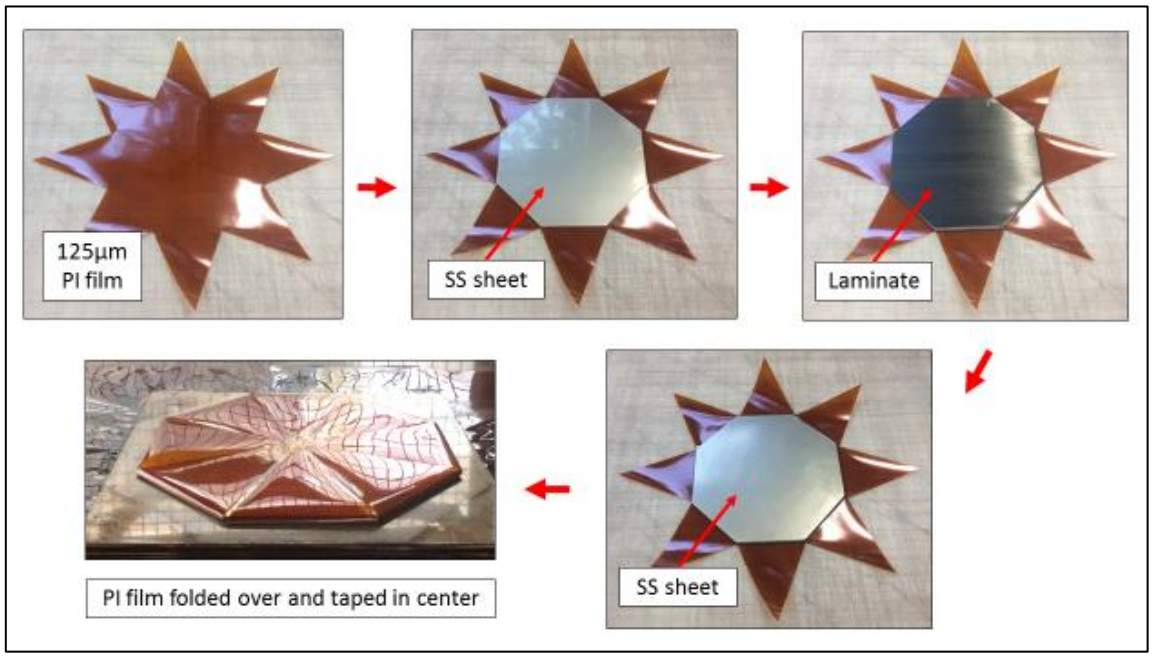

Figure 82 - UD laminate consolidation process sequence

b. For fabric materials the spot-welded plies were wrapped in sections of 50mm wide aluminum adhesive backed tape (item 19 in Table 7) to help contain any resin that flows out during consolidation. A depiction of the steps is shown in Figure 83. Note that two sections of tape are not shown in the right-hand side of the picture, but were added to create a complete perimeter around the laminate.

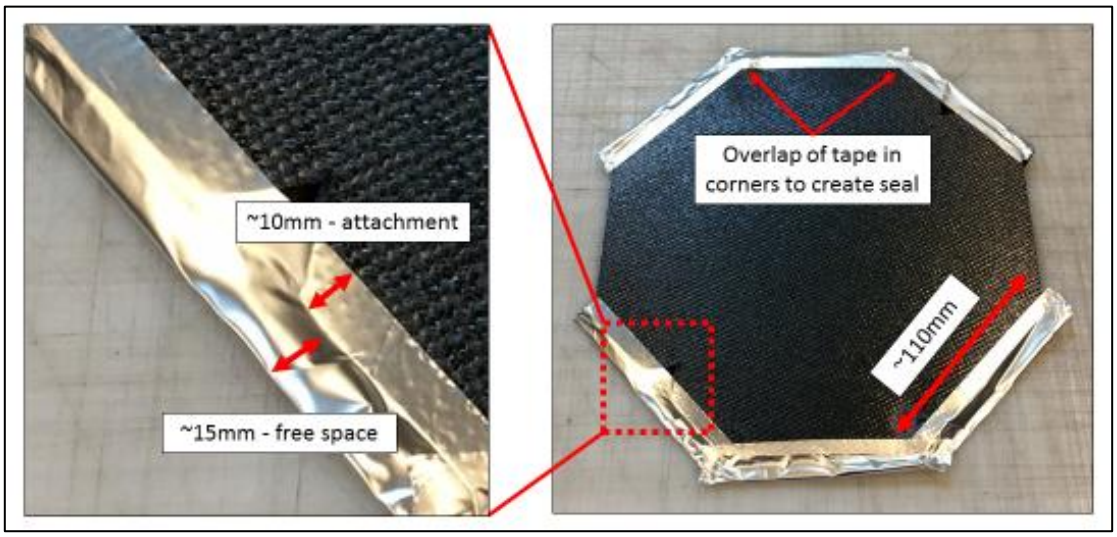

Figure 83 - Fabric laminate consolidation preparation

4) The prepared laminate assemblies were then put into the platen press with the configuration of components and materials as shown in Figure 84. Two laminate assemblies were consolidated at each time in the press to save on time. A single 1mm thick SS sheet was used to separate the laminate assemblies. The temperature and heating cycle shown in Figure 18 was used with requested temperatures of 320^0C and 6bar of pressure for PPS materials and 380^0C and 6bar of pressure for PEEK materials.

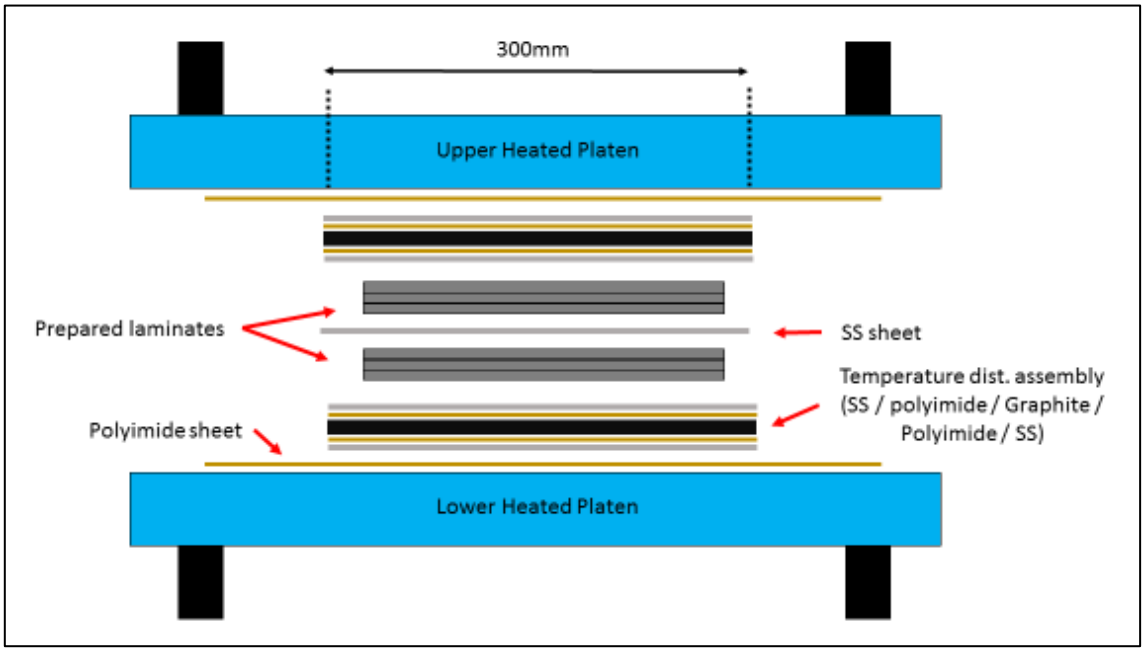

Figure 84 - Press layout for consolidating two laminates

The consolidation process for laminates used for MPT specimens is different than that of the SBS, and CLC laminates described previously and consists of the following steps:

1) Composite plies of UD and fabric were first embedded respectively with ~20µm and ~50µm VACNTs at 200^{0}C and 1 bar of pressure following the above-noted processes. The embedded composite plies were stacked in the orientation as called in Table 3. For UD materials, the VACNTs were embedded on the top side of the -5^0 ply in the [0_{13} /-5/+5/0] ply orientation. For fabric materials, the VACNTs were embedded into the top side of the 11th of the total 12 plies used in the $[(0/90)/(0/90)]_{3s}$ ply orientation. A 12.5µm PI film (item # 8 in Table 7) was as a ply separator for the laminates made for the MPT specimens which would allow for the peel arm of the specimens to be made. The layout of this sheet and the laminate plies is shown in Figure 85. The plies were first stacked and welded using a Rinco RL35 hand-held ultrasonic welder at the two corners opposite the location of the PI film as shown in Figure 86. As with laminates made for SBS and CLC specimens with UD materials this process of spot-welding was difficult to accomplish and local downward pressure around the spot-welded area was needed to hold the plies in place during welding. For fabric materials, the spot-welding process did not present any issues. For each spot-weld, a dwell time of 2 seconds was used for the welding, and downward pressure was held on the weld for roughly 30 seconds after the welding impulse to allow the weld to cool sufficiently.

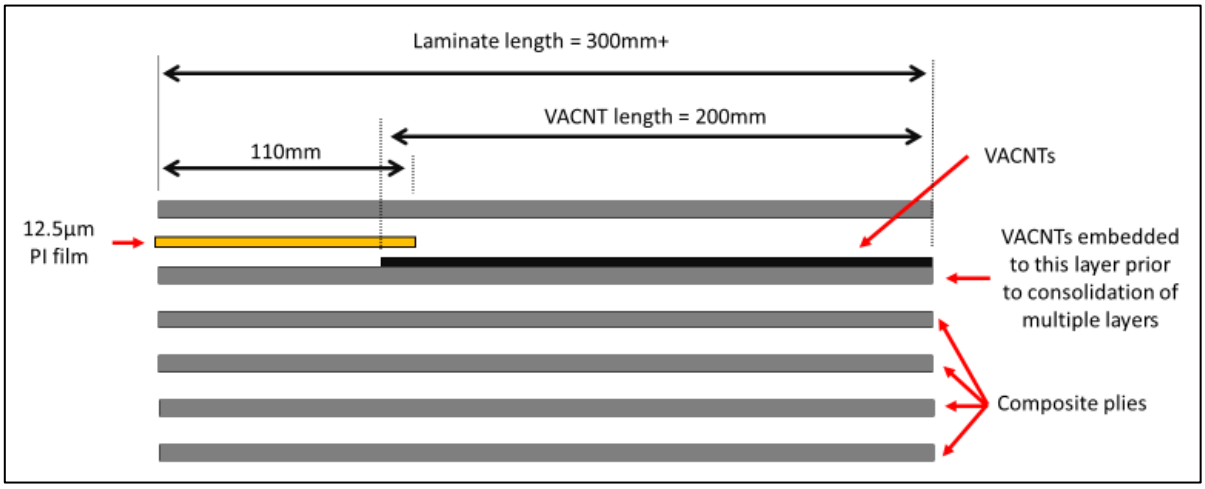

Figure 85 - MPT composite ply orientation - side-view

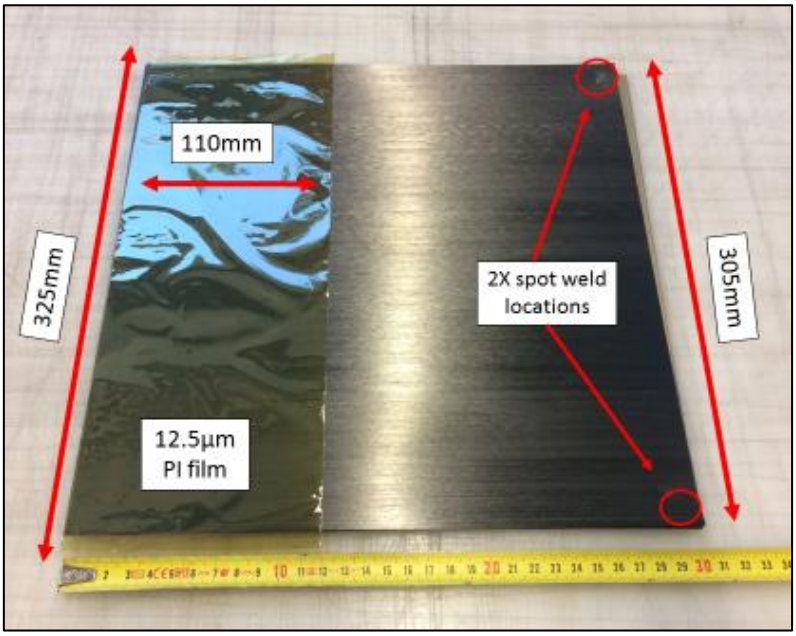

Figure 86 - Stacking of plies for MPT laminate – shown without uppermost ply(s)

3) The stacked and welded plies were prepared for consolidation depending on the composite material.

    a. For UD materials the spot-welded plies were placed in a sandwich of materials consisting of 1mm thick SS plates cut 300mm x 300mm shape shown in Figure 87. These plates were coated with Marbocote 227-CEE mold release (item 17 in Table 7) as per the instructions. Around the sandwich of materials, a 430mm x 430mm square sheet of 125µm PI film was tightly wrapped around the assembly to help physically constrain the UD plies during consolidation.

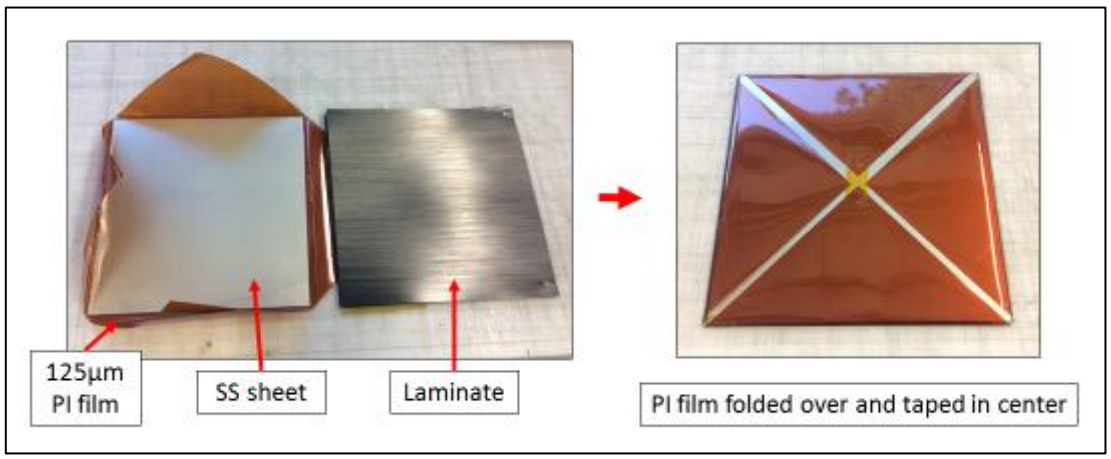

Figure 87 - UD laminate consolidation process sequence for MPT specimens

b. For fabric materials, the spot-welded plies were wrapped in sections of 50mm wide aluminum adhesive backed tape (item 19 in Table 7) to help contain resin that flows out during consolidation. The application of the tape was done similarly to that shown in Figure 83 but for the larger 305mm x 305mm square laminate size.

The prepared laminate assemblies were then put into the platen press with the configuration of components and materials as shown in Figure 84. Two laminate assemblies were consolidated at each time in the press to save on time. A single 1mm thick SS sheet was used to separate the laminate assemblies. The temperature and heating cycle shown in Figure 18 was used with requested temperatures of 320^0C and 6bar of pressure for PPS materials and 380^0C and 6bar of pressure for PEEK materials.

E) Mandrel Peel Test calculation example

The calculations for the fracture toughness values obtained via the MPT method used in section 5.5 required several steps to accomplish. While other researchers have spelled out this process [71], [72], [74], [83], a review of the steps taken by the author to obtain the values reported in this project are listed here for clarity. These steps were reviewed in person with F. Sacchetti (lead author of [83]) before testing. The process is spelled out in the following steps with pictures and notations as deemed relevant.

1) The raw data were imported into Excel and relabeled for the *Peel Force* and *Align Force* which correspond to *Fp* and *Fa* forces of the test shown in Figure 53. From this, the data the forces were graphed versus time along with their difference as seen. The width value used is an average of three measurements made along the length of each specimen as indicated in section 5.5.1. A judgment was made for the area of the test that corresponds to the peeling of the peel arm only and removes any end effects. It is from this range data that the corresponding G_c will be calculated.

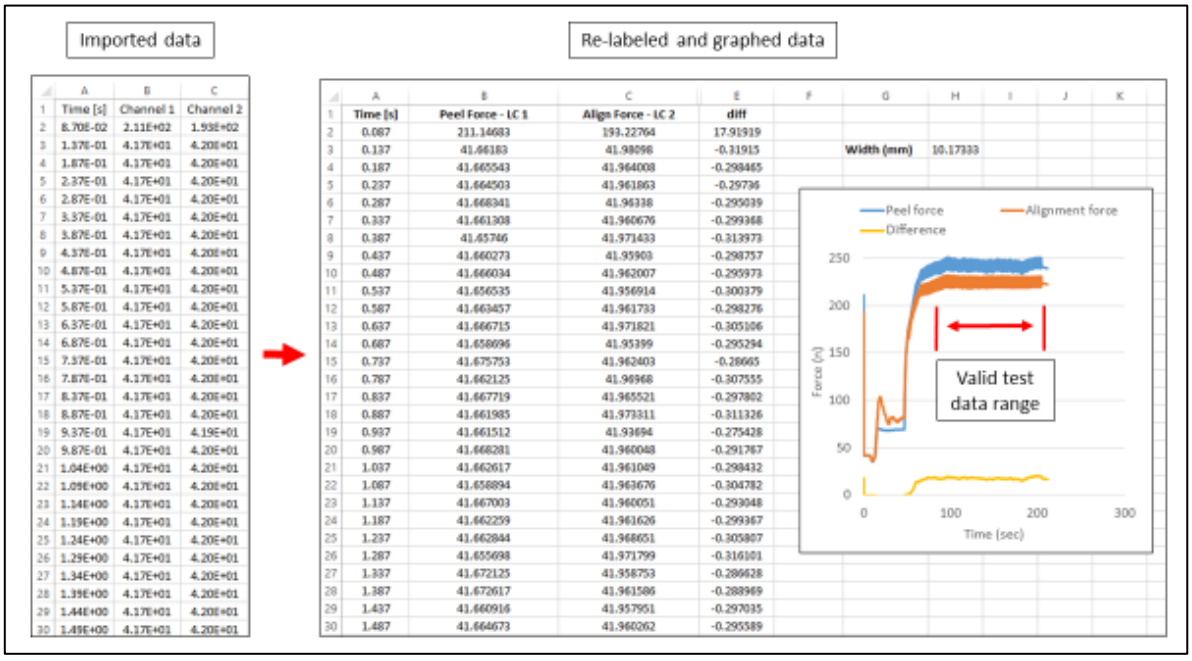

Figure 88 - MPT calculation – step 1

2) The calculation of the μ frictional force is calculated using equation (4) and as shown in Figure 89. From this, the data is graphed over versus time, and a judgment of the range of frictional force is calculated based on the input data which is shown. The μ that is used for the calculation of the ending G_c is an average value of all the specimens tested in a sample set, of which five specimens per sample set were tested within this project.

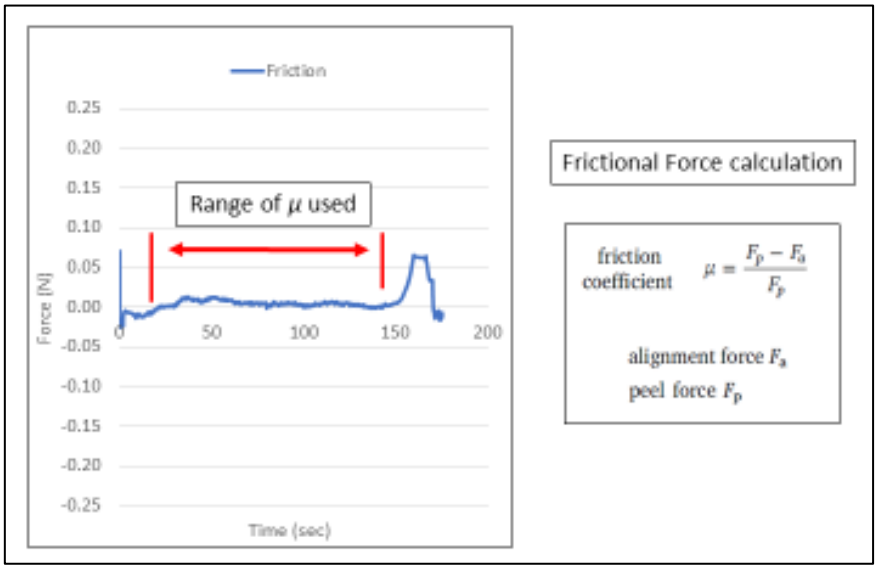

Figure 89 - MPT calculation – step 2

3) The G_c could be calculated using this total average μ and graphed as shown in Figure 90. Again, a judgment call of the range of G_c to be used was from which to calculate an average G_c as shown. This average value is what is used as the graph shown in Figure 54.

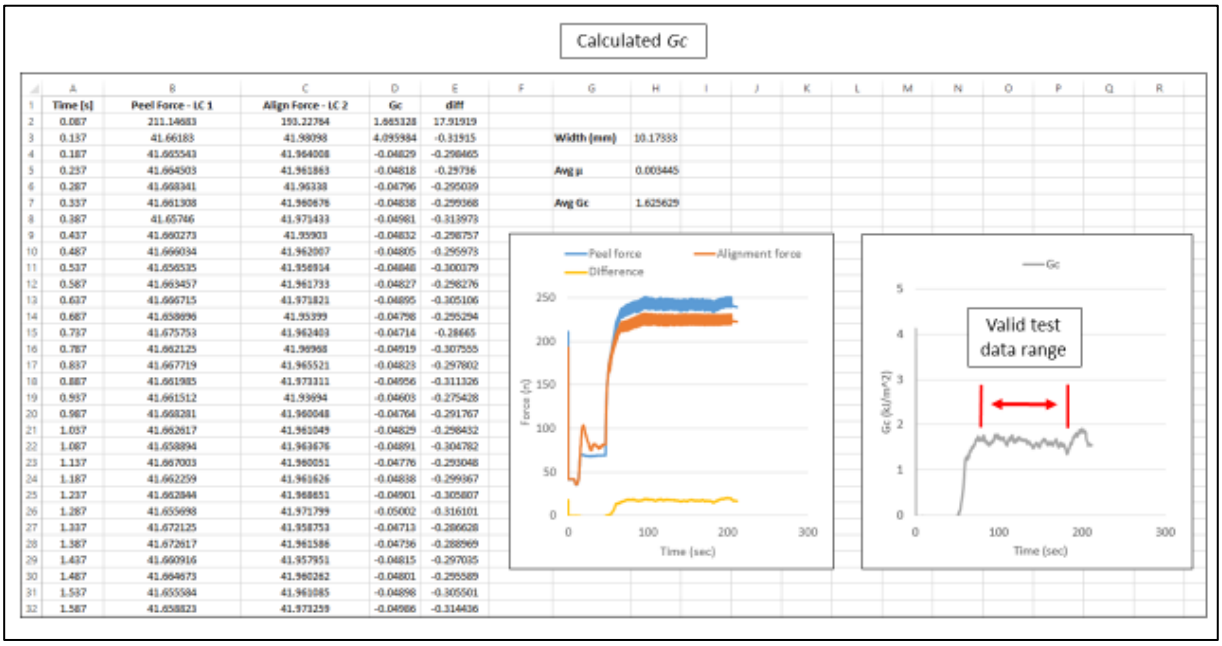

Figure 90 - MPT calculation – step 3

It is the author's opinion that the steps used to calculate the fracture toughness values are have three specific areas that require subjective *selection* of data from which to use which can could lead unexpected or inaccurate results.

F) VACNT and Thermoplastic film investigations

As mentioned in section 6.2, some preliminary work with the embedding of ~50µm VACNTs into PPS TP films was performed. This was done as a trial to see if it would be possible to embed VACNTs into a film substrate which could be used as a conductive layer for induction welding of thermoplastics. It was hypothesized that the VACNT structure would create a conductive field to be produced in the PPS film in the area where the VACNTs would be embedded. The details of this trial are listed here with the appropriate comments on materials and process used. This testing was done in collaboration with Michiel Hagenbeek on 5/7/2018 at TU Delft

The VACNTs were ~50µm in length and the substrate it was on was cut to 30mm x 30mm wide. A pre-consolidated PPS film measuring roughly 100mm x 100mm and 160µm thick was used. This was constructed from previously consolidated amorphous PPS film measuring 80µm thick.

The arrangement of the material is similar to that used for the embedding of VACNTs with a PI film vacuum bag as described in detail in Appendix A and shown in Figure 59 but on a smaller scale. The layout of the materials is shown in Figure 91. Note that while the PPS film is shown to be held in place to the vacuum PI film with PI tape in two locations, the VACNT substrate also had two small sections of PI tape attached to opposite corners to hold the substrate in place during handling. The entire assembly was placed onto the lower platen of the Joos platen press described previously with the same four standoffs described in Appendix A.

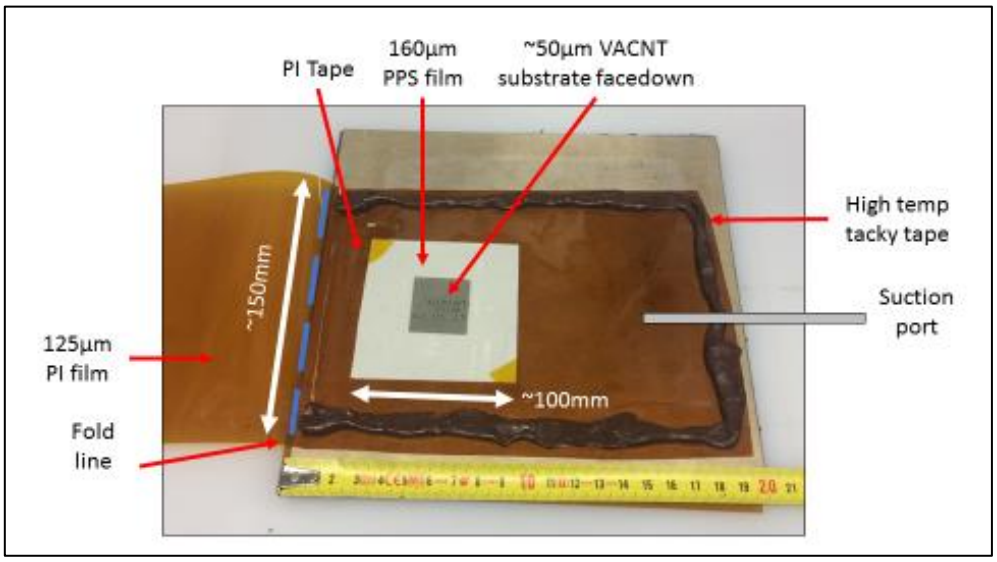

Figure 91 – Vacuum bag assembly for PPS film embedding

The temperature and pressure profile that was requested is shown in Figure 92. The five-minute hold time at 320^0C was chosen since the PPS film was thought to be able to become briefly completely melted and allow the VACNTs located above it to become embedded. The pressure of 0.2bar was chosen based on the hypothesis that since there was no fiber material in the PPS film, it would readily wet and embed with the VACNTs and that further pressure could matt or buckle the VACNTs.

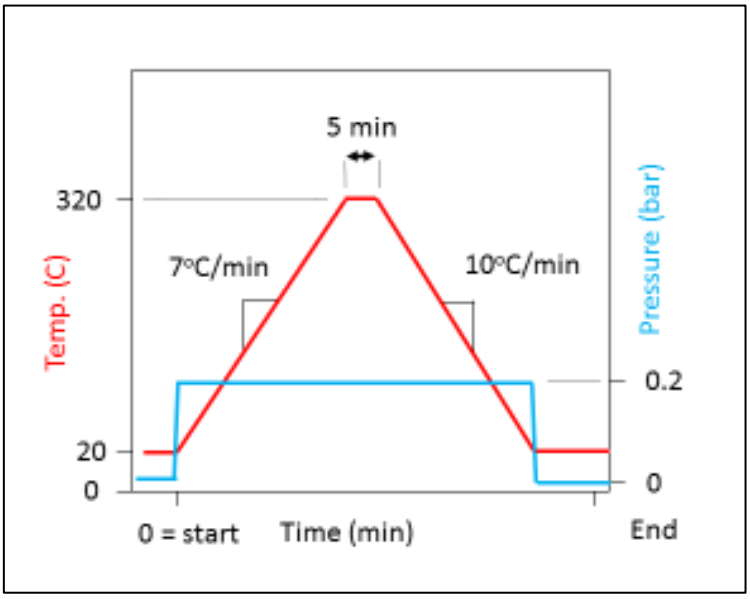

Figure 92- Temperature/pressure/time profile for PPS film embedding

The resulting embedding is shown in Figure 93. From this, both sides of the film are shown with one corner of the film missing which was broken off during handling. From Figure 93 the VACNTs can be seen to have nearly 100% transfer from the substrate. Some of the black color from the VACNTs can be seen coming through on the opposite side of the PPS film from where the substrate was located. There appeared to be little to no run-out or flowing of the PPS film from its original shape. Given that the location of the black color on the backside being roughly the same shape and location as where they were originally placed seems to indicate that there was little to no matting or shearing of the VACNTs during the embedding process. Some browning of the PPS film was noticed but was attributed to either slight oxidation or transfer of the from the PI film used for the vacuum bag material.

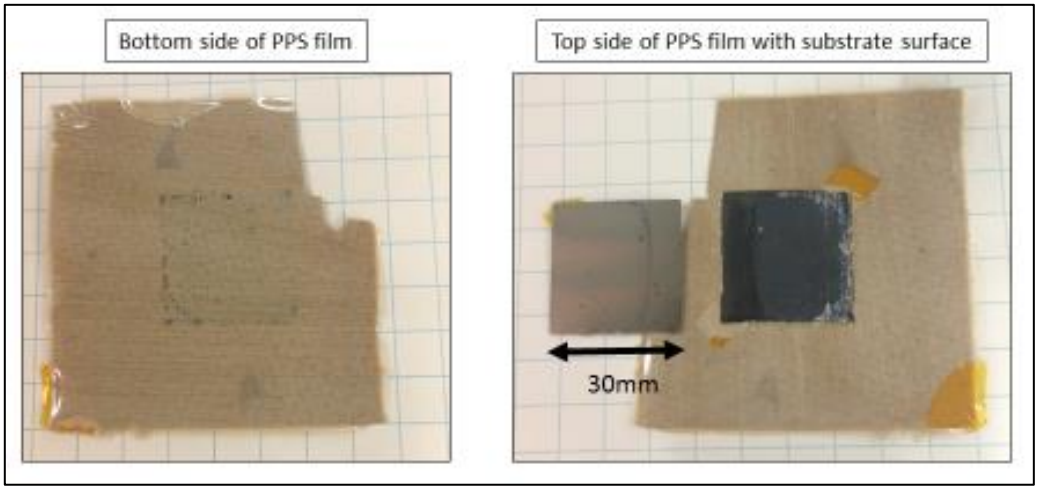

Figure 93 – PPS film after embedding – top and bottom side.

The entire PPS specimen as shown in Figure 93 was placed into an induction welding setup as shown Figure 94. The induction welder used is an Ambrell Systems brand EasyHeat station with a

maximum power of 10kVa and a frequency range of 140-410kHz. A thermal imaging video camera was placed directly above the heating element to observe the resultant temperature change of the PPS film with VACNTs as a result of the induced induction current. If the film was conductive, a corresponding increase in temperature of the film would be expected but was not observed over several settings used. This indicated that the VACNTs in the PPS film as tested did not form a substantial conductive material. Several settings for the induction heating were used with a maximum being 500amps of power. A starting distance of 1mm was used initially and reduced to approximately 0.25mm with no observable change in the heating of the PPS film. The frequency of the induction coil was automatically set internally within the induction welder within the stated range.

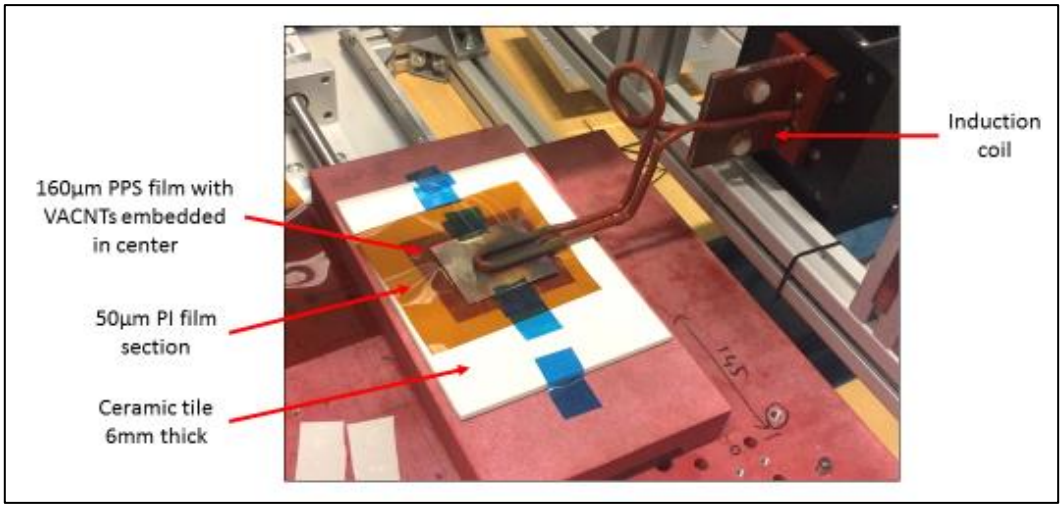

Figure 94 - Induction coil testing arrangement

After the induction heating trials were tested, the specimen was sectioned and reviewed with the JEOL SEM used for the previous observations as seem in Figure 95. From this, a film can be seen on the top of the VACNTS similar to that seen in Figure 25 for embedding of ~20µm VACNTs into PPD CF/TP UD materials. Additionally, the orientation of the VACNTs was observed to largely intact with very little matting or buckling of the VACNTs. The vertical orientation of the VACNTs matches with the findings from the induction testing. The highly conductive nature along the long-axis of the CNTs would not react to the induction current with the bulk vertical orientation of the CNTs. It is thought that the VACNTs would have to be matted over to create this possible conductive field. This opens the door to further work to see if a matting of the VACNTS can be produced by possibly using a lower temperature, one below the TM of PPS, where by the VACNTs are partially embedded in the film and can then be manually matted or *knocked over* to produce a morphology that responds to induction heating. Additionally, while the specific results of the embedding VACNTs into PPS films did not produce the hypothesized results, it does present a promising method for embedding VACNTs into PPS and other TP films where by the orientation of the VACNTs possibly be maintained better than through the embedding processes trialed throughout the bulk of this project.

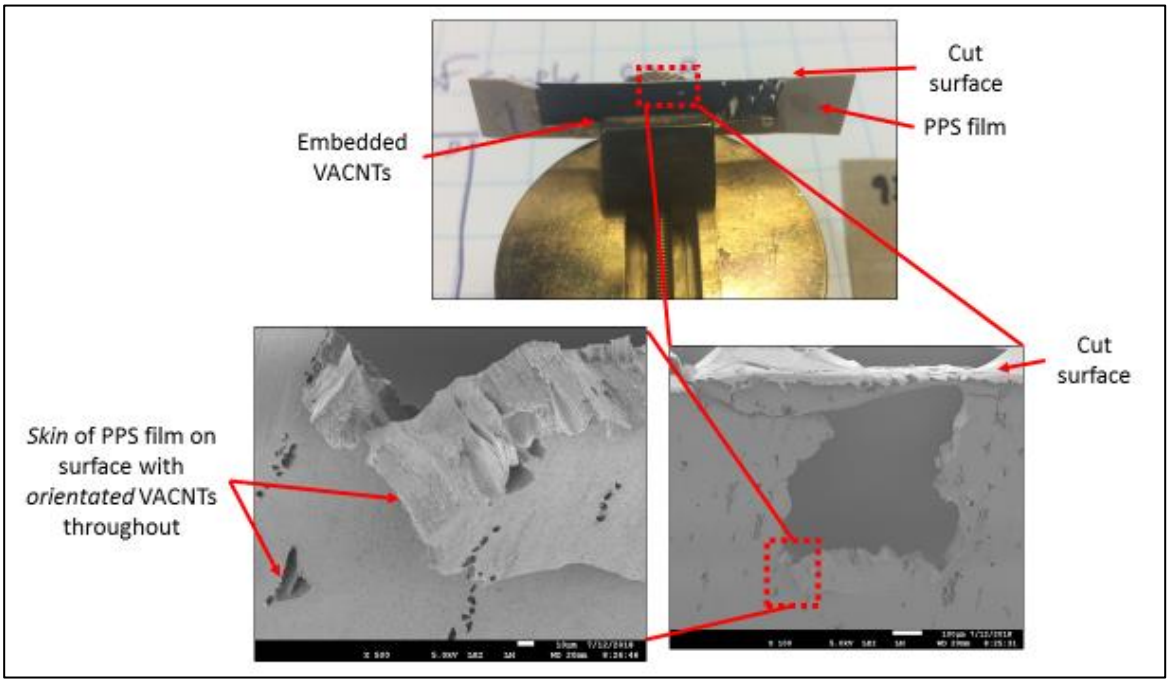

Figure 95 – Sectioned PPS film with VACNTs

8 References

[1] S. Iijima, "Helical microtubules of graphitic carbon," *Nature*, vol. 354, pp. 56–58, 1991.

[2] P. C. Ma, N. A. Siddiqui, G. Marom, and J. K. Kim, "Dispersion and functionalization of carbon nanotubes for polymer-based nanocomposites: A review," *Compos. Part A Appl. Sci. Manuf.*, vol. 41, no. 10, pp. 1345–1367, 2010.

[3] A. H. Barber, R. Andrews, L. S. Schadler, and H. D. Wagner, "On the tensile strength distribution of multiwalled carbon nanotubes," *Appl. Phys. Lett.*, vol. 87, no. 20, pp. 1–3, 2005.

[4] O. Gorhardani, M. Elola Chapartegui, and C. Elizetxea, "Potential and prospective implementation of carbon nanotubes on next generation aircraft and space vehicles," *Prog. Aerosp. Sci.*, vol. 70, pp. 42–68, 2014.

[5] H. Golnabi, "Carbon nanotube research developments in terms of published papers and patents, synthesis and production," *Sci. Iran.*, vol. 19, no. 6, pp. 2012–2022, 2012.

[6] E. J. Garcia, B. L. Wardle, and A. John Hart, "Joining prepreg composite interfaces with aligned carbon nanotubes," *Compos. Part A Appl. Sci. Manuf.*, vol. 39, no. 6, pp. 1065–1070, 2008.

[7] S. Béland, *High Performance Thermoplastic Resins and their Composites*. Park Ridge, New Jersey, USA: National Research Council of Canada, 1991.

[8] W. Callister and D. Rethwisch, *Materials Science and Engineering*, 9th ed. Wiley, 2001.

[9] M. Bannister and A. Mouritz, *Introduction to Aerospace Materials*. Woodhead, 2009.

[10] P. K. Mallick, *Fiber Reinforced Composites*, 3rd ed. CRC Press, 2007.

[11] B. Esp, *Practical Analysis of Aircraft Composites*, 1st ed. Grand Oak Publishing, 2017.

[12] A. Baker, *Composite Materials for Aircraft Structures*, 2nd ed. Reston, VA USA: AIAA Education Series, 2004.

[13] A. P. Mouritz, K. H. Leong, and I. Herszberg, "A review of the effect of stitching on the in-plane mechanical properties of fibre-reinforced polymer composites," *Compos. Part A Appl. Sci. Manuf.*, vol. 28, no. 12, pp. 979–991, 1997.

[14] K. A. Dransfield, L. K. Jain, and Y.-W. Mai, "On the effects of stitching in CFRPs - Mode I delamination toughness," *Compos. Sci. Technol.*, vol. 58, no. 6, pp. 815–827, 1998.

[15] S. L. Donaldson, "Fracture toughness testing of graphite/epoxy and graphite/PEEK composites," *Composites*, vol. 16, no. 2, pp. 103–112, 1985.

[16] G. Doray, S. M. Bishop, and P. T. Curtis, "On the impact performance of carbon fibre laminates with epoxy and PEEK matrices," *Compos. Sci. Technol.*, vol. 23, no. 3, pp. 221–237, 1986.

[17] S. M. Bishop, "The mechanical performance and impact behaviour of carbon-fibre reinforced PEEK," *Compos. Struct.*, vol. 3, no. 3–4, pp. 295–318, 1985.

[18] B. Vieille, V. M. Casado, and C. Bouvet, "Comparative Study on the Impact Behavior and Damage Tolerance of Woven Carbon Fiber Reinforced Thermoplastic – and Thermosetting – Composites," in *ECCM15 - 15TH EUROPEAN CONFERENCE ON COMPOSITE MATERIALS*,

Venice, Italy, 2012, no. June, pp. 24–28.

[19] M. Biron, *Thermoplastics and Thermoplastic Composites (2nd Edition)*. 2013.

[20] H. Golnabi, "Carbon nanotube research developments in terms of published papers and patents, synthesis and production," *Sci. Iran.*, vol. 19, no. 6, pp. 2012–2022, 2012.

[21] L. Gorbatikh, B. L. Wardle, and S. V. Lomov, "Hierarchical lightweight composite materials for structural applications," *MRS Bull.*, vol. 41, no. 9, pp. 672–677, 2016.

[22] F. H. Gojny, M. H. G. Wichmann, B. Fiedler, and K. Schulte, "Influence of different carbon nanotubes on the mechanical properties of epoxy matrix composites - A comparative study," *Compos. Sci. Technol.*, vol. 65, no. 15–16 SPEC. ISS., pp. 2300–2313, 2005.

[23] D. D. L. Chung, *Carbon Fiber Composites*. Butterworth-Heinemann, 1994.

[24] A. Peigney, C. Laurent, E. Flahaut, R. R. Bacsa, and A. Rousset, "Specific surface area of carbon nanotubes and bundles of carbon nanotubes," *Carbon N. Y.*, vol. 39, no. 4, pp. 507–514, 2001.

[25] R. Vidu, M. Rahman, M. Mahmoudi, M. Enachescu, T. D. Poteca, and I. Opris, "Nanostructures: a platform for brain repair and augmentation," *Front. Syst. Neurosci.*, vol. 8, no. June, pp. 1–24, 2014.

[26] M. Arai, Y. Noro, K. ichi Sugimoto, and M. Endo, "Mode I and mode II interlaminar fracture toughness of CFRP laminates toughened by carbon nanofiber interlayer," *Compos. Sci. Technol.*, vol. 68, no. 2, pp. 516–525, 2008.

[27] X. Xu, Z. Zhou, Y. Hei, B. Zhang, J. Bao, and X. Chen, "Improving compression-after-impact performance of carbon-fiber composites by CNTs/thermoplastic hybrid film interlayer," *Compos. Sci. Technol.*, vol. 95, pp. 75–81, 2014.

[28] M. Siegfried, C. Tola, M. Claes, S. V. Lomov, I. Verpoest, and L. Gorbatikh, "Impact and residual after impact properties of carbon fiber/epoxy composites modified with carbon nanotubes," *Compos. Struct.*, vol. 111, no. 1, pp. 488–496, 2014.

[29] P. C. Ma, S. Y. Mo, B. Z. Tang, and J. K. Kim, "Dispersion, interfacial interaction and re-agglomeration of functionalized carbon nanotubes in epoxy composites," *Carbon N. Y.*, vol. 48, no. 6, pp. 1824–1834, 2010.

[30] X. L. Xie, Y. W. Mai, and X. P. Zhou, "Dispersion and alignment of carbon nanotubes in polymer matrix: A review," *Mater. Sci. Eng. R Reports*, vol. 49, no. 4, pp. 89–112, 2005.

[31] M. R. Loos and K. Schulte, "Is It Worth the Effort to Reinforce Polymers with Carbon Nanotubes?," *Carbon Nanotub. Reinf. Compos. CNR Polym. Sci. Technol.*, pp. 207–232, 2014.

[32] M. R. Loos, V. Abetz, and K. Schulte, "Dissolution of MWCNTs by using polyoxadiazoles, and highly effective reinforcement of their composite films," *J. Polym. Sci. Part A Polym. Chem.*, vol. 48, no. 22, pp. 5172–5179, 2010.

[33] L. Gorbatikh, S. V. Lomov, and I. Verpoest, "Nano-engineered composites: A multiscale approach for adding toughness to fibre reinforced composites," *Procedia Eng.*, vol. 10, pp. 3252–

3258, 2011.

[34] A. Godara *et al.*, “Influence of carbon nanotube reinforcement on the processing and the mechanical behaviour of carbon fiber/epoxy composites,” *Carbon N. Y.*, vol. 47, no. 12, pp. 2914–2923, 2009.

[35] E. J. Garcia, B. L. Wardle, A. John Hart, and N. Yamamoto, “Fabrication and multifunctional properties of a hybrid laminate with aligned carbon nanotubes grown In Situ,” *Compos. Sci. Technol.*, vol. 68, no. 9, pp. 2034–2041, 2008.

[36] N. Yamamoto *et al.*, “High-yield growth and morphology control of aligned carbon nanotubes on ceramic fibers for multifunctional enhancement of structural composites,” *Carbon N. Y.*, vol. 47, no. 3, pp. 551–560, 2009.

[37] S. S. Wicks, W. Wang, M. R. Williams, and B. L. Wardle, “Multi-scale interlaminar fracture mechanisms in woven composite laminates reinforced with aligned carbon nanotubes,” *Compos. Sci. Technol.*, vol. 100, pp. 128–135, 2014.

[38] S. S. Wicks, “Manufacturing and Fracture of Hierarchical Composite Materials Enhanced with Aligned Carbon Nanotubes,” MIT, 2014.

[39] V. Koissin, T. Bor, Ž. Kotanjac, L. Lefferts, L. Warnet, and R. Akkerman, “Carbon Nanofibers Grown on Large Woven Cloths: Morphology and Properties of Growth,” *C*, vol. 2, no. 3, 2016.

[40] G. Gardiner, “The End of delamination,” 2015. [Online]. Available: http://www.compositesworld.com/blog/post/the-end-of-delamination. [Accessed: 14-Jan-2017].

[41] E. G. Rakov, “Materials made of carbon nanotubes. The carbon nanotube forest,” *Russ. Chem. Rev.*, vol. 82, no. 6, pp. 538–566, 2013.

[42] M. Terrones *et al.*, “Controlled production of aligned-nanotube bundles,” *Nature*, vol. 388, no. 6637, pp. 52–55, 1997.

[43] S. Pacheco Benito and L. Lefferts, “The production of a homogeneous and well-attached layer of carbon nanofibers on metal foils,” *Carbon N. Y.*, vol. 48, no. 10, pp. 2862–2872, 2010.

[44] N. K. Reddy, J. L. Meunier, and S. Coulombe, “Growth of carbon nanotubes directly on a nickel surface by thermal CVD,” *Mater. Lett.*, vol. 60, no. 29–30, pp. 3761–3765, 2006.

[45] K. Lafdi, L. Li, M. Boehle, and A. Lagounov, “Receptor-Catalyst Growth Process for Carbon Nanotubes,” 2014.

[46] V. Choudhary and A. Gupta, “Polymer / Carbon Nanotube Nanocomposites,” 1st ed., Shanghai: Intech, 2011.

[47] R. Hashaikeh, P. Krishnamachari, J. K. P. Pandey, H. Takagi, A. N. N. Nakagaito, and H.-J. Kim, *Handbook of Polymer Nanocomposites. Processing, Performance and Application*, vol. C. 2015.

[48] I. Lahiri, D. Lahiri, S. Jin, A. Agarwal, and W. Choi, “Carbon nanotubes: How strong is their bond with the substrate?,” *ACS Nano*, vol. 5, no. 2, pp. 780–787, 2011.

[49] S. S. Wicks, R. G. de Villoria, and B. L. Wardle, “Interlaminar and intralaminar reinforcement

of composite laminates with aligned carbon nanotubes," *Compos. Sci. Technol.*, vol. 70, no. 1, pp. 20–28, 2009.

[50] H. Cebeci, R. G. de Villoria, A. J. Hart, and B. L. Wardle, "Multifunctional properties of high volume fraction aligned carbon nanotube polymer composites with controlled morphology," *Compos. Sci. Technol.*, vol. 69, no. 15–16, pp. 2649–2656, 2009.

[51] R. Guzman de Villoria, P. Hallander, L. Ydrefors, P. Nordin, and B. L. Wardle, "In-plane strength enhancement of laminated composites via aligned carbon nanotube interlaminar reinforcement," *Compos. Sci. Technol.*, vol. 133, pp. 33–39, 2016.

[52] J. Blanco, E. J. García, R. Guzmán De Villoria, and B. L. Wardle, "Limiting mechanisms of mode i interlaminar toughening of composites reinforced with aligned carbon nanotubes," *J. Compos. Mater.*, vol. 43, no. 8, pp. 825–841, 2009.

[53] R. Guzman de Villoria, L. Ydrefors, P. Hallander, K. Ishiguro, P. Nordin, and B. Wardle, "Aligned Carbon Nanotube Reinforcement of Aerospace Carbon Fiber Composites: Substructural Strength Evaluation for Aerostructure Applications," *53rd AIAA/ASME/ASCE/AHS/ASC Struct. Struct. Dyn. Mater. Conf. AIAA/ASME/AHS Adapt. Struct. Conf. AIAA*, pp. 3–10, 2012.

[54] E. Kalfon-Cohen, D. Lewis, J. Ravine, and B. L. Wardle, "Structure-Process-Property Study of Aligned Carbon Nanotube Interlaminar Reinforcement in Woven Carbon Fiber Prepreg Laminate," *57th AIAA/ASCE/AHS/ASC Struct. Struct. Dyn. Mater. Conf.*, no. January, pp. 1–6, 2016.

[55] B. Wardle, "Nanostitched Composites with Improved Interlaminar and Intralaminar Strengths for Advanced Airframes in Sea-based Aviation," Cambridge, MA USA, 2017.

[56] X. Ni *et al.*, "Interlaminar Reinforcement of Carbon Fiber Composites Using Aligned Carbon Nanotubes," in *21st International Conference on Composite Materials (ICCM)*, 2017.

[57] D. Lewis, B. L. Wardle, and D. Lewis, "Interlaminar Reinforcement of Carbon Fiber Composites from Unidirectional Prepreg Utilizing Aligned Carbon Nanotubes By SUBMITTED TO THE DEPARTMENT OF AERONAUTICS AND ASTRONAUTICS IN PARTIAL Interlaminar Reinforcement of Carbon Fiber Composites from Unidi," Massachusetts Institute of Technology, 2016.

[58] D. Lewis and B. L. Wardle, "Interlaminar shear strength investigation of aligned carbon nanotube-reinforced prepreg composite interfaces," in *56th AIAA/ASCE/AHS/ASC Structures, Structural Dynamics, and Materials Conference*, 2015, no. January.

[59] Y. Zhang *et al.*, "Void Reduction in Out-of-Autoclave Processing of Carbon Fiber Epoxy Composites By Reinforcing Interlaminar Regions Using Vertically Aligned Carbon Nanotubes," no. June, pp. 26–30, 2016.

[60] C. Furtado, "Mechanics of Hierarchical Nanoengineered Aerospace Composite Materials -

(Unpublished)," Porto, Portugal, 2017.

[61] B. G. Falzon, S. C. Hawkins, C. P. Huynh, R. Radjef, and C. Brown, "An investigation of Mode I and Mode II fracture toughness enhancement using aligned carbon nanotubes forests at the crack interface," *Compos. Struct.*, vol. 106, pp. 65–73, 2013.

[62] A. T. Rhead, J. F. Morais, H. Conway, and D. Chebot, "Compression after impact strength of laminates with VACNT interply toughening produced with an industrially scalable process," *Compos. Part A Appl. Sci. Manuf.*, vol. 0, pp. 1–8, 2017.

[63] H. Conway, D. Chebot, C. Gouldstone, and R. Williams, "Fatigue response of carbon fiber epoxy laminates with vertically-aligned carbon nanotube interfacial reinforcement," 2015.

[64] C. Gouldstone, D. Degtiarov, and R. D. Williams, "Reinforcing Ply Drop Interfaces Using Vertically-Aligned Carbon Nanotube Forests," in *Sampe Conference*, 2014.

[65] H. Conway, B. Bancroft, D. Chebot, M. Devoe, and C. Gouldstone, "Impact Resistance and Residual Strength of Carbon Fiber Epoxy Laminates With Vertically- Aligned Carbon Nanotube Interfacial Reinforcement," 2017.

[66] S. H. Tseng and N. H. Tai, "Fabrication of a transparent and flexible thin film transistor based on single-walled carbon nanotubes using the direct transfer method," *Appl. Phys. Lett.*, vol. 95, no. 20, pp. 1–4, 2006.

[67] S. Park, M. Vosguerichian, and Z. Bao, "A review of fabrication and applications of carbon nanotube film-based flexible electronics," *Nanoscale*, vol. 5, no. 5, p. 1727, 2013.

[68] E. Sunden, J. K. Moon, C. P. Wong, W. P. King, and S. Graham, "Microwave assisted patterning of vertically aligned carbon nanotubes onto polymer substrates," *J. Vac. Sci. Technol. B Microelectron. Nanom. Struct.*, vol. 24, no. 4, p. 1947, 2006.

[69] F. Sacchetti, "Interlaminar Toughness of Fusion Bonded Thermoplastic Composites," University of Twente, 2017.

[70] Y. Su, M. De Rooij, W. Grouve, and L. Warnet, "Characterisation of metal-thermoplastic composite hybrid joints by means of a mandrel peel test," *Compos. Part B Eng.*, vol. 95, pp. 293–300, 2016.

[71] W. J. B. Grouve, L. L. Warnet, and R. Akkerman, "Critical assessment of the mandrel peel test for fiber reinforced thermoplastic laminates," *Eng. Fract. Mech.*, vol. 101, pp. 96–108, 2013.

[72] L. Kawashita, A. Kinloch, D. Moore, and J. Williams, "a Critical Investigation of the Use of a Mandrel Peel," pp. 2304–2323, 2006.

[73] P. Method, "A Protocal for Determination of Adhesvie Fracture Toughness of Flexible laminates by Peel Testing: Mandrel Peel Method," *J. Adhesion*, vol. 81, p. 561, 2005.

[74] L. F. Kawashita, D. R. Moore, and J. G. Williams, "The development of a mandrel peel test for the measurement of adhesive fracture toughness of epoxy-metal laminates," *J. Adhes.*, vol. 80, no. 3, pp. 147–167, 2004.

[75] TenCate, “TenCate - PPS processes and properties.” .

[76] E. W. Andrew, *Biron , M . (2016) Material Selection for Thermoplastic Parts - Practical and Advanced Information for Plastics Engineers* -. 2016.

[77] S. Esconjauregui *et al.*, “Measurement of area density of vertically aligned carbon nanotube forests by the weight-gain method,” *J. Appl. Phys.*, vol. 113, no. 14, 2013.

[78] “ASTM Standard D2344/D2344M, 2016 - Standard Test Method for Short-Beam Strength (SBS) of Polymer Matrix Composite Materials and Their Laminates.” ASTM International, West Conshohocken, PA, PA.

[79] “ASTM Standard D6641/D6641M, 2016 - Standard Test Method for Compressive Properties of Polymer Matrix Composite Materials Using a Combined Loading Compression (CLC) Test Fixture.” ASTM International, West Conshohocken, PA, PA.

[80] S. G. Ivanov, D. Beyens, L. Gorbatikh, and S. V. Lomov, “Damage development in woven carbon fibre thermoplastic laminates with PPS and PEEK matrices: A comparative study,” *J. Compos. Mater.*, vol. 51, no. 5, pp. 637–647, 2017.

[81] B. Vieille, V. M. Casado, and C. Bouvet, “About the impact behavior of woven-ply carbon fiber-reinforced thermoplastic- and thermosetting-composites: A comparative study,” *Compos. Struct.*, vol. 101, pp. 9–21, 2013.

[82] L. C. Lopez and G. L. Wilkes, “Poly(p-Pheny1ene Sulfide]-An Overview of an Important Engineering Thermoplastic,” *J. Macromol. Sci. Part C*, vol. 29, no. 1, pp. 83–151, 1989.

[83] F. Sacchetti, W. J. B. Grouve, L. L. Warnet, and I. Fernandez Villegas, “Interlaminar fracture toughness of 5HS Carbon/PEEK laminates. A comparison between DCB, ELS and mandrel peel tests,” *Polym. Test.*, vol. 66, no. October 2017, pp. 13–23, 2018.

[84] J. Ding *et al.*, “Graphene–Vertically Aligned Carbon Nanotube Hybrid on PDMS as Stretchable Electrodes,” *Nanotechnology*, 2017.